AD-766 472

GENERATION AND PROPAGATION OF INFRASONIC WAVES

Allan D. Pierce, et al

Massachusetts Institute of Technology

Prepared for:

Air Force Cambridge Research Laboratories

30 April 1973

DISTRIBUTED BY:

NTIS

National Technical Information Service
U. S. DEPARTMENT OF COMMERCE
5285 Port Royal Road, Springfield Va. 22151

Unclassified
Security Classification

DOCUMENT CONTROL DATA - R & D

Security classification of title, body of abstract and indexing annotation must be entered when the overall report is classified)

ORIGINATING ACTIVITY (Corporate author) Massachusetts Institute of Technology Cambridge, Massachusetts 02139	2a. REPORT SECURITY CLASSIFICATION Unclassified 2b. GROUP

3. REPORT TITLE

GENERATION AND PROPAGATION OF INFRASONIC WAVES

4. DESCRIPTIVE NOTES (Type of report and inclusive dates)
Scientific. Final: 1 February 1970 - 31 January 1973. Approved 22 May'73

5. AUTHOR(S) (First name, middle initial, last name)
Allan D. Pierce
Charles A. Moo
Joe W. Posey

6. REPORT DATE April 30, 1973	7a. TOTAL NO. OF PAGES 140 / 31	7b. NO. OF REFS 158
8a. CONTRACT OR GRANT NO. F19628-70-C-0008 b. PROJECT, TASK, AND WORK UNIT NOS. 7639-10-01 c. DOD ELEMENT 63731F d. DOD SUBELEMENT 679977	9a. ORIGINATOR'S REPORT NUMBER(S) 9b. OTHER REPORT NO(S) (Any other numbers that may be assigned this report) AFCRL-TR-73-0135	

10. DISTRIBUTION STATEMENT

A - Approved for public release; distribution unlimited.

11. SUPPLEMENTARY NOTES TECH, OTHER	12. Air Force Cambridge Research Laboratories (LW) L. G. Hanscom Field Bedford, Massachusetts 01730

13. ABSTRACT

A review is given of theoretical studies on infrasound generation and propagation through the atmosphere which were carried out under the contract. These studies include (1) further development and application of a computer program for the prediction of pressure signatures at large distances from nuclear explosions, (2) development of an alternative approximate model for waveform synthesis based on Lamb's edge mode, (3) development of a geometrical acoustics theory incorporating nonlinear effects, dispersion, and wave distortion at caustics, and (4) a theoretical model for the prediction of acoustic gravity wave generation by rising and oscillating fireballs. Numerical studies are reviewed which indicate the dependence of far field waveforms on energy yield and burst height. Implications of the Lamb edge mode theory include a new method for estimating energy yield from waveforms and an explanation of amplitude anomalies in terms of focusing or defocusing of horizontal ray paths.

DD FORM NOV. 1473

Unclassified
Security Classification

14 KEY WORDS	LINK A		LINK B		LINK C	
	ROLE	WT	ROLE	WT	ROLE	WT
Acoustics						
Wave Propagation						
Nuclear Explosions						
Gravity Waves						
Acoustic-gravity Waves						
Infrasonic Waves						

AFCRL - TR - 73 - 0135

Generation and Propagation of Infrasonic Waves

by

Allan D. Pierce, Charles A.Moo, and Joe W. Posey

Massachusetts Institute of Technology
Cambridge, Massachusetts 02139

Contract No. F19628-70-C-0008
Project No. 7639
Task No. 763910
Work Unit No. 76391001

FINAL REPORT

Period Covered: February 1, 1970 through January 31, 1973

30 April, 1973

Contract Monitor: Elisabeth F. Iliff
Terrestrial Sciences Laboratory

Approved for public release; distribution unlimited.

Prepared
for

AIR FORCE CAMBRIDGE RESEARCH LABORATORIES
AIR FORCE SYSTEMS COMMAND
UNITED STATES AIR FORCE
BEDFORD, MASSACHUSETTS 01730

ABSTRACT

A review is given of theoretical studies on infrasound generation and propagation through the atmosphere which were carried out under the contract. These studies include (1) further development and application of a computer program for the prediction of pressure signatures at large distances from nuclear explosions, (2) development of an alternative approximate model for waveform synthesis based on Lamb's edge mode, (3) development of a geometrical acoustics' theory incorporating nonlinear effects, dispersion, and wave distortion at caustics, and (4) a theoretical model for the prediction of acoustic gravity wave generation by rising and oscillating fireballs. Numerical studies are reviewed which indicate the dependence of far field waveforms on energy yield and burst height. Implications of the Lamb edge mode theory include a new method for estimating energy yield from waveforms and an explanation of amplitude anomalies in terms of focusing or defocusing of horizontal ray paths.

Preceding page blank

CONTENTS

1.0 Introduction..... 13
1.1 Scope of the Report..... 13
1.2 Background of the Report..... 14

2.0 Papers and Theses..... 17
2.1 Contents of Papers Written during the Contract..... 17
2.2 Contents of Theses Written during the Contract..... 20

3.0 The Modal Synthesis of Infrasonic Waveforms..... 23
3.1 Status of INFRASONIC WAVEFORMS..... 23
3.1.1 Earth curvature effects..... 23
3.1.2 Other modifications in the program..... 26
3.1.3 Further suggestions for program users..... 27
3.2 Source Models..... 29
3.2.1 Above ground explosions..... 29
3.2.2 Near surface explosions..... 37
3.3 Variation of Waveforms with Energy Yield and with Burst Height..... 38

4.0 An Approximate Theory Based on Lamb's Atmospheric Edge Mode..... 47
4.1 Introduction..... 47
4.2 Dispersion of Lamb's Mode..... 51
4.3 Theoretical Expressions for Edge Mode Waveforms..... 56
4.4 Comparison with Multimodal Computations..... 61
4.5 Implications of the Edge Mode Theory..... 66
4.5.1 Variation of waveform period with distance..... 66
4.5.2 Ratios of successive periods..... 66
4.5.3 Record begins with pressure rise..... 66
4.5.4 Ratio of successive peaks..... 67
4.5.5 Variation of waveform amplitude with distance..... 67
4.5.6 Determination of explosion energy from pressure waveforms..... 67
4.5.7 The anomalous spatial variations in amplitude may be explained in terms of focusing or defocusing of horizontal ray paths..... 74

5.0 A Short Period Model for Waves Generated by Explosions..... 83
5.1 Introduction..... 83
5.2 Ray Paths..... 83
5.3 Propagation along a Ray Segment..... 86
5.3.1 Dispersion effects..... 87
5.3.2 Nonlinear effects..... 90
5.3.3 Composite numerical method..... 95
5.4 Initial Conditions..... 95
5.5 Propagation past Caustics and Ground Reflection..... 97
5.6 Remarks..... 103

Preceding page blank

CONTENTS (cont'd)

6.0 A Model for Acoustic-Gravity Wave Excitation by Fireball Rise 105
6.1 Introduction 105
6.2 Dynamical Model of Fireball Rise 106
6.3 Approximate Solution of Fireball Rise Equations 110
6.4 Derivation of Source Terms 115
6.4.1 Monopole source terms 116
6.4.2 Mass dipole source 118
6.5 Remarks 119

7.0 Conclusions and Recommendations 121
7.1 Multimode Synthesis 121
7.2 Lamb Edge Mode Synthesis 122
7.3 Higher Frequency Model 123
7.4 Waves Excited by Fireball Rise 123
7.5 Other Topics 124
7.6 Concluding Remarks 125

REFERENCES 127

ILLUSTRATIONS

Figure 1. Comparison of nuclear-explosion generated acoustic-gravity waves upwind, crosswind, and downwind from the source. In each case, the observer is 10,000 km from the source in a subtropical summer atmosphere. The contributing modes, as well as their sum, are shown for each direction..... 24

Figure 2. Sketch illustrating the various idealizations incorporated in the mathematical formulation of the problem of acoustic-gravity wave propagation from a nuclear blast..... 30

Figure 3. Acoustic pressure per megaton of the source yield for ground bursts of 1, 10, and 100 megatons as a function of time. The observer is on the ground 10,000 km north of the source in a subtropical summer atmosphere..... 40

Figure 4. Plot of the amplitude dependence on yield found in the present calculations and a curve showing the $Y^{0.6}$ dependence derived from Harkrider's computations and made to agree with the first curve at 5 MT..... 42

Figure 5. Time variation of ground-level acoustic pressure 10,000 km north of 1 MT explosions at altitudes of 0, 50, and 70 km in a subtropical summer atmosphere..... 43

Figure 6. Height of burst dependence of the pressure amplitude per megaton of the source as found in the theoretical syntheses of ground-level wave forms for yields of 1, 10, 100 MT..... 44

Figure 7. Comparison of amplitude dependence upon height of burst as predicted by the Lamb edge mode hypothesis and by syntheses based on the summation of fully-ducted normal modes. The choice of ω_{char} is $0.0185\ sec^{-1}$..... 46

Figure 8. Model of edge mode propagation from an explosive source in an almost-stratified atmosphere above a spherical earth..... 48

ILLUSTRATIONS (cont'd)

Figure 9. Comparison of approximate edge mode dispersion curve (dashed line) with guided mode dispersion curves obtained by numerical solution of the acoustic-gravity wave eigenvalue problem (solid lines). The nomenclature labelling the acoustic-gravity wave modes is that of Press & Harkrider [1962]..... 55

Figure 10. Comparison of multi-mode and edge mode group velocity curves. These curves are appropriate for propagation 35° north of east in the atmosphere of Table I..... 57

Figure 11. Source function, $M(\mu)$, describing the time variation of the effective source for Lamb mode excitation by nuclear explosions. Here $\mu = t/T_Y$, where T_Y is a characteristic time for the explosion..... 59

Figure 12. Variation of the waveform factor $\psi(t)$ with the parameter T_Y/τ_D. Here ψ is normalized with respect to T_Y/τ_D and the time is plotted relative to τ_a in units of τ_D..... 62

Figure 13. Predicted ratios a_3/a_1 and a_2/a_1 of successive peak to trough amplitudes a_1, a_2, and a_3 in far-field edge mode waveforms produced by nuclear explosions..... 63

Figure 14. Observed and theoretical pressure waveforms at Berkeley, California, following the Housatonic detonation at Johnson Island on 1962, October 30. The observed waveform is taken from Donn and Shaw [1967]. The energy yield assumed in the theoretical computations was 10 MT. The maximum peak to trough amplitude of the experimental waveform is about 350 μbar..... 65

Figure 15. Comparison of observed and theoretical variation of maximum amplitude with distance from the source. The results of a series of Lamb mode syntheses are compared with observations reported by Wexler and Hass [1962] and with the results of waveform syntheses performed by Harkrider [1964] using a multi-mode formulation. (Harkrider's reported amplitudes are here corrected by the factor $p_o(z_o)/p_o(z_g)$ suggested by Pierce [1965], which in this case is about 0.76.)..... 68

ILLUSTRATIONS (cont'd)

Figure 16. Comparison of data with the theoretical relation between amplitude and period of infrasonic waveforms generated by nuclear explosions. The data points are lettered a to n corresponding to particular events defined in the text..... 75

Figure 17. Observed arrival time of an infrasonic wave. The source of the wave is the Soviet thermonuclear blast over Novaya Zemlya, October 30, 1961, at about 0830 GMT, and the recording instruments are barographs at weather stations or on ships. The dashed rectangle indicates the portion of the northern hemispheric map shown in Figs. 19-21. (Extracted from paper by Wexler and Hass [1962].)..... 76

Figure 18. Maximum observed amplitude of an infrasonic wave. This map is for the same disturbance as in Fig. 17, and is derived from the same records. The amplitude is given in mbars. (Extracted from paper by Wexler and Hass [1962].)..... 77

Figure 19. Sea level synoptic weather map for the Northern Pacific Ocean and North America. The portion of the northern hemispheric map indicated by the dashed box in Fig. 17 is shown here..... 79

Figure 20. 500 mbar synoptic weather map for the Northern Pacific Ocean and North America. The portion of the northern hemispheric map indicated by the dashed box in Fig. 17 is shown here..... 80

Figure 21. High and low ambient pressure centers. The high and low pressure centers shown in Fig. 20 are labeled and the direction of circulation about each noted. The location of the Soviet explosion of October 30, 1961, is indicated by a star..... 81

Figure 22. Computer generated plots of ray paths from a point source to the east in summer. (Extracted from paper by Donn and Rind [1971].)..... 85

Figure 23. Sketch of the effects of gravitationally induced dispersion on an originally N-shaped waveform. Successive plots correspond to later values of time. The parameter $ is equivalent to distance along a ray path..... 91

ILLUSTRATIONS (cont'd)

Figure 24. Sketch of the application of the equal area rule to construct shock locations from a multi valued waveform..... 92

Figure 25. Sketch of rays in the vicinity of a caustic (which forms the locus of points of intersection of adjacent rays). Here, for simplicity, the radius of curvature of the caustic is considered to be substantially less than that of the rays, although this is not always the case..... 98

Figure 26. Three simple pulse shapes and their Hilbert transforms. (Extracted from paper by Sachs and Silbiger [1971].)..... 101

Figure 27. Sketch of how nonlinear effects reduce a logarithmic singularity to a shock of finite amplitude. (a) Unmodified multivalued waveform, illustrating application of equal area rule. (b) Modified waveform with constructed shock..... 102

Figure 28. Sketch of the prediction of the theory outlined in the text in regards to the height of a rising fireball (or hot gaseous bubble) as a function of time..... 113

ACKNOWLEDGEMENTS

Appreciation is expressed for the long-term guidance, cooperation, assistance, and interest given by Mrs. E. F. Iliff of AFCRL. The authors would also like to thank B. L. Murphy of Mt. Auburn Research Associates, G. M. Daniels of Avco Everett Research Laboratory, and J. Reed of Sandia Laboratories for helpful discussions concerning the research reported here.

Chapter I

INTRODUCTION

1.1 SCOPE OF THE REPORT

The present report summarizes investigations carried out by the authors during the years 1970-1972 on the propagation of low frequency pressure disturbances under Air Force Contract No. F19628-70-C-0008 with the Air Force Cambridge Research Laboratories, Bedford, Massachusetts. The study performed was theoretical in nature.

The central topic of this study was the generation and propagation of infrasonic waves in the atmosphere. The principal emphasis was on waves from man made nuclear explosions although certain aspects of the study pertain to waves generated by natural phenomena including, in particular, severe weather.

Specific topics considered during the study include the following:

1.) The further development and application of a computer program INFRASONIC WAVEFORMS for the prediction of pressure signatures as would be detected at large horizontal distances following the detonation of a nuclear device in the atmosphere. The original version of this program was developed by two of the authors [Pierce and Posey, 1970] under a previous Air Force Contract (F19628-67-C-0217).

2.) The development of an alternative and considerably simpler theoretical model for waveform synthesis based on the hypothesis that dominant features of the early arriving low frequency part of the pressure wave are carried by the real atmosphere's counterpart of Lamb's edge mode.

3.) The development of a preliminary theoretical model applicable to the prediction of shorter period pressure disturbances at intermediate to moderate distances from lower yield (1 to 500 kT) nuclear explosions.

4.) The source mechanisms by which fireball rise and subsequent near field phenomena may excite acoustic-gravity waves.

5.) The preliminary development of a theoretical model for the generation of acoustic-gravity waves by severe weather.

6.) The effects of atmospheric turbulence on guided infrasound propagation.

Preceding page blank

During the course of the research reported here, the study of some of the above topics reached the point where a definable phase of the research was sufficiently complete that it was logical to summarize the results in a form appropriate for publication. Such results have been given in seven published papers, in one M.S. thesis and in one Ph.D. thesis. The abstracts of these are listed in Chapter II of the present report.

In subsequent chapters, a brief summary of the accomplishments under the contract are given. These include what the authors believe to be the principal highlights of the work already published under the contract plus a somewhat more detailed description of the work, some of which is only partially complete, not previously reported. In Chapter VII, some recommendations are made for future work in this field.

1.2 BACKGROUND OF THE REPORT

The general topics of infrasonic wave propagation, generation, and detection have been of considerable interest to a large segment of the scientific and defense communities for some time. A recently published bibliography (the existence of which allows us to omit extensive citations here) lists [Thomas, Pierce, Flinn, and Craine, 1971] over 600 titles, most of which are directly concerned with infrasound. Literature pertaining to the infrasonic detection of nuclear explosions constitutes a considerable portion of these. Earlier work by Rayleigh [1890], Lamb [1908,1910], G. I. Taylor [1929,1936], Pekeris [1939,1938] and Scorer [1950], among others, which was concerned with waves from the Krakatoa eruption [Symond, 1888] and from the great Siberian meteorite [Whipple, 1930] is also directly applicable to the understanding and interpretation of nuclear explosion waves.

The present report thus merely summarizes a continuation of a small number of facets of a lengthy pattern of research which has been carried on by a large number of investigators in the past. In a more restricted sense, the work reported here represents a continuation of work done in two previous studies performed under contract for Air Force Cambridge Research Laboratories. The first of these was Air Force Contract No. AF19(628)-3891 with Avco Corporation during 1964-1966; the second was Air Force Contract No. AF19628-67-C-0217 with the Massachusetts Institute of Technology during 1967-1969. Summaries of this earlier work may be found in the appropriate final reports by Pierce and Moo [1967] and by Pierce and Posey [1970].

One of the principal results of the two aforementioned previous contracts was a computer program INFRASONIC WAVEFORMS; the deck listing of the then current version of which is given in the report by Pierce and Posey [1970]. This program enables one to compute the pressure waveform

at a distant point following the detonation of a nuclear explosion in the atmosphere. The primary limitation on the program's applicability to realistic situations is that the atmosphere is assumed to be perfectly stratified. However, the temperature and wind profiles may be arbitrarily specified. The general theory underlying this program is somewhat similar to that developed by Harkrider [1964] but differs from his in that it incorporates background winds and in that it has a different source model for a nuclear explosion.

Chapter II

PAPERS AND THESES

2.1 CONTENTS OF PAPERS WRITTEN DURING THE CONTRACT

A. D. Pierce, J. W. Posey, and E. F. Iliff, Variation of Nuclear Explosion Generated Acoustic-Gravity Wave Forms with Burst Height and with Energy Yield, J. Geophys. Res. 76 , 5025-5042 (1971) .

A formulation of a method for synthesizing theoretical infrasonic far-field pressure wave forms generated by nuclear explosions is described which differs from that described by Harkrider in 1964 primarily in the method by which the source presence is incorporated. The rationale of the model is described and a number of predicted wave forms created by the detonation of nuclear explosions in temperature-stratified and wind-stratified atmospheres are presented to illustrate the effects of winds and the effect of the varying energy yield and of the height of burst. Theoretical wave forms are compared with a number of observed wave forms previously exhibited by Harkrider. Discrepancies are pointed out among the predictions of Scorer, of Weston, of Hunt, Palmer, and Penney, and of Harkrider as to the effects of height of burst. Our formulation predicts the early portion of wave forms received on the ground to be nearly proportional to yield and to increase slowly with height of burst up to a height of the order of 40 km (which depends on yield) and then to decrease rapidly with further increasing height. These predictions are explained in simpler terms if the early portion of the wave form is assumed to be carried in a single composite guided mode analogous to that predicted by Lamb for the isothermal atmosphere.

A. D. Pierce and J. W. Posey, Theory of the Excitation and Propagation of Lamb's Atmospheric Edge Mode from Nuclear Explosions, Geophys. J. R. astr. Soc. 26 , 341-368 (1971) .

A relatively simple theoretical model of near-surface pressure pulse propagation from nuclear explosions is developed from the hypothesis that the early portion of the pulse travels in the real atmosphere's counterpart of Lamb's edge mode. Various concepts of geometrical acoustics are used in the construction of the model. The pulse travels along horizontal ray paths which may be refracted by horizontal variations in the height-averaged effective sound speed and wind velocity. The dispersion of the pulse as it propagates along such paths is governed by a one-dimensional wave equation similar to that derived by Korteweg and de Vries in 1895. Coefficients are found by comparison with the dispersion relation derived by

Garrett in 1969 as an expansion in terms of a parameter ϵ describing deviations of the atmospheric profile from isothermal. The method of incorporation of terms governing accumulative far-field non-linear effects is indicated. Height variations in propagating variables are approximated to zeroth order in ϵ. Variations along horizontal ray paths are governed by the principle of conservation of modal wave action. The excitation of the edge mode is found by matching the general form of the far-field quasi-geometrical solution to the near-field solution for a point energy source in an isothermal atmosphere. Explicit expressions are given for the far-field pressure disturbance. Computations agree favourably with those based on a multimode theory for the first few cycles of the waveform. The edge mode theory leads to a number of implications, which may be compared with existing data. These include the prediction that the energy of the explosion yield may be estimated from a knowledge of the first peak-to-peak period and first peak-to-trough pressure amplitude in far-field records with very little information concerning atmospheric structure, and the prediction that anomalous azimuthal variations in waveform amplitudes may be caused by focusing or defocusing of horizontal ray paths for the edge mode.

J. E. Thomas, A. D. Pierce, E. A. Flinn, and L. B. Craine, Bibliography on Infrasonic Waves, Geophys. J. R. Astr. Soc. 26, 399-426 (1971).

This bibliography is current through 1970 and is composed of references related to the generation, propagation, and detection of sound radiation at ground level and ionospheric heights. The frequency range of the pressure signals considered here encompasses those normally associated with acoustics, infrasonic, acoustic-gravity and gravity waves.

C. A. Moo and A. D. Pierce, Generation of Anomalous Ionospheric Oscillations by Thunderstorms, in Effects of Atmospheric Acoustic Gravity Waves on Electromagnetic Propagation, AGARD Conference Proceedings No. 115 (Harford House, London, 1972) pp. 17-1 to 17-6.

Recent experimental evidence, based on radio HF Doppler sounding of the ionosphere, shows oscillations of the upper atmosphere during periods of thunderstorm activity. These oscillations have periods in the range of 2 min to 5 min, frequently for many hours duration. The coherence of the oscillations is consistant with the interpretation generally given that they are caused by the passage of long wavelength infrasonic waves. There are apparently no similar distinct oscillations with the same period range associated with air motion in the troposphere during severe weather. However, convective activity is known to generate fluctuations and internal

waves with periods near and above Brunt-Vaisala periods. The present paper proposes a theory for the generation of these ionospheric 2-5 min period waves, based on concepts similar to those used by Lighthill in the theory of aerodynamic sound. That the periods of the ionospheric oscillations are substantially lower than tropospheric Brunt-Väisälä periods is explained as being due to the fact that the predominant radiated frequencies are obtained as a summation, via non-linear processes, of the frequencies of the interacting velocity fields generated by the weather system. These radiated frequencies are not necessarily observed in the near field.

A. D. Pierce, A Model for Acoustic-Gravity Wave Excitation by Buoyantly Rising and Oscillating Air Masses, in Effects of Atmospheric Acoustic Gravity Waves on Electromagnetic Wave Propagation, AGARD Conference Proceedings No. 115 (Harford House, London, 1972), pp. 4-6 to 4-10.

A somewhat general mathematical model is developed for the study of the excitation of acoustic-gravity waves by rising and oscillating air masses. Sources are initially described by distributions of fluid dynamic quantities over a moving closed surface. Analysis then indicates that insofar as wave generation is concerned, such surface distributions are equivalent to concentrated point sources at the center of the volume. The resulting linearized inhomogeneous wave equations are derived and solved in terms of Green's functions. The case of an isothermal atmosphere is discussed in some detail.

J. W. Posey and A. D. Pierce, Explosive Excitation of Lamb's Atmospheric Edge Mode, in Effects of Atmospheric Acoustic Gravity Waves on Electromagnetic Wave Propagation, AGARD Conference Proceedings No. 115 (Harford House, London, 1972), pp. 12-1 to 12-8.

It has been previously demonstrated that far-field ground-level pressure observations of explosively generated acoustic-gravity waves are often dominated by the Lamb atmospheric edge mode for the first cycle or two. In this paper, particular attention is given to the excitation of this mode by a blast wave from a large atmospheric explosion. It is found that the strength of the excitation is strongly dependent upon the tail of the blast wave. However, information on the precise form of the blast wave tail is unavailable, so that any analytical representation must be somewhat arbitrary.

A theoretical development shows that, for the pure Lamb mode, a simple analytical relation exists between the energy of the source and the initial amplitude and period of the far-field pressure waveform. This relation is compared with some empirical data and appears to be in fair agreement with yield estimates based on seismic observations.

J. W. Posey and A. D. Pierce, Estimation of Nuclear Explosion Energies from Microbarograph Records, Nature 232 , 253 (1971)

A theoretical relation derived from the edge mode theory developed by the authors is compared with microbarograms published by Donn and Shaw and by Harkrider. Energy yields are taken as estimated by Båth. The comparison of theory and data indicates the energy yield may be estimated from a knowledge of the first peak to peak amplitude and from the period between the first two successive positive peaks.

2.2 CONTENTS OF THESES WRITTEN DURING THE CONTRACT

J. W. Posey, Application of Lamb Edge Mode Theory in the Analysis of Explosively Generated Infrasound, Ph.D. thesis, Department of Mechanical Engineering, Massachusetts Institute of Technology, August 1971 .

The propagation theory for Lamb's atmospheric edge mode of acoustic-gravity waves is presented. The excitation of this mode by large atmospheric explosions is investigated and observations of explosively generated infrasound obtained from the literature are examined for the presence of the edge mode. The theory utilizes Bretherton's and Garrett's previous results for the phase velocity and dispersion of this mode and incorporates various techniques from geometrical acoustics and guided wave theory. The result is a two dimensional model for transient pulse propagation over the surface of a curved earth through an atmosphere which is not necessarily perfectly stratified. It is found that the excitation of acoustic-gravity waves by the blast wave from a nuclear explosion is primarily governed by the tail of the blast wave. The analytical approximation introduced by Glasstone is selected to represent the pulse primarily because of its mathematical simplicity, although its limitations are discussed in some detail. The form of the far field edge mode pressure waveform is examined, and the effects of some possible variations in parameters of the medium and of the source are investigated. An approximate relation giving the source yield Y_{KT} (in equivalent kilotons of TNT) in terms of the first peak-to-trough amplitude p_{FPT}, and the time between the first two peaks $T_{1,2}$, of the ground level Lamb mode pressure waveform is

$$Y_{KT} = 0.034 \sin^{1/2}(R/r_e)\, T_{1,2}^{3/2} p_{FPT}$$

which is derived for bursts in the troposphere . Here p_{FPT} is in μbars

and $T_{1,2}$ in sec. Comparison of the theory with experiment suggests that the first cycle or two in each of the relevant empirical microbarograms, although not necessarily the part of the record with the largest amplitude, is often dominated by the Lamb mode.

L. Tang, Propagation of Guided Acoustic Gravity Waves in a Turbulent Atmosphere, M.S. thesis, Department of Mechanical Engineering, Massachusetts Institue of Technology, June, 1971.

The effects of atmospheric turbulence on the propagation of Lamb mode acoustic gravity waves are studied. A general variational principle for acoustic gravity waves is first derived and then used to obtain the set of approximate partial differential equations for the propagation of guided Lamb mode waves in an inhomogenous atmosphere. This set of equations is then solved for the scattering of waves by turbulence using the Born approximation. A stochastic integral is subsequently derived to describe the random behavior of the scattered wave. With the assumption that the correlation function of temperature fluctuations obeys the Kolmogorov two-thirds law, the effective cross sectional length of scattering is obtained.

Chapter III

THE MODAL SYNTHESIS OF INFRASONIC WAVEFORMS

3.1 STATUS OF INFRASONIC WAVEFORMS

INFRASONIC WAVEFORMS is a digital computer program, the first version of which was written by Pierce and Posey [1970] under Air Force Contract AF19628-67-C-0217. The nature of the program is such that it produces, among other quantities, a synthesized plot of pressure versus time (Fig. 1) which would correspond to the infrasonic waveform signature expected at a given far field point in the atmosphere following the detonation of a nuclear device in the atmosphere. Input presupposes the atmosphere to be approximated by a sequence of horizontal layers of constant temperature and wind velocity.

In the time following its original writing, INFRASONIC WAVEFORMS has been adapted for use at a number of research laboratories. These include the following:

1. Air Force Cambridge Research Laboratories (Mrs. E. F. Iliff)
2. National Oceans and Atmospheres Administration (Dr. J. M. Young)
3. Lamont-Doherty Geological Observatory of Columbia University (Dr. W. L. Donn and Dr. N. K. Balachandran)
4. University of Idaho (Dr. J. E. Thomas)
5. Avco Everett Research Laboratory (Mr. G. M. Daniels)

The various versions of the program in operation at these laboratories differ primarily in the manner in which the computer interfaces with the plotter for the plotting of waveforms.

In the present section, we describe some minor modifications which have been made to the program during the past three years. We also give some additional guidelines to the program's use.

3.1.1 Earth Curvature Effects

In the deck listing of the subroutine TMPT which is given on pages 287-290 of the report by Pierce and Posey [1970], we have made one minor

Preceding page blank

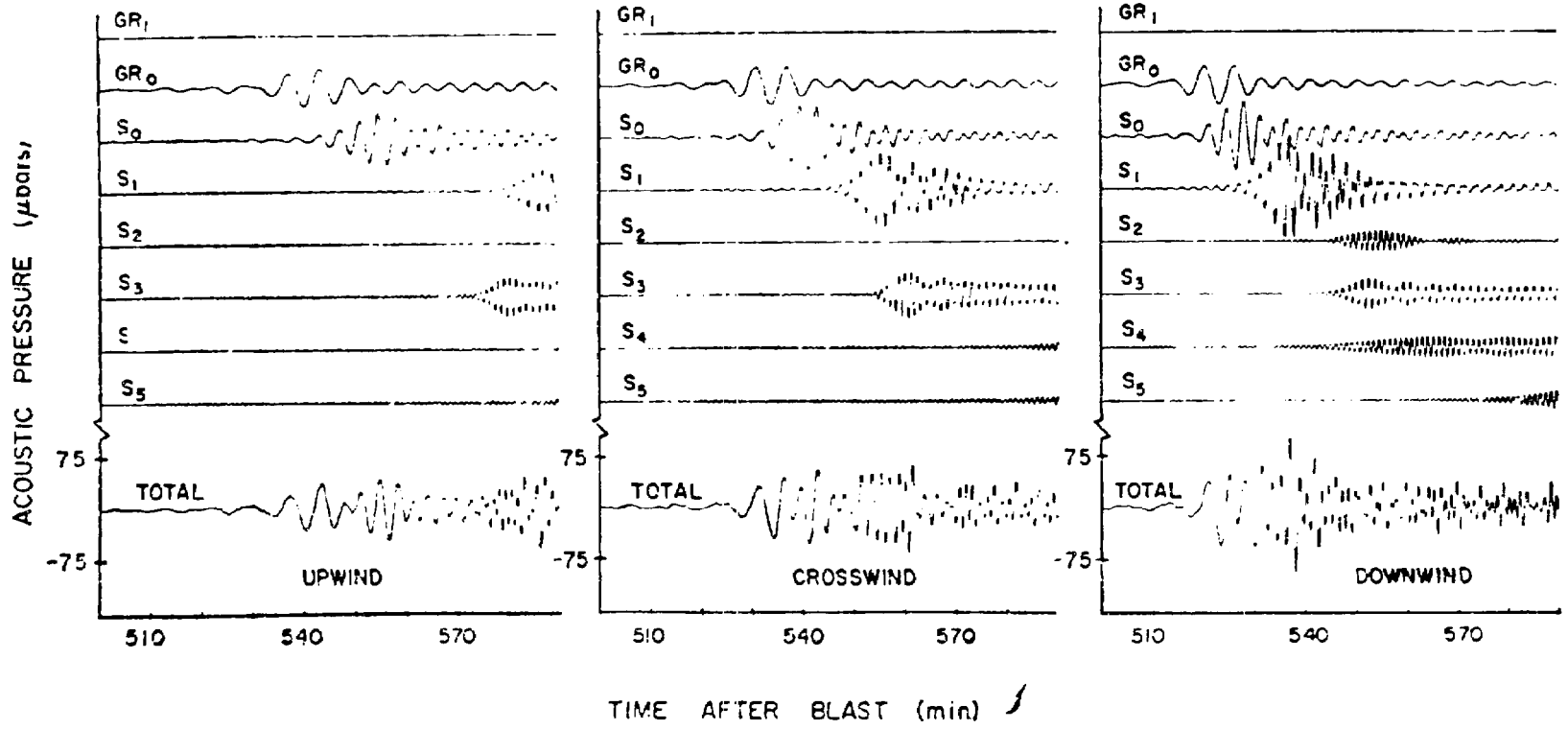

Figure 1. Comparison of nuclear-explosion generated acoustic-gravity waves upwind, crosswind, and downwind from the source. In each case, the observer is 10,000 km from the source in a subtropical summer atmosphere. The contributing modes, as well as their sum, are shown for each direction.

change to take into account the curvature of the earth. On page 288 following the statement NOFN = KFIN(N) which follows FORTRAN statement 11 we have added the following cards

```
C
C DETERMINE THE EARTH CURVATURE CORRECTION TIMES ROBS**(-0.5)
      RAD = ROBS / 6374.
      CF = ( 1. / ( 6374. * SIN(RAD) ) )**0.5
C
```

The program then resumes with the COMMENT card "THE MODE N RESPONSE IS FOUND...". Then FORTRAN statement 51 is changed to read

```
   51 TNINT(N,IT) = CF * TNINT(N,IT)
```

such that the factor (ROBS)**(-0.5) in the previous version is replaced by CF.

The change just described thus replaces the amplitude factor $(1/r)^{1/2}$ appropriate to cylindrical spreading by a factor $[r_e \sin(r/r_e)]^{-1/2}$ appropriate to circular spreading of waves over a surface of a sphere of radius r_e. Here r_e = 6374 km is the radius of the earth and r is the great circle distance of the observation point from the source. The theory underlying the incorporation of this earth curvature correction has been described previously by Weston [1961] and by Harkrider [1964], among others. One may note that the correction is minor if $r \ll r_e$. It corrects the amplitude upwards by about 7% at a distance of 5600 km. At the antipode where $r = \pi r_e$ the theory underlying the approximation breaks down and we have not yet modified the program to take this case into account.

The program, however, with relatively minor changes can still be used to estimate pressure waveforms of waves which have traveled over half way around the globe, i.e. past the antipode, providing the wave has traveled at least, say, 1000 km past the antipode. Following the theoretical development of Brune, Nafe, and Alsop [1961], one finds that the appropriate modifications needed are (1) to replace $\sin(r/r_e)$ by its absolute magnitude: (2) to shift the Fourier transforms of each modal waveform by a phase of $\pi/2$ radians; and (3) to reinterpret r (ROBS in the program) as the total distance the wave has traveled (which in this case would be between πr_e and $2\pi r_e$). These modifications can be accomplished by replacing the above definition of CF in subroutine TMPT by

```
      CF = ( 1. / ( 6374. * ABS(SIN(RAD ))))**0.5
```

Then, also in the deck listing of TMPT, between lines TMPT 149 and TMPT 150

as given on page 289 of the report by Pierce and Posey [1970], one should insert a card

```
PH2 = PH2 + 1.570796
```

An identical card should also be inserted between lines TMPT 166 and TMPT 167. The input value of ROBS should also be selected to correspond to the longer propagation path.

One should note that, in regard to the above suggested modifications for antipodal arrivals, the underlying theoretical basis presumes the atmosphere to be cylindrically symmetric about an axis passing through the point of detonation. Since this is a rather stringent idealization, considerable caution should be used in the interpretation of the results of the computations.

3.1.2 Other Modifications in the Program

Also, in regards to subroutine TMPT, a minor change in the FORMAT statement 104 was to change the FORMAT specification F12.2 to F12.4 to allow more significant figures to be printed in the output tabulation of TNINT (JOPT,IT).

One minor error in the deck listing of the subroutine NXTPNT was pointed out to the authors by T. H. Kuckertz of the University of Idaho. In FORTRAN statement 26 of this subroutine, the number -5 should have been punched +5. As best we can tell, this error will never affect the output of the program since, for any conceivable atmosphere model, IDR can never be 5 at a point when statement 26 is reached.

In subroutine SOURCE, the present version at M.I.T. has set TAS = 0.33 instead of 0.48 as was done in the original listing. The revised source model theory described here in Sec. 3.2 and by Pierce, Posey, and Iliff [1971] suggests that this should be the appropriate choice if the source is sufficiently high that there is no appreciable nonlinear interaction between the incident shock and the ground reflected shock.

If the explosion is relatively close to the ground, the subroutine SOURCE should be modified following a suggestion made to the authors by J. Reed. In accordance with the theory outlined in the next section, one should replace the statement computing the quantity PAS in the subroutine by

```
PAS = ((21.4E+3)/1.0)*(1.61)
```

and the statement defining TAS by

```
TAS = 0.416
```

Just when a given explosion should be classified as near ground or above ground depends primarily on the ratio of the height of burst h to the explosion characteristic length $(E/p_o)^{1/3}$ where E is the energy yield and p_o is the atmospheric pressure. If the ratio is greater than, say 5, the above ground source model would appear to be more appropriate. If it is less than 1, the near ground source model would appear appropriate. For intermediate ranges of altitude, just which choice is better remains a topic of investigation. (Dr. B. L. Murphy and his colleagues at Mt. Auburn Research Associates are currently developing an improved source model which takes the nonlinear interaction between incident and reflected shocks into account.)

We would suggest for the present that one take

$$z_o < 500\ (Y_{KT})^{1/3} \text{ft}$$

as defining a surface burst, where Y_{KT} is the yield in KT.

3.1.3 Further Suggestions for Program Users

In the usage of the program by ourselves and by our colleagues in other laboratories we have become aware of a number of possible pitfalls in its use. In order to increase the effectiveness of future use of the program it would seem appropriate to mention these here. The present discussion amends that of Chapter III in the previous report by Pierce and Posey [1970].

While, apriori, one should not expect the temperature in the uppermost layer (a halfspace in the theory) to affect waveforms observed near the ground, the actual computations may indicate otherwise. This would appear to be due to the neglect of leaking modes in the theoretical formulation. Any mode or portion of a mode which leaks energy into the upper halfspace is associated with a complex wavenumber and appears formally to be damped with propagation in the horizontal direction. The possible values of phase velocity v_p and angular frequency ω which could in principle correspond to a nonleaking mode is limited primarily by the choice of temperature in the uppermost halfspace. The forbidden regions where all conceivable modes must be leaky correspond to values of ω and v_p for which the normal mode dispersion function does not exist. Such domains in the ω vs v_p plane correspond to the regions containing X's in computer generated plots, of normal mode dispersion waves such as shown in Figs. 3.3 and 3.4 of the previous report by Pierce and Posey. Interestingly, if one takes the atmosphere to be of some very large but finite height h terminated by either a rigid surface or a free surface, the modes are all non leaky (there's nowhere to leak) and the dispersion curves and height

profiles for modes which propagate primarily in the lower atmosphere are nearly the same in both cases. If, however, one terminates the atmosphere by an isothermal halfspace extending above h, certain portions of the lower atmosphere modes will become leaky. Since the computer program discards such modes, regardless of how small the leakage may actually be, it is difficult to say whether more nearly correct results will be obtained with the unbounded atmosphere model than with one terminated above by either a free surface or a half space.

A specific suggestion for circumventing this problem without actually revising the computational procedure to include leaky modes is that one always choose the temperature of the upper halfspace to be sufficiently high that $\omega_B = (\gamma-1)^{1/2}g/c$ for the upper halfspace is smaller than any frequency one suspects should be dominant in the synthesized waveform. Also, one should want the sound speed in the upper half space to exceed the horizontal phase velocity of any wavelet which contributes substantially to the overall waveform. We suggest that one check his output after the computation to see if his choice of a model atmosphere satisfies these criteria. If not, he should either revise his model to accomplish this, subject to whatever constraints one imposes on the relation of the model to reality, or else he should be very careful in the interpretation of his computational results.

Other problems which arise in the use of the program are associated with the truncation of the integration over frequency in the synthesis of individual modal waveforms. When one chooses his input parameters OM1, OM2, V1, and V2, he implicitly limits the frequency range for the Fourier inversions to an interval contained between OM1 and OM2 radians. The interval is also limited by the fact that the dispersion curve for the non-leaking portion of any given mode may not exist for all frequencies between OM1 and OM2 and also by the fact that its phase velocities may not fall between V1 and V2 km/sec. Thus the integration represents an approximation and one should make some assessment as to whether the app oximation has any validity.

One possible simple means of checking whether the truncation approximation is applicable is to examine the range of group velocities printed out by the program for the individual modes. Suppose the group velocities vary in magnitude between $v_{g,min}$ and $v_{g,max}$ for an individual mode. Then one would expect the contribution from that mode to be of significant magnitude at best only for times between $r/v_{g,max}$ and $r/v_{g,min}$ with a possible extension of perhaps one or two cycles on either side of this interval. If this is not the case, then the approximation is probably insufficient. If one suspects it to be insufficient, then he should next check to see if the mode in question gives a substantial contribution to the overall waveform for the time interval of interest. If it doesn't, then one probably need not worry about the error introduced by truncation in as far as

that mode's contribution is concerned. If it does, then one should alter his input parameters to improve the situation either by extending the range of frequencies and phase velocities considered or else by changing the assumed form of the upper atmosphere to make the mode not taking over a wider frequency interval.

Anyone who has attempted to use the program to synthesize waveforms at relatively close in distances may have noted that the individual modal waveforms may not be causal, i.e., the program may formally predict a disturbance before the time of detonation, which, of course, is meaningless. In principle, the superposition of all the modes should result in a causal waveform, but there is no apriori reason in the mathematical theory why any given individual waveform should so be. At larger distances, this lack of modal causality is not a significant factor since the noncausal portions of the synthesized waveform tend to be of negligible amplitude compared to the portions which arrive at times corresponding to the group velocity.

Another question one should consider is whether one has incorporated enough modes in his synthesis. If one is seeking to describe the disturbance in a given time interval at range r then he probably need only consider those modes and frequency intervals which correspond to group velocities r/t where t falls within the desired time interval. In general, modal contributions tend to decrease with increasing mode number, so if, for example, one has convinced himself that contributions from the S_4, S_5, S_6 modes are all negligible, then the same should be true for the S_7, S_8, etc.

3.2 SOURCE MODELS

The source model for INFRASONIC MODES has been somewhat modified since the writing of the report by Pierce and Posey [1970]. Here we outline the revised theory for the present source model. The first part of the discussion follows that outlined in the paper by Pierce, Posey and Iliff [1971].

3.2.1 Above Ground Explosions

The basic mathematical model is the linearized equations of hydrodynamics for a temperature-stratified and wind-stratified compressible atmosphere. The geometry is sketched in Fig.2. The presence of the source is assumed to be taken into account by the addition of a source term to that equation corresponding to energy conservation. Thus, the governing equations for acoustic pressure deviation p from ambient pressure p_c, acoustic density deviation ρ, and fluid velocity deviation $\vec{u}$, are taken as

$$\rho_o[D_t\vec{u} + (\vec{u}\cdot\nabla)\vec{v}] = -\nabla p - g\rho\vec{e}_{up} \qquad (3.1a)$$

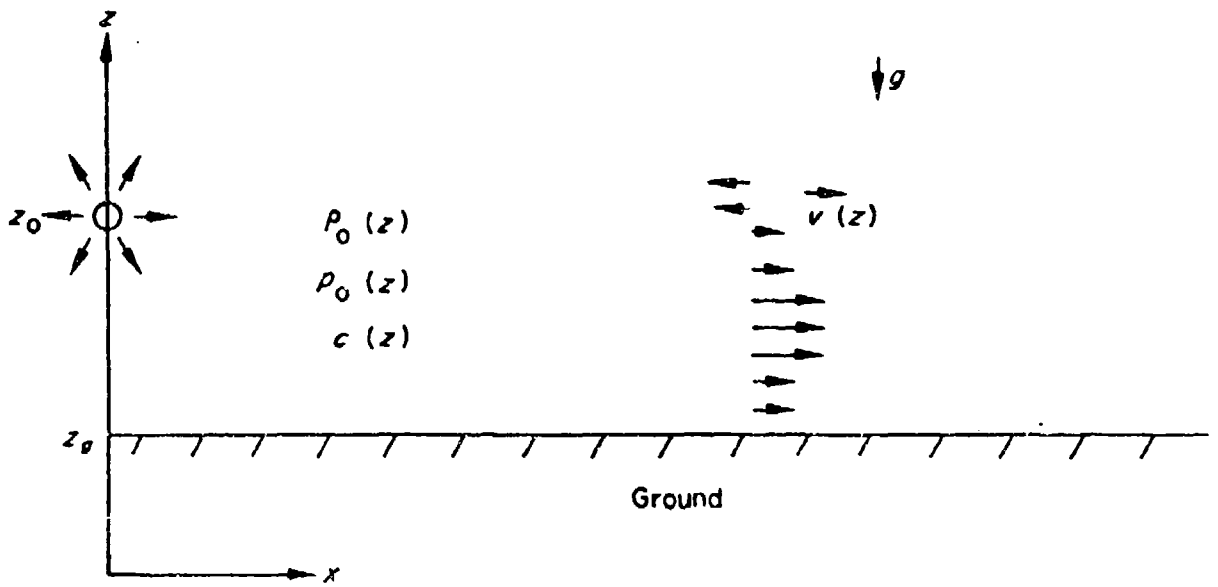

Figure 2. Sketch illustrating the various idealizations incorporated in the mathematical formulation of the problem of acoustic-gravity wave propagation from a nuclear blast.

$$D_t \rho + \nabla \cdot (\rho_o \vec{u}) = 0 \qquad (3.1b)$$

$$[D_t p + \vec{u} \cdot \nabla p_o] - c^2 [D_t \rho + \vec{u} \cdot \nabla p_o]$$

$$= 4\pi c^2 f_E(t)\ \delta(\vec{r} - \vec{r}_o) \qquad (3.1c)$$

where

$$D_t = (\partial/\partial t) + \vec{v} \cdot \nabla$$

is the time derivative corresponding to an observer moving with the ambient wind velocity $\vec{v}$. The quantity $\vec{e}_{up}$ is the unit vector in the vertical direction, while $\vec{r}_o$ denotes the source location; $c = [\gamma p_o/\rho_o]^{1/2}$ is the speed of sound. The source term (and, in particular, the form of the function $f_E(t)$ on the right-hand side of Eq. (3.1c)) is chosen with the objective of insuring that, at larger distances, the solution of Eqs. (3.1a, b, c) should agree with what might be expected if the nonlinear terms were retained and a more realistic source model were used.

To explain our choice for the energy source function $f_E(t)$, the basic nonlinear hydrodynamic model for a nuclear explosion [Taylor, 1950; Brode, 1955, 1968] is reviewed, which consists of an initially isothermal sphere of very small radius in an unbounded isothermal atmosphere with negligible gravity. The initial sphere has ambient density and fluid velocity, but is assumed to have very high temperature and pressure. The total initial potential energy (the specific heat of air is assumed independent of temperature) inside the sphere is assumed to be some fixed fraction of the total energy Y_{KT} (in kilotons of TNT, where 1 KT = 4.2×10^{19} ergs) released by the explosion. According to The Effects of Nuclear Weapons (ENW) [Glasstone, 1957, 1962], this initial potential energy (which should be the same as the total hydrodynamic energy) is roughly one-half of Y_{KT}. We assume this proportionality factor does not vary with yield or with height of burst. It would appear from comments in sections 2.119, 7.25, and from Figure 1.22 in ENW[Glasstone, 1962] that this is a good approximation for bursts below 100,000 feet (30 km) and a fair approximation at altitudes up to 350,000 feet (100 km), although no quantitative description of the variation of this fraction is given. (In any event, the results of this study will not be invalidated by such a variation, provided energy yield is always interpreted as twice the hydrodynamic energy of the explosion.)

The pressure wave form in this idealized basic nonlinear model corresponds

to hydrodynamic scaling, i.e., at distance R,

$$p = p_o F(R/cT_Y,\ t/T_Y) \tag{3.2}$$

where F is a universal function of two dimensionless quantities and where T_Y is a characteristic time that may be defined as any convenient constant times $(Y_{KT}/p_o)^{1/3}/c$. We choose T_Y to be defined such that, when p_o and c correspond to a standard reference pressure (p_{ref} = 1 atm) and sound speed (c_{ref} = 331 m/sec) and when Y_{KT} is 1 KT, then T_Y is equal to the time duration t_{ref} of the blast wave at a distance R_{ref} (which we take as 1 mile) from a 1-KT explosion. (As explained later, the appropriate numerical choice of t_{ref} would appear to be 0.33 sec.) Thus,

$$T_Y = (p_{ref}/p_o)^{1/3}(c_{ref}/c)Y_{KT}^{1/3}t_{ref} \tag{3.3}$$

(where, to maintain dimensional purity, Y_{KT} is here interpreted as the ratio of the explosion's energy to a reference energy of 4.2×10^{19} ergs).

Since, in the homogeneous atmosphere case currently being considered, the amplitude of F may be expected to fall off nearly inversely with R (spherical spreading in linear acoustics), Eq. (3.2) should be rewritten in the form

$$p = (\Delta p)_{ref}(p_o/p_{ref})[cT_Y/(c_{ref}t_{ref})](R_{ref}/R)$$

$$\times \psi([t - R/c]/T_Y, R/(cT_Y)) \tag{3.4}$$

where, at large distances R, ψ should be a relatively slowly varying function of its second argument. Here $(\Delta p)_{ref}$ is the shock overpressure at the reference distance R_{ref} (1 mile) from a 1-KT air burst in a standard reference atmosphere. $(\Delta p)_{ref}$ is taken to be 34 mbar; the function ψ is dimensionless and is normalized such that it has a value of unity immediately behind the shock.

With reference to the nonlinear model described above, a suitable choice for $f_E(t)$ would appear to be that function which would lead to a solution of Eqs. (3.1a, b, c) which agrees with Eq. (3.4) at moderate distances from the source when gravity is neglected and when the atmosphere is assumed to be homogeneous. The ambient atmosphere for this matching process is taken as that characteristic of the burst location. The distance selected for the matching is $\{cT_Y/[c_{ref}t_{ref}]\}$ (i.e., the scaled counterpart of 1 mile from 1 KT in the reference atmosphere), such that cT_Y/R is identically equal to $c_{ref}t_{ref}/R_{ref}$.

Since the linearized equations, with the neglect of gravity and inhomogeneities, give

$$p = R^{-1}f_E'(t - R/c) \tag{3.5}$$

the matching of the two solutions under the circumstances described above gives

$$f_E(t) = B_o p_o c T_Y^2 Q(t/T_Y) \tag{3.6}$$

where the dimensionless constant B_o is given by

$$B_o = [(\Delta p)_s/p_{ref}]\{R_{ref}/[c_{ref}t_{ref}]\} \tag{3.7}$$

(Its value for the choice of numerical values described previously is 0.40.) The function $Q(t/T_Y)$ is simply the integral of ψ, i.e.,

$$Q(\xi) = \int_{-\infty}^{\xi} \psi(\xi, A_o)\, d\xi \tag{3.8}$$

where the integration constant is such that $f_E(t)$ vanishes at sufficiently early times. The quantity A_o is just $[R_{ref}/c_{ref}t_{ref}]$ (which turns out to have a numerical value of 14).

The apparent arbitrariness in the selection of the distance R_{ref} is largely immaterial insofar as the prediction of the far-field wave form is concerned. It turns out that the low-frequency pulse predicted at large

distances (as well might be expected for any low-frequency pulse) is largely governed by the first few terms in the power series expansion in angular frequency ω of the Fourier transform (over time) of $f_E(t)$. Thus, a key parameter (which may be considered as proportional to the zeroth order term in this expansion) would be

$$4\pi \int_{-\infty}^{\infty} f_E(t)\, dt = (\gamma - 1)(K/c^2)E \qquad (3.9)$$

where $E = 4.2 \times 10^{19} Y_{KT}$ ergs is the total energy released by the explosion and where K is a dimensionless constant given by

$$K = 4\pi(\gamma - 1)^{-1}(\Delta p)_{ref} R_{ref} (t_{ref} c_{ref})^2$$

$$\times \int_{-\infty}^{\infty} Q(\xi)\, d\xi / (4.2 \times 10^{19} \text{ ergs}) \qquad (3.10)$$

It is assumed here that $f_E(t)$ is integrable, and, in particular, that it vanishes as $t \to \infty$. This would seem to be a necessary requirement since (at least in the acoustic limit implied by Eq. (3.5)) the particle displacement is proportional to f_E/R. If $f_E(t)$ were to approach a non-zero limit as $t \to \infty$, this would tend to imply that the net amount of work done in expanding or compressing the gas behind the shock diverges (rather than approaches a limit) as the shock radius increases without limit, which in turn implies that the energy associated with the source is unlimited.

The actual near-field blast form can be inferred from Brode's [1955] calculations with the hydrodynamic energy (which Brode denotes as E_{tot}) interpreted as one-half the total energy released by the explosion. Brode's calculations show the blast beginning with a shock whose overpressure decreases faster than $1/R$, followed by a positive phase whose duration is nearly constant with R and equal to $1.22\,(E_{tot}/p_o)^{1/3}/c$. Although very little information can be inferred from Brode's paper concerning the wave form after the negative phase, it seems (from extrapolation of the calculated wave form) that there is a very small oscillation whose period is roughly of the order of twice the negative phase and whose amplitude decreases fairly rapidly. The energy feeding this oscillation is the energy dissipated at the start of the positive phase. On this basis, one can argue that the value of the constant K, as computed from Eq. (3.10) should be independent of the choice of R_{ref}, providing that $(\Delta p)_{ref}$, t_{ref}, and $Q(\xi)$ correspond

to whatever choice is made. The rationale of this conclusion is that the internal energy relative to ambient is $p/(\gamma - 1)$ per unit volume; if p is taken as given by Eq.(3.4), and if R/cT_γ in the second argument of ψ is approximated by $R_{ref}/(cT_\gamma)$, and if the total internal energy (a spatial integral) is evaluated at the instant the shock radius is the scaled counterpart of R_{ref}, one finds, after an integration by parts, that this energy at large t approaches $(K)(E)$ where K is defined in Eq. (3.10). The fact that the major contribution to the integral comes at larger R justifies one setting $R = R_{ref}$ in the second argument of ψ .

Since we would expect this limit to exist (even the dissipated energy must eventually be transformed into internal energy) we must conclude that K is independent of R_{ref} at sufficiently large R_{ref}. Another conclusion which seems warranted is that K should not exceed one-half since the increase in internal energy cannot exceed the total hydrodynamic energy released by the explosion.

Concerning the choices of R_{ref}, t_{ref}, ψ, $(\Delta p)_{ref}$, we take R_{ref} = 1 mile, since this seems amply large for a 1-KT explosion, the overpressure being of the order of 3% ambient at this distance. The actual value of $(\Delta p)_{ref}$ can then be determined from Brode's calculations to be 34 mbar. The same number can also be inferred from Figure 3.946 in the 1957 edition of ENW [Glasstone, 1957]. (The figure gives the overpressure at the ground at a distance of 1 mile from a 1-KT air burst as 1.00 psi. Since nonlinear effects are small at this distance, we expect the overpressure, if the presence of the ground were neglected, to be one-half of this or 0.50 psi = 34 mbar.) The choice of t_{ref} as inferred from Brode's results (with an extrapolation based on the theory of weak spherically diverging shocks [Bethe and Fuchs, 1947; Landau, 1945; Whitham, 1950]) is found to be 0.33 sec. On the other hand, Figure 3.96 in the 1957 edition of ENW, with an appropriate extrapolation, gives t_{ref} = 0.48 sec. Since the latter is not documented and hardly constitutes an adequately reported piece of research, we prefer to adopt the number based on Brode's computations of t_{ref} = 0.33 sec. In addition, as discussed below, energy considerations would tend to suggest that the ENW figure is inappropriate.

With regard to the functional form of ψ , it would appear adequate to use a fairly simple analytic approximation, represented by the function [Glasstone, 1962]

$$\psi(\xi, A_o) = (1 - \xi)e^{-\xi}U(\xi) \qquad (3.11)$$

when $U(\xi)$ is the Heaviside step function and ξ is measured from the onset

of the shock. While this function has the disadvantages of giving more 'sag' to the positive phase decay than implied by Brode's fit as represented by his equations 22 and 23 and of having a negative phase of unlimited duration, it does have the desired features of leading to an $f_E(t)$, which vanishes at sufficiently large t, and of giving a finite value to K in Eq. (3.10), although it is not clear to what extent its predicted integral over Q, which turns out to be 1, would agree with that for the true wave form. Considering the fact that the integral simply denotes the center of gravity of the wave form $\psi(\xi, A_Q)$ with respect to the start of the blast wave, one would doubt that this center of gravity would fall too far from the location of the end of the positive phase (which is at $\xi = 1$). One ancillary reason for adopting Eq. (3.11) is that the same function has been used previously by Harkrider, and we wish to compare our results with his.

With ψ given by Eq. (3.11), the source function becomes

$$f_E(t) = (4\pi)^{-1}(\gamma - 1)(K)(E/c^2) \cdot (t/T_\gamma^2)e^{-t/T_\gamma}U(t) \qquad (3.12)$$

where (with $t_{ref} = 0.33$ sec) the value of K in Eq. (3.10) is taken as 0.50. In contrast, if we used $t_{ref} = 0.48$ sec, we would have found $K = 1.1$. Since, as pointed out previously, there are strong theoretical grounds for supposing K to be less than one-half, the choice of $t_{ref} = 0.33$ sec based on Brode's calculations appears preferable. The time origin in Eq. (3.12) was chosen so that the shock would arrive at the matching distance at a time equal to this distance divided by the ambient sound speed. While this does not necessarily coincide with the time of detonation (due to finite amplitude effects), the choice of origin is immaterial insofar as the amplitude and relative shape of the received wave form are concerned.

A shortcoming of the source model described above is its neglect of gravitational effects and of sound speed and density gradients during the early history of the blast. Apart from the desire for a relatively simple model, the justification for this neglect is that the influence of these effects accumulates at a relatively slow rate and does not become appreciable until relatively late during the history of the formation of the blast wave. Since we are interested primarily in the earliest portion (say, the first 15 to 30 minutes) of the pressure pulse which propagates through the lower atmosphere (which is frequently all that is detected by ground-level microbarographs), we may view the early portion of the blast wave (including the first positive and negative phases) as the source of the pulse.

It would appear that waves generated by fireball rise due to buoyancy may be excluded on the basis that they would arrive too late.

From the discussion accompanying Eq. (3.9), it would also appear that, insofar as the low-frequency far-field pulse is concerned, the only critical assumptions are (i) that the energy radiated by the near-field blast be radiated isotropically and (ii) that the total additional internal energy in the atmosphere caused by the explosion be of the order of one-half the total energy yield. It would appear that these assumptions would be valid provided the formation of the positive phase (which spreads isotropically and which includes the bulk of the hydrodynamic energy at very early times) should not be altered significantly (in terms of energy content) by gravity and inhomogeneities. A possible quantitative criterion is that the time for the positive phase to form (which may be taken as being of the order T_Y) be less than one-fourth (since the positive phase resembles one-fourth of a full cycle of a sine wave) of the characteristic period for acoustic-gravity waves in the atmosphere. This period [Väisälä, 1925; Brunt, 1927] is generally greater than 5 minutes. Thus, we could take $T_Y < 1$ minute as a possible restriction. This would restrict the model to yields of less than about 10^4 MT at sea level and to yields of less than 1 MT at 65 km. We should emphasize that the prominence of periods of the order of the Brunt-Väisälä period in the far-field wave forms does not necessarily indicate the inappropriateness of the model, as these periods can arise through the accumulative long-range dispersion of the early portion of the blast wave form.

3.2.2 Near Surface Explosions

The following describes the appropriate source model for near surface explosions which was developed following a suggestion by J. Reed of Sandia Corporation. Suppose Y is the total energy yield of a near ground explosion. Then the blast wave at moderate distances might appear (from symmetry considerations) to be the same as from an air burst of yield $2Y$ when the presence of the ground is neglected. On the basis of this assertion and the reasoning outlined in the previous section, we would infer that the blast overpressure $(\Delta p)^*_{ref}$ and positive phase duration t_{ref} of the blast wave waveform on the ground at a distance of R_{ref} from the explosion should be jointly taken as (for $Y_{KT} = 1$ KT)

$$R_{ref} = 2^{1/3} \text{ miles}$$

$$\Delta p^*_{ref} = 34 \text{ mbar}$$

$$t_{ref} = 0.33 \times 2^{1/3} \text{ sec}$$

If we wish to have a linear source model such as is implicit in the existing theories, we would have to interpret Δp^{*}_{ref} to be twice that overpressure which would be observed if the ground were not present. This means we would want $\Delta p_{ref} = 17$ mbar. If, in addition, we were to assume that spherical spreading holds reasonably well between 1 and $2^{1/3}$ miles, then one would take $\Delta p_{ref} = 17 \times 2^{1/3}$ when one backs up to $R_{ref} = 1$ mile.

All this suggests that the program's output should be more satisfactory for near surface bursts were one to jointly set

$$R_{ref} = 1 \text{ mile}$$

$$\Delta p_{ref} = 17 \times 2^{1/3} = 21.4 \text{ mbar}$$

$$t_{ref} = 0.32 \times 2^{1/3} = 0.42 \text{ sec}$$

in the existing computer program. The method in which this is done is as described in Sec. 3.1.2.

3.3 VARIATION OF WAVEFORMS WITH ENERGY YIELD AND WITH BURST HEIGHT

One of the principal results obtained with the use of the modal synthesis program during the past reporting period was a clarification of the effects of burst height and energy yield on the waveforms generated by nuclear explosions [Pierce, Posey, and Iliff, 1971]. Literature published previous to this had certain discrepancies which were apparently not well understood. Scorer's and Hunt, Palmer, and Penney's results would indicate that the earliest portion of the pulse received at large distances (2000 km or greater) should have amplitudes directly proportional to energy yield. On the other hand, a plot (which we omit here for brevity) of the amplitudes computed numerically by Harkrider (Figure 15 in his paper) would suggest that these should vary with yield Y as $Y^{0.6}$ for yields above 5 MT.

The two relevant sets of calculations on burst height effects exhibited by Weston [1962] indicate that the amplitudes decrease drastically as burst height is increased (although this fact is not noted explicitly in Weston's text). His figures indicate the amplitudes of the earlier portion of the pulse to be down by factors of about 1/60 and 1/300 for bursts at 39 km and 76 km, respectively, from the amplitudes for a burst at ground level. In contrast, Harkrider's altitude effect prediction as exhibited in Figure 17 of his paper (with the correction suggested by Pierce [1965]) indicates that,

for altitudes up to 17 km, the decrease in amplitude with burst height is much smaller than one would expect from an extrapolation of Weston's results. Harkrider's results would suggest the net decrease to only be of the order of 30% when the explosion is raised from 2 to 17 km.

Our findings by use of INFRASONIC WAVEFORMS tend to more nearly support the predictions of Scorer and of Hunt, Palmer, and Penney as regards yield-amplitude proportionality than the predictions of Harkrider's $Y^{0.6}$ dependence. As regards the height of burst dependence, we agree neither with Harkrider nor with Weston. We find a small increase of amplitude with increasing height up to an altitude of the order of 40 km followed by a decrease with increasing altitude.

In Fig. 3, a number of waveforms computed for fixed height of burst and fixed observer location, but for variable energy yield, are simultaneously plotted. In each case, the overpressure divided by the yield (in megatons) is plotted rather than the overpressure. Thus, the near coincidence of the curves during the early portion of the wave form indicates that this portion of the wave form is nearly directly proportional to energy yield.

That this proportionality should hold in the range of lower yields is evident from the general theoretical formulation. If, during the early portion of the wave form, the bulk of the contribution to the dominant modes comes primarily from lower frequencies where $\omega T_Y << 1$, then the sum of the modal waveforms will appear proportional to T_Y^3 (and hence to E) at these times.

An estimate of the range of yields over which this proportionality should hold may be obtained if one takes ω in the condition $\omega T_Y << 1$ to be the frequency corresponding to the period between the first two prominent peaks in the wave form. Since this period is typically about 4 minutes (see, for example, the data exhibited by Donn and Shaw [1967]) one requires $T_Y << 40$ sec, or, for sea-level bursts, E << 500 MT. The condition becomes much more stringent when the height of burst is raised.

It is suggested that some slight improvement over the yield-amplitude proportionality law might be obtained if one took the amplitude to vary with yield Y_{KT} as

$$p_{amp} = DY_{KT}/[1 + (Y_{KT}/Y_o)^{2/3}] \qquad (3.13)$$

where D is independent of yield and where Y_o is given by (units in

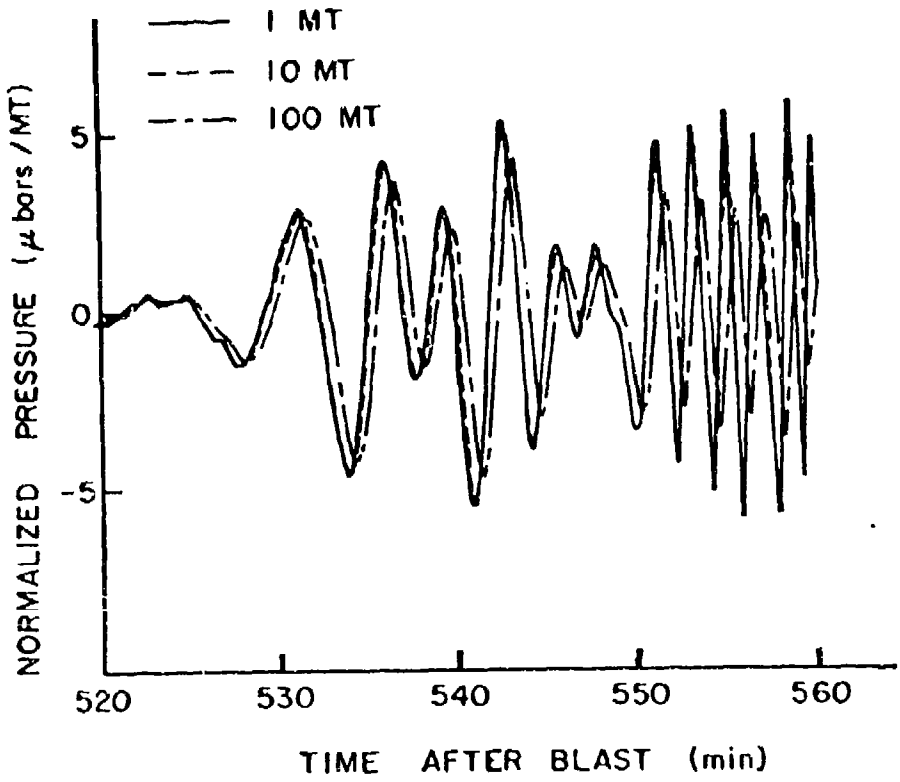

Figure 3. Acoustic pressure per megaton of the source yield for ground bursts of 1, 10, and 100 megatons as a function of time. The observer is on the ground 10,000 km north of the source in a subtropical summer atmosphere.

kilotons of TNT)

$$Y_o = (p_o/p_{ref})(c/c_{ref})^3/(\omega_{char} t_{ref})^3 \qquad (3.14)$$

where p_o and c are evaluated at z_o and where ω_{char} is a characteristic frequency designating the early portion of the wave form. Typically, Y_o should be of the order of 5×10^6 KT for sea-level explosions. For the amplitudes (first principal peak to trough) of the computed wave forms shown in Fig. 3, we find that the best fit to Eq. (3.13) gives $D = 0.0075$ dynes/cm^2 KT and $Y_o = 4.4 \times 10^6$ KT. The degree of fit is indicated in Fig. 4. For contrast, the line $p = D' Y_{KT}^{0.6}$ (derived from Harkrider's computations) is also plotted, where D' is selected such that the curve agrees with (3.13) at a yield of 5 MT. The discrepancy shows that this model more nearly exhibits yield-amplitude proportionality than does Harkrider's. For reasons discussed during the derivation of (3.12) we are not sure that our source model is adequate in the quantitative description of the deviation from yield-amplitude proportionality. However, the fact that the computed wave forms conform to this proportionality over such a wide range of yields tends to support our thesis that the model is insensitive to the choice of R_{ref} provided that the constant K in Eq. (3.10) is correct.

In Fig. 5, three computed waveforms are shown for a given yield, a given observer location, and a given model atmosphere, but for a variable height of burst. The amplitude of the entire wave train is seen to increase with height of burst below some altitude (seen in Fig. 6 to be a function of yield), above which the amplitude decreases. The decrease in amplitude is greater for the later arriving high-frequency 'acoustic' portion of the wave form.

In Fig. 6, the normalized amplitude p_{emp}/Y (see Fig. 5) is plotted versus height of burst for a number of yields Y. Although the details vary, the general shape of all such curves is similar. At lower altitudes, the amplitude increases slowly with height of burst, reaches a maximum at a height somewhere between 25 and 50 km, then decreases at a relatively rapid rate with subsequent increasing height.

The general shape of the amplitude-burst height curves may be interpreted with the aid of the general formulation and a few additional considerations. For the most part, we expect that the earlier low-frequency portion may be considered as carried by a single composite mode [Bretherton, 1969; Garrett, 1969a, b] which is the real atmosphere's counterpart of the edge mode discovered by Lamb [1910] for the isothermal atmosphere. That the numerical computations of dispersion curves suggest the existence of such a mode has been pointed out by Press and Harkrider [1962], who use the descriptive phrase 'pseudo mode' to denote the fact that its dispersion curve coincides with those

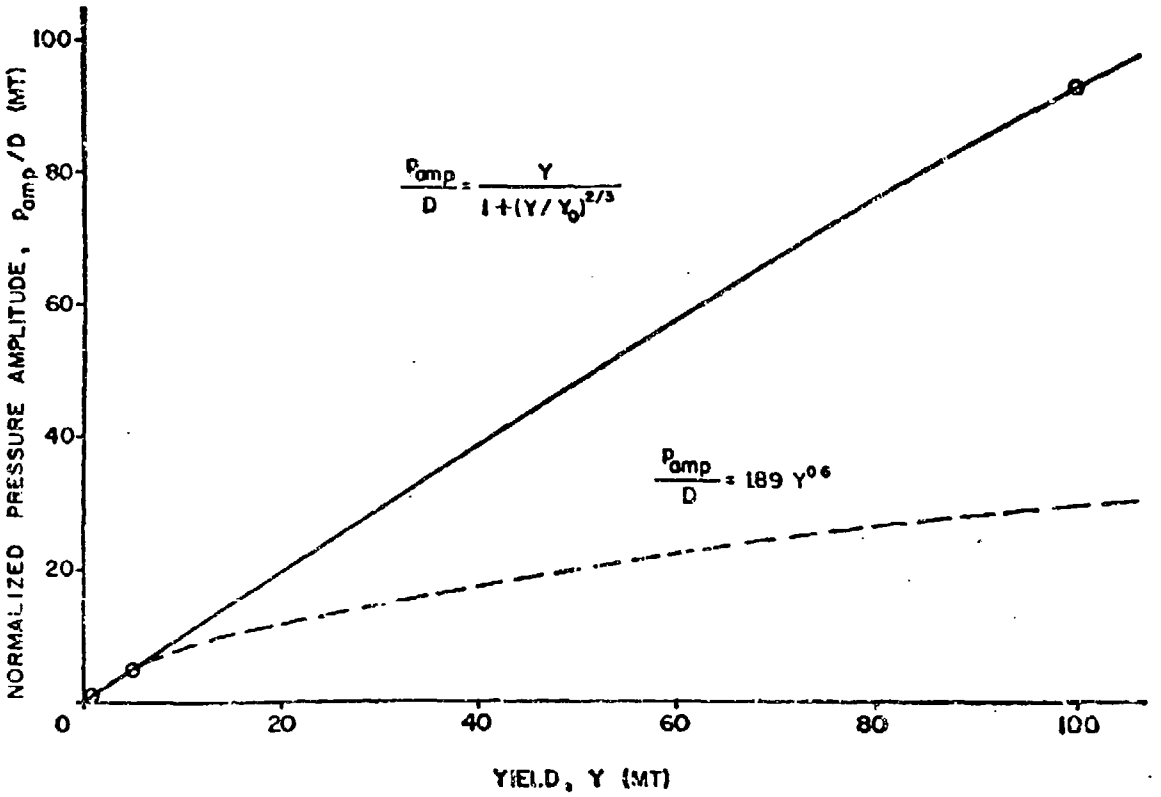

Figure 4. Plot of the amplitude dependence on yield found in the present calculations and a curve showing the $Y^{0.6}$ dependence derived from Harkrider's computations and made to agree with the first curve at 5 MT.

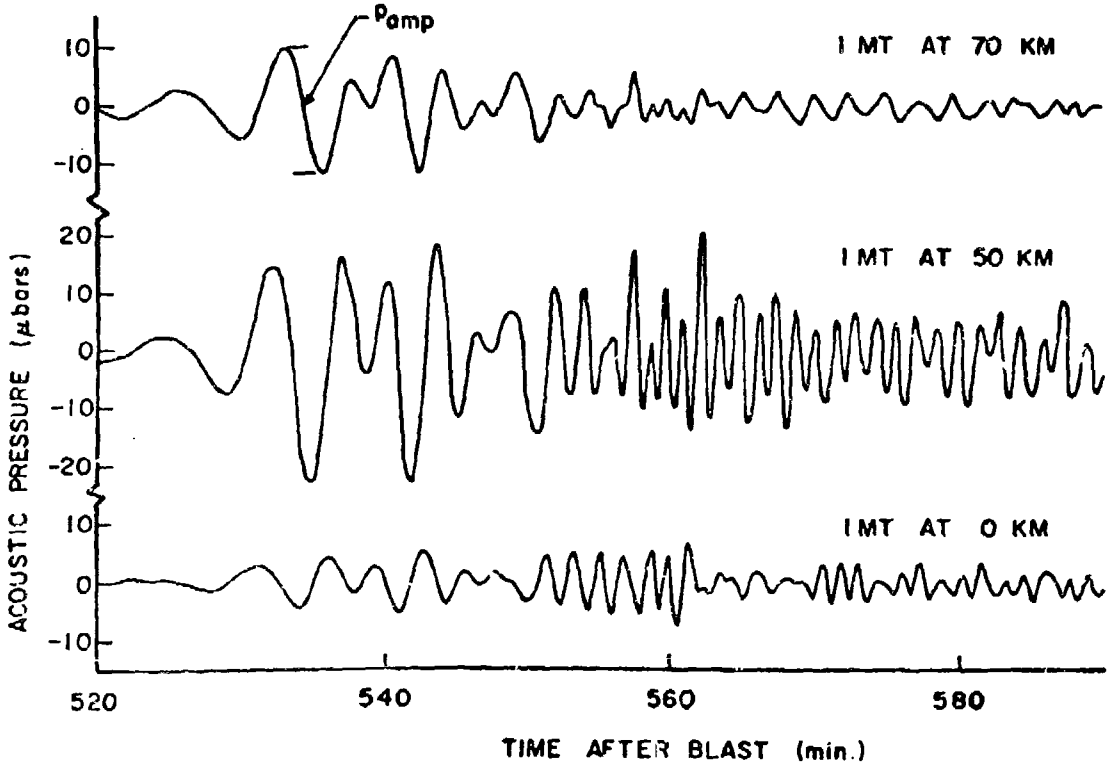

Figure 5. Time variation of ground-level acoustic pressure 10,000 km north of 1 MT explosions at altitudes of 0, 50, and 70 km in a subtropical summer atmosphere.

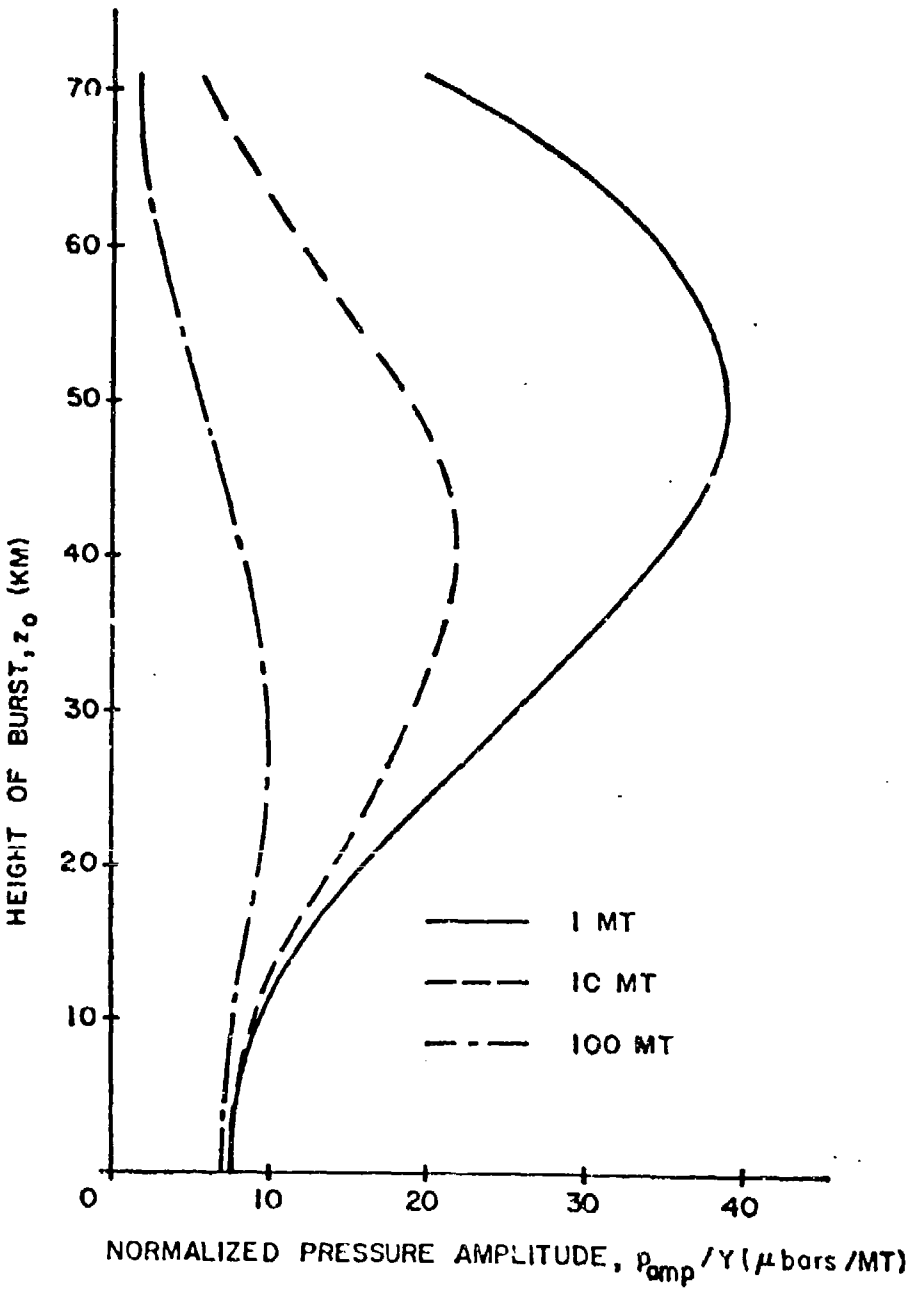

Figure 6. Height of burst dependence of the pressure amplitude per megaton of the source as found in the theoretical syntheses of ground-level wave forms for yields of 1, 10, 100 MT.

of mathematically distinct modes over different frequency ranges.

In the paper by Pierce, Posey, and Iliff [1971] it is argued on this basis that the lower frequency portion of the waveform should vary with height of burst z_o as

$$p_{amp} = JY_{KT}[p_{ref}/p_o(z_o)]^{(\gamma-1)/\gamma}/[1 + (\omega_{char}T_Y)^2] \qquad (3.15)$$

where J is a constant, independent of burst height and of yield. Note that T_Y does, however, depend on height.

The factor $[1/p_o]^{(\gamma-1)/\gamma}$ in (3.15) increases monotonically with height, although at a relatively slow rate compared with $1/p_o$ since $(\gamma - 1)/\gamma$ is only 2/7 . Thus, were it not for the denominator $[1 + (\omega T_Y)^2]$, the quantity (Eq. 3.15) would increase indefinitely with height. As it is, the expression reaches a maximum at some finite height, then decreases due to the increase of T_Y with height of burst as $1/p_o^{1/3}$. The altitude at which this maximum is obtained depends on yield and clearly decreases with increasing yield. This is in accord with the results shown in Fig. 6.

To check to what extent Eq. (3.15)quantitatively accounts for the variation exhibited in Fig. 6, we plot a selected portion of these curves in Fig. 7 along with corresponding plots of Eq.(3.15) The values $\omega_{char} = 0.018$ sec^{-1} and J = 390 μbars/MT were determined taking $Y_o = 4.4 \times 10^3$ MT and D = 7.5 μbars/MT for a ground-level burst. Considering the limitations of the approximation, we consider the agreement to be relatively good. In effect, a good prediction of amplitude-height dependence was made using only a knowledge of amplitude-yield dependence for a ground-level burst.

It should be pointed out that the validity of the source model is open to question (more so than for low-yield low-altitude bursts) when $\omega_{char}T_Y$ becomes comparable to 1. Nevertheless, it is gratifying that the model does predict the amplitude to eventually decrease when the burst height is raised beyond a certain point. Any other behavior would certainly be unacceptable on physical grounds.

We are unable to explain the discrepancy between our derived height of burst effect and those presented in the figures in Weston's [1962] paper. We have not found any errors in Weston's formulation which might account for this. However, in view of the fact that we can quantitatively account for discrepancies between our results and those obtained independently by Harkrider [1964], we are of the opinion that there was a coding error in the computation of Weston's wave forms.

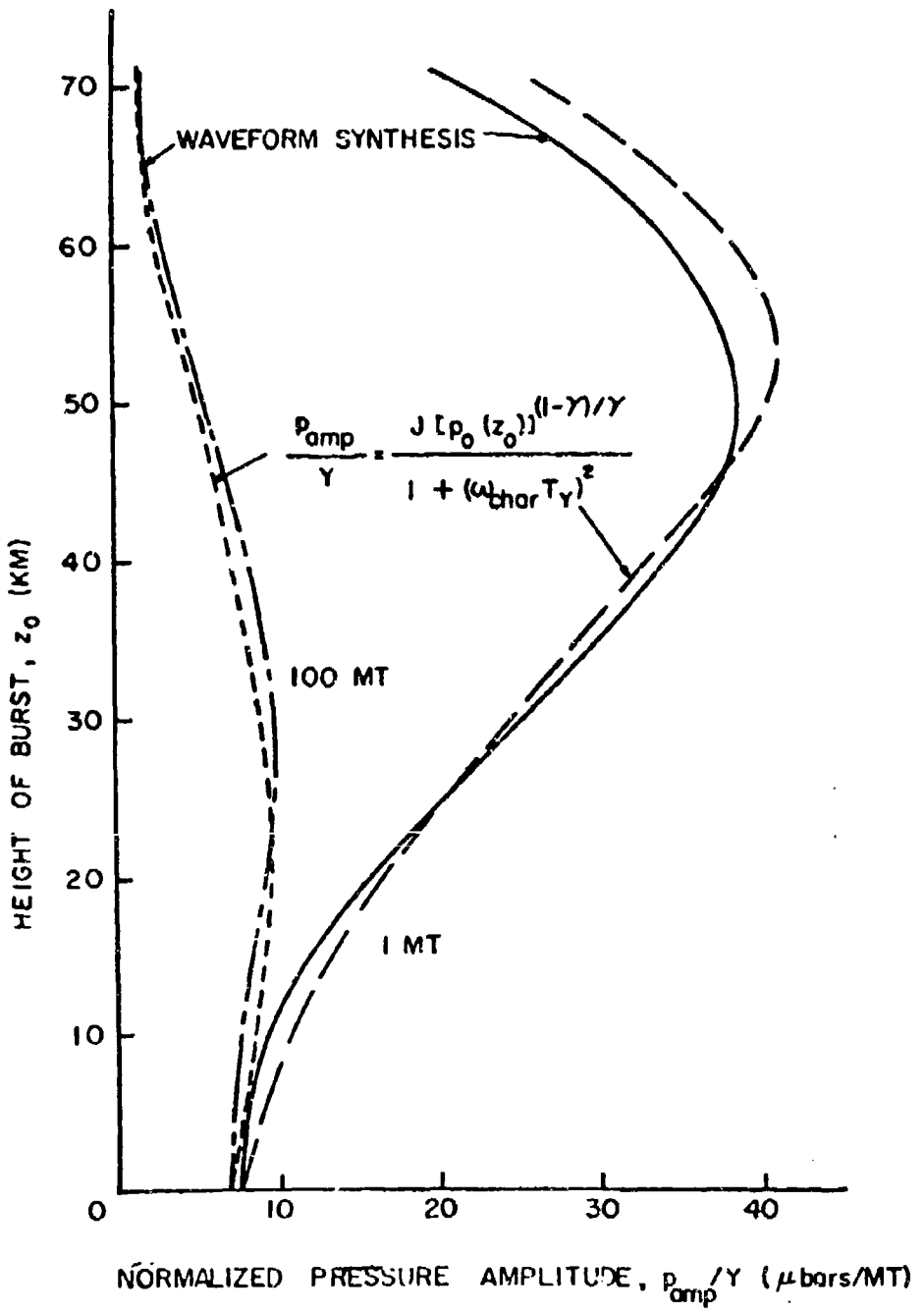

Figure 7. Comparison of amplitude dependence upon height of burst as predicted by the Lamb edge mode hypothesis and by syntheses based on the summation of fully-ducted normal modes. The choice of ω_{char} is $0.0185\ sec^{-1}$.

Chapter IV

AN APPROXIMATE THEORY BASED ON LAMB'S ATMOSPHERIC EDGE MODE

4.1 INTRODUCTION

The Lamb edge mode theory has previously been described in some detail in the papers by Pierce and Posey [1971], Posey and Pierce [1971], Posey and Pierce [1972], and in the doctoral thesis by Posey [1971]. The present chapter summarizes some of the salient aspects of this theory and its implications.

The basic idea of the theory, in somewhat simplified terms, is that the wave may be regarded as traveling along the ground rather than through the atmosphere. The situation is analogous to water waves, which one regards as waves on the surface of water even though there is in principle some water movement at arbitrary depths below the surface. That such a description is possible for pressure pulses in the atmosphere was demonstrated for the special case of a constant temperature atmosphere by Lamb in 1910.

However, the counterpart of this type of motion for realistic (nonisothermal) atmospheres was not clearly recognizable in theories of wave propagation until Bretherton (1969) and Garrett (1969a,b) derived formulas governing the propagation of constant frequency (sinusoidal) waves of this type. Of key importance in this respect is the wave dispersion, whereby waves of lower frequency travel faster than waves of higher frequency. The Lamb type of wave (called Lamb's mode) does not exhibit any dispersion for the isothermal atmosphere and this would clearly be inadequate to explain the data since the shape of the waveform changes radically with increasing distance from the explosion. Bretherton and Garrett's contribution was to show how one might derive formulas governing this dispersion in a fairly simple manner.

Given the basic idea that the wave is propagating as a surface wave in the real atmosphere's counterpart of Lamb's guided mode, one can consider the wave arriving at a given point to have travelled along a curved path (horizontal ray path) which connects the explosion and the recording site. [See Fig. 8.] The determination of these paths may be made using the same principles which explain why light rays are bent when they pass from air to water. The speed of waves in traveling along these paths is an average of the sound speed and wind velocity profiles above the path. The distortion of the waveform as it moves along the path is governed by an equation similar to that used in the study of sonic boom shock waves in the atmosphere and to that derived by Korteweg and de Vries in 1895 to explain why water waves do not necessarily break. As the wave

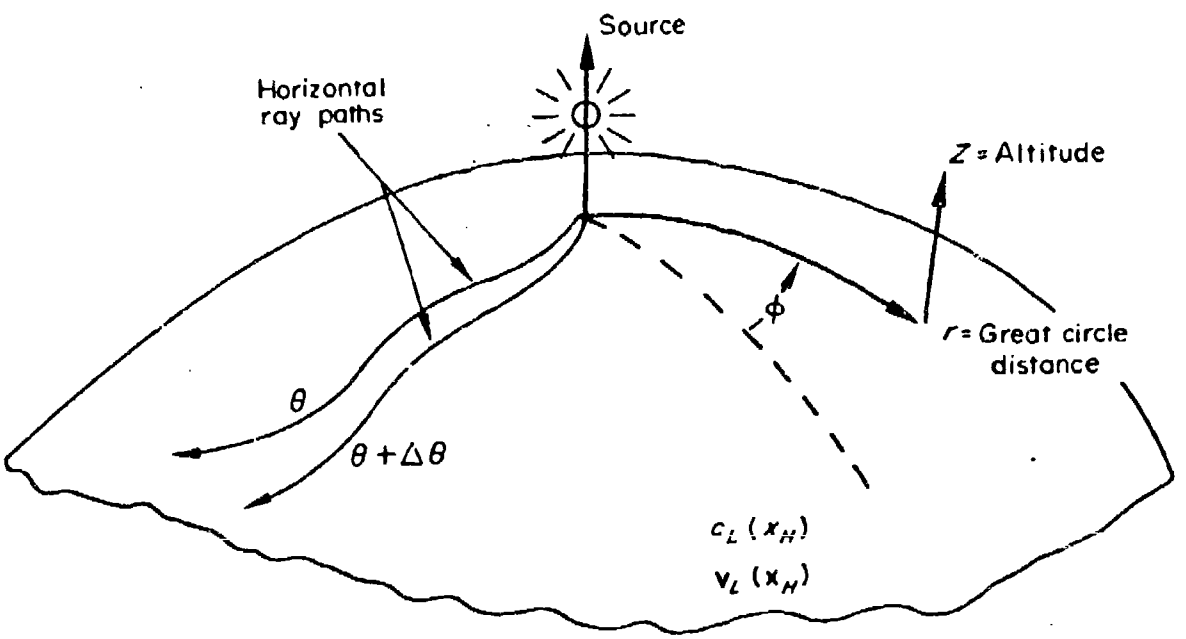

Figure 8. Model of edge mode propagation from an explosive source in an almost-stratified atmosphere above a spherical earth.

moves from point to point along the path, its amplitude continuously adjusts itself such that wave action (a quantity similar to energy) is conserved. The pertinent formulas representing just how this guided wave is excited by the detonation of a nuclear explosion are derived by matching the guided wave onto a solution valid at close-in distances.

An important result of the theory is that the shape of the waveform recorded at any given point (providing the clock recording the wave is speeded up or slowed down just the right amount) depends on just one number, the ratio of a characteristic time for the explosion itself to a quantity (also having the units of time) which is an average of the properties of the atmosphere over the range of profiles above the path. The amplitude of the waveform depends on a number of quantities, the most important probably being the spread of the ray paths. If a number of paths should be caused to focus (just as light is focused by a magnifying glass) larger amplitudes may be expected. This appears to be the explantion of the data reported by Wexler and Hass [1962].

In regards to the relation of the Lamb mode theory to the multimode theory on which INFRASONIC WAVEFORMS is based, a principal virtue of the Lamb mode theory is its simplicity. One may note that the development of the theory of long-range atmospheric pressure pulse propagation since the early pioneering work of Rayleigh [1890], Lamb [1910], Taylor [1929], Solberg [1936], Pekeris [1939,1948] and Scorer [1950] has largely been towards progressively more complicated, albeit realistic, models [e.g. Yamamoto 1957; Hunt, Palmer and Penney 1960; Gazaryan 1961; V. H. Weston 1961, 1962; Pfeffer and Zarichny 1962; Press and Harkrider 1962; Weston and Van Hulsteyn 1962; Clarke 1963; Harkrider 1964; Van Hulsteyn 1965; Pierce 1965, 1967; MacKinnon 1967, 1968; Balachandran and Donn 1968; Nelson, Singhaus and McNiel 1968; Balachandran 1968, 1970; Pierce, Posey and Iliff 1971.] Notable exceptions to this general trend are the works of Row [1967], Hines [1967] and Tolstoy and Herron [1970], although these are concerned with waves which are propagating primarily in the ionosphere rather than near the Earth's surface.

Even with the aid of a large digital computer, agreement with data of multimodal calculations tends to be spasmodic. The reasons for this are not entirely clear; it may be due to incorrect assumptions concerning the atmospheric profiles or concerning the source mechanisms, to the neglect of horizontal variations in the atmosphere, or of dissipative processes in the upper atmosphere, or accumulative far-field non-linear effects. Since the implications of existing multi-mode theories such as those of Harkrider [1964], MacKinnon [1967] or Pierce and Posey [1970] are difficult to explore without the aid of a large digital computer, the inverse problem of determining imperfectly known aggregate properties of the source or atmosphere from empirical waveforms appears formidable. Even if the computer-assisted solution of the inverse problem were feasible, one's confidence in its predictions should be at best marginal in view of the inherent meagre insight

afforded by a theory which relies on a lengthy sequence of computations, which tends to obscure the causal relationships between input and output variables. One does not know, in addition, just what a priori realistic extensions to the existing simplified model are necessary, without first making such extensions and then exploring their consequences by numerical experiment. A possible trend could be towards an overly detailed model, rather than towards the achievement of the simplest possible model adequate to explain the existing data. That the latter is a desirable goal is a premise which with we believe most investigators will agree.

One theme which has pervaded much of the discussions of the empirical data [see, for example, Donn and Ewing 1962] is that the early portion of the waveform may be considered as being that of a single composite mode. Press and Harkrider [1962] noted that the phase velocity versus period curves for a realistic atmospheric profile tend to be arranged such that a single curve of nearly constant phase velocity extending over a wide range of periods may be constructed by the connection of the horizontal segments of a number of individual modal dispersion curves. This composite mode is evidently the real atmosphere's counterpart of the edge mode (with constant phase velocity equal to the sound speed) predicted by Lamb [1910] for the isothermal atmosphere model. The fact that Scorer [1950] found only one mode for a profile with the atmosphere above the tropopause idealized by an isothermal halfspace suggests that the other portions of the Press and Harkrider dispersion curves correspond to waves guided at relatively high altitudes. This has been supported by various numerical experiments [see, for example, Harkrider and Wells 1968] as well as by examination of the height profiles associated with different frequencies and different modes [Pfeffer and Zarichny 1963].

As mentioned above, the development of an analytical theory for the propagation of Lamb's edge mode in realistic atmospheres was initiated only relatively recently by Bretherton [1969] and by Garrett [1969a, b]. Bretherton showed how the mode's phase velocity may be found to first order in deviations of the sound speed profile from that of an isothermal atmosphere and to first order in the wind velocity, while Garrett extended the method to higher orders and thus succeeded in finding the dispersion of the mode. The latter paper by Garrett [1969b] gives a detailed discussion of the applications of the theory based on the edge mode to the analysis of empirical waveforms, as well as of the limitations of the theory. In spite of the relative simplicity of the Bretherton-Garrett model, it appears to be adequate for the explanation of the gross propagation speeds and dispersive characteristics of empirical waveforms, although it does not (at least to the extent which the perturbation series has yet been carried) explain more subtle features such as the inverse dispersion suggested by the data analysis of Donn and Ewing [1962].

The work by the present authors in regards to the edge mode theory has concentrated on the development of a relatively simple model for theoretical synthesis of transient waveforms recorded at large distances from nuclear

explosions. The model developed would appear to give a relatively simple explanation of (i) the magnitude of the amplitudes of the first few peaks, (ii) the periods between the first few peaks, (iii) the fact that records almost always begin with a positive pressure rise, and (iv) the anomalies in the spatial distribution of recorded peak overpressures that have been reported by Wexler and Hass [1962]. (Item (iii) above is unfortunately not widely appreciated, due to the fact that noise often obscures the early part of the record and that some of the published records have inadvertently been published with the positive pressure axis extending downwards. Professor Donn has informed us that this was the case in the paper by Donn and Shaw [1967]. The first three items are also explained by the more elaborate multimode theories [see, for example, Harkrider 1964] and we accordingly demonstrate that the edge mode model gives results similar to the multimode calculations of Pierce, Posey, and Iliff [1971] for the first few cycles. The advantage of the edge mode model is its simplicity, which allows an exploration of effects whose consideration may have been prohibitively difficult within the context of existing multimode theories. Such effects include accumulative far-field non-linear effects, the effects of terrain variations and the effects of horizontal atmospheric variations.

4.2 DISPERSION OF LAMB'S MODE

In our development of a theory for the propagation of Lamb's edge mode, we considered a sequence of idealized models. The mode's dispersion relation was taken for a temperature and wind-stratified atmosphere above a rigid flat ground at $z = z_g$, with only slight and unimportant modifications from that previously derived by Garrett [1969a, b]. The resulting expression relating angular frequency ω and horizontal wave number $\vec{k}$ as given by Pierce and Posey [1971] is to first order in ϵ given by

$$\omega = (c_L + v_{Lk})k + 0(\epsilon^2), \tag{4.1}$$

Here ϵ is any convenient parameter characterizing the order of magnitude of $[c(z) - c_L]/c_L$ where $c(z)$ is the height dependent sound speed and c_L (L for Lamb) is some constant value representative of the lower atmosphere. One may choose c_L and also a mean wind velocity $\vec{v}_L$ in such a manner that they are given by the equations

$$1/c_L^2 = \langle 1/c^2 \rangle; \quad \vec{v}_L = \langle \vec{v} \rangle, \tag{4.2}$$

where, for any $f(z)$,

$$f = \int \mathcal{E} f dz \Big/ \int \mathcal{E} dz \tag{4.3}$$

with

$$\mathcal{E} = p_o^{2/\gamma}(z)/\rho_o(z) \tag{4.4}$$

representing the height profile of what, in the isothermal case, may be construed as the kinetic energy density for Lamb's edge wave. Here $p_o(z)$ and $\rho_o(z)$ represent the ambient pressure and density of the actual atmosphere. The integration limits should be z_g and some relatively large value of z. In Eq. (4.1), v_{Lk} is an abbreviation for $\vec{v}_L \cdot \vec{e}_k$ where $\vec{e}_k$ is the unit vector pointing in the direction of the horizontal wave number $\vec{k}$. Thus, to first order in ϵ, the dispersion relation is that appropriate to an isothermal atmosphere (sound speed c_L) with constant horizontal wind velocity $\vec{v}_L$.

The definitions one may adopt for c_L and $\vec{v}_L$ are restricted only to first order in ϵ. There is no a priori reason for preferring any one of alternate definitions which differ in second order. The definitions we took were chosen such that the resulting second order terms (which actually govern the dispersion) are of relatively simple form.

To second order in ϵ, the dispersion relation obtained by Garrett [1969a] may be rewritten (albeit with some lengthy manipulation) in the form

$$\omega = k(c_L + v_{Lk} + a_{kk}) - k(k^2 - k_{BL}^2)h_{kk}, \tag{4.5}$$

where

$$a_{kk} = [1/(2c_L)]\left\langle [(\vec{v}(z) - \vec{v}_L) \cdot \vec{e}_k]^2 \right\rangle \tag{4.6a}$$

$$h_{kk} = \frac{1}{2} c_L^5 \left\langle [C + 2\vec{D}\cdot\vec{e}_k/c_L^3]^2 \right\rangle \tag{4.6b}$$

with

$$C(z) = \mathcal{E}^{-1}(z) \int_{z_g}^{z} \mathcal{E}(z)(c_L^{-2} - c^{-2})dz \tag{4.6c}$$

$$D(z) = \mathcal{E}^{-1}(z) \int_{z_g}^{z} \mathcal{E}(z)(\vec{v} - \vec{v}_L)dz. \tag{4.6d}$$

It should be noted that the latter two quantities both remain bounded at high altitudes by virtue of the definitions in Eqs. (4.2-4). The quantity k_{BL} which appears in Eq. (4.5) is ω_{BL}/c_L, where $\omega_{BL} = (\gamma - 1)^{1/2} g/c_L$ is

the Brunt-Väisäla frequency for an isothermal atmosphere with sound speed c_1. The form of the second-order terms in the dispersion relation would tend to suggest that the approximation is best for frequencies of the order of the Brunt-Väisäla frequency, rather than in the limit of low frequency. Fortunately, the dominant frequencies in pressure waveforms at large distances from nuclear explosions are of the same order of magnitude. [A detailed derivation of the above equations is given by Posey (1971).]

One may note that Eq. (4.5) may also be written in the form

$$\omega = c_E k - h_{kk} k^3 \tag{4.7}$$

where

$$c_E = c_L + v_{Lk} + a_{kk} + h_{kk} k_{BL}^2 \tag{4.8}$$

In order to facilitate comparison of Eq. (4.7) with the numerically determined multi-mode dispersion curves, it may be expressed in a form expressing frequency ω as a function of phase velocity $v_p = \omega/k$.

$$\omega = v_p [(v_p - c_E)/h_{kk}]^{1/2} \tag{4.9}$$

Figure 9 is a representative comparison between this relation and the multi-mode curves for the same atmosphere. The lower 225 km of the model atmosphere used, as listed in Table 1, was selected to represent average conditions between Johnston Island and Berkeley, California for the month of October, based on data from the Handbook of Geophysics and Space Environments [Valley, 1965] and from the 1965 COSPAR International Reference Atmosphere [COSPAR, 1965]. The direction of propagation is along the great circle path from Johnston Island to Berkeley, 35° north of east. Since the Lamb mode dispersion is only weakly affected by conditions above 115 km [Posey, 1971], the computation of Eq. (4.9) uses only the model atmosphere below this altitude. The edge mode propagation parameters are found to be $c_E = 0.318$ km/sec and $h_{kk} = 0.132$ km^3/sec. Notice that the agreement is within 0.2% in the flat portions of GR_o, S_o and S_1 for frequencies up to 0.07 sec^{-1} (periods down to about 90 sec), which, as discussed by Posey [1971], are relatively insensitive to the atmosphere above 110 km.

Garrett [1969b] has discussed the effect of imposing an arbitrary boundary impedance at a given altitude $z = H_o$. He finds that the relative variation in the phase velocity of the edge mode is of the order $e^{-H/(2H_s)}$

MODEL ATMOSPHERE OF 34 LAYERS

LAYER	ZB	ZT	H	C	VX	VY
34	225.00	INFINITE	INFINITE	0.8014	0.0	0.0
33	205.00	225.00	20.00	0.7655	0.0	0.0
32	195.00	205.00	10.00	0.7469	0.0	0.0
31	185.00	195.00	10.00	0.7279	0.0	0.0
30	175.00	185.00	10.00	0.7097	0.0	0.0
29	165.00	175.00	10.00	0.6882	0.0	0.0
28	155.00	165.00	10.00	0.6584	0.0	0.0
27	145.00	155.00	10.00	0.6093	0.0	0.0
26	135.00	145.00	10.00	0.5413	0.0	0.0
25	125.00	135.00	10.00	0.4783	0.0103	0.0
24	115.00	125.00	10.00	0.4007	0.0206	0.0
23	105.00	115.00	10.00	0.3168	0.0309	0.0
22	95.00	105.00	10.00	0.2833	0.0103	0.0
21	85.00	95.00	10.00	0.2718	-0.0051	0.0000
20	75.00	85.00	10.00	0.2725	0.0077	0.0
19	65.00	75.00	10.00	0.2869	0.0206	0.0
18	55.00	65.00	10.00	0.3104	0.0216	0.0
17	45.00	55.00	10.00	0.3230	0.0216	0.0
16	40.00	45.00	5.00	0.3261	0.0175	0.0
15	35.00	40.00	5.00	0.3161	0.0082	0.0
14	30.00	35.00	5.00	0.3084	0.0021	0.0
13	25.00	30.00	5.00	0.3019	-0.0021	0.0000
12	20.00	25.00	5.00	0.2938	-0.0072	0.0000
11	18.00	20.00	2.00	0.2869	-0.0058	-0.0021
10	16.00	18.00	2.00	0.2819	0.0055	0.0055
9	14.00	16.00	2.00	0.2869	0.0100	0.0040
8	12.00	14.00	2.00	0.2938	0.0139	0.0
7	10.00	12.00	2.00	0.3005	0.0154	0.0
6	8.00	10.00	2.00	0.3078	0.0129	0.0
5	6.00	8.00	2.00	0.3161	0.0098	0.0
4	4.00	6.00	2.00	0.3230	0.0046	0.0
3	2.00	4.00	2.00	0.3292	0.0046	0.0
2	1.00	2.00	1.00	0.3400	0.0011	-0.0011
1	0.0	1.00	1.00	0.3424	0.0011	-0.0011

ZB=HEIGHT OF LAYER BOTTOM IN KM
ZT=HEIGHT OF LAYER TOP IN KM
H =WIDTH OF LAYER IN KM
C =SOUND SPEED IN KM/SEC
VX=X COMP. OF WIND VEL. IN KM/SEC
VY=Y COMP. OF WIND VEL. IN KM/SEC

Table I. Representative wind and sound speed profiles above 30°N, 140°W for October. This model is based on Valley's [1965] Figs. 2.2, 2.4, 2.5 and 4.11 and table 4.21 and on the data on p. 46 in COSPAR [1965].

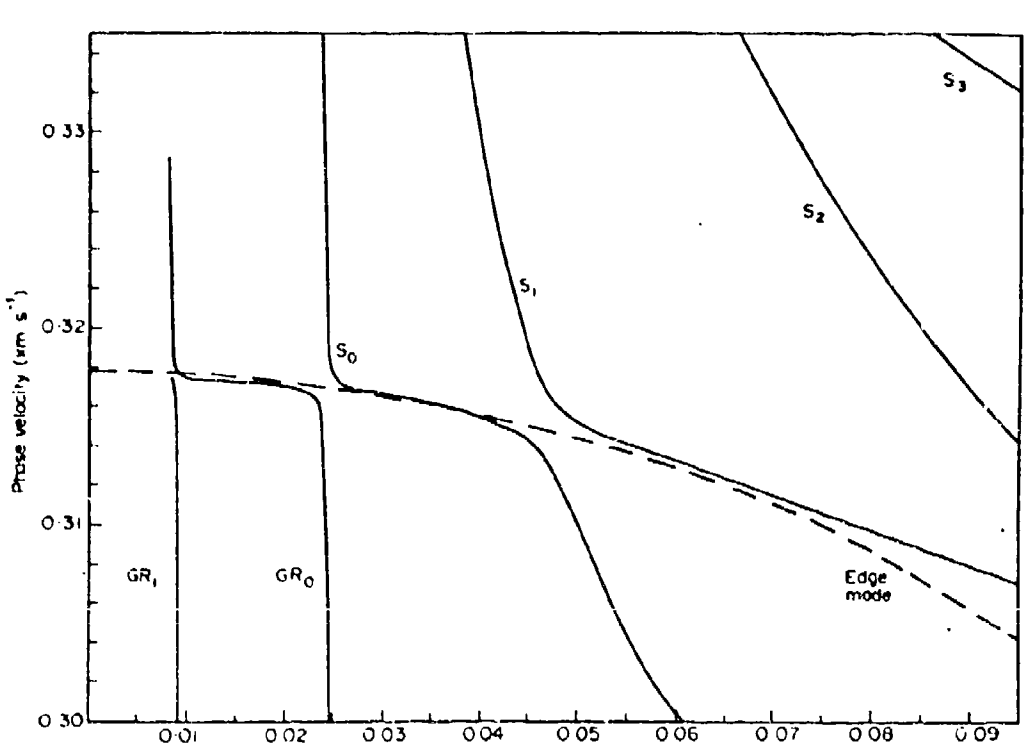

Figure 9. Comparison of approximate edge mode dispersion curve (dashed line) with guided mode dispersion curves obtained by numerical solution of the acoustic-gravity wave eigenvalue problem (solid lines). The nomenclature labelling the acoustic-gravity wave modes is that of Press and Harkrider (1962).

(where H_g is a scale height) for plausible variations in the boundary impedance. The agreement between the independently derived dispersion relations shown in Fig. 9 seems to substantiate this.

A relation for the group velocity, $v_g = d\omega/dk$, can also be found from Eq. (4.7),

$$v_g = c_E - 3h_{kk}(\omega/c_E)^2 \tag{4.10}$$

and a comparison of this with the multi-mode curves for the same model as described above is shown in Fig. 10.

A FORTRAN computer program which, among other quantities, evaluates the various Lamb mode propagation constants c_L, $\vec{v}_L$, h_{kk}, c_E, etc., for an arbitrary multilayered atmosphere was written during the contract and is given in Posey's doctoral thesis [Posey, 1971].

4.3 THEORETICAL EXPRESSIONS FOR EDGE MODE WAVEFORMS

The general results of the theoretical development by Pierce and Posey [1971] of the excitation and propagation of Lamb's atmospheric edge mode from nuclear explosions is summarized here. The general expression for the acoustic pressure signature at a point $\vec{x}$ at times t is given by

$$p(\vec{x},t) = \left\{ \frac{DV(\vec{x},\vec{x}_0)gE}{(c_{L0}T_Y)^{3/2} c_{L0}^{\,2} (db/d\theta)^{1/2}} \right\} \psi(t,s,\theta), \tag{4.11}$$

where D is a numerical constant given by ($K \approx 0.50$)

$$D = K\sqrt{2}(\gamma - 1)(2 - \gamma)4\pi \approx 0.013 \tag{4.12}$$

while $V(\vec{x},\vec{x}_0)$ is a dimensionless quantity given by

$$V(\vec{x},\vec{x}_0) = \frac{\Lambda(\vec{x})\Lambda(\vec{x}_0)c_{L0}^{\,1/2}(c_L + v_{Lk})_0}{p_o(\vec{x}_0)c_L^{\,1/2}|c_L\vec{e}_k + \vec{v}_L|^{1/2}(c_L + v_{Lk})^{1/2}} \tag{4.13}$$

with

$$\Lambda(\vec{x}) = p_o^{\,1/\gamma}(\vec{x})/p_o(\vec{x}_g)^{(1/\gamma) - (1/2)} \tag{4.14}$$

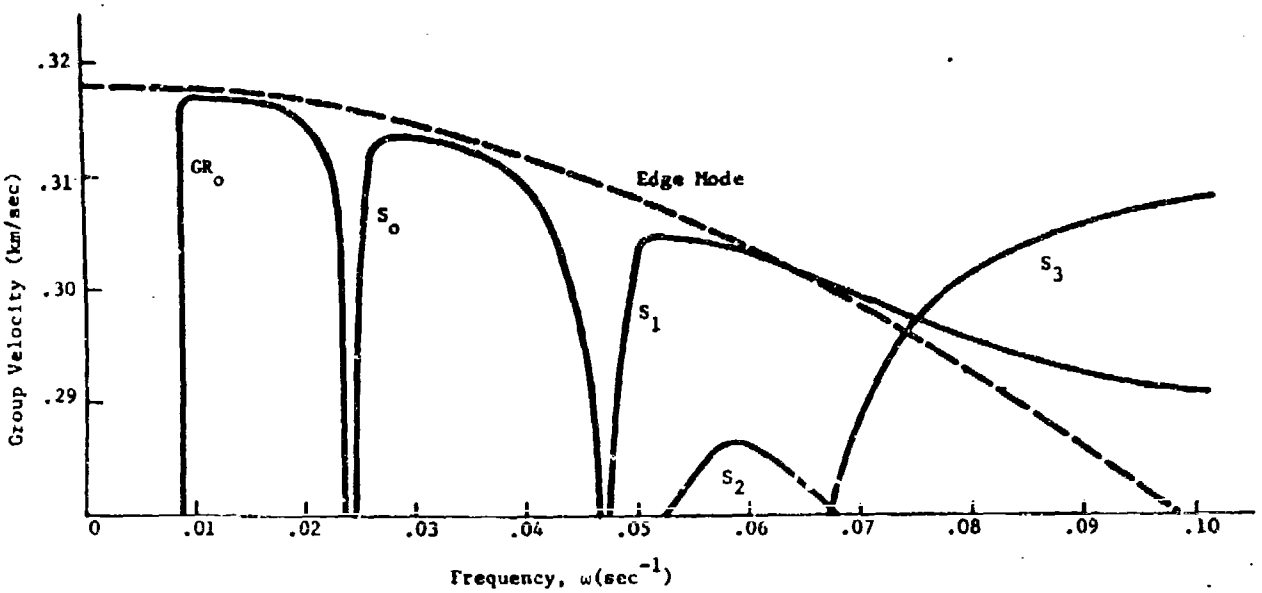

Figure 10. Comparison of multi-mode and edge mode group velocity curves. These curves are appropriate for propagation 35° north of east in the atmosphere of Table I.

Here $\vec{x}$ denotes the observation location, $\vec{x}_0$ the source location, $\vec{x}_g$ (or $\vec{x}_{0g}$) the point on the ground directly below the observer (or source). The subscript 0 implies the corresponding quantity is evaluated for the atmosphere at the source location. The quantity g in Eq. (4.11) is the acceleration of gravity, E is the total energy released by the explosion, T_Y is the source characteristic time defined by Eq. (3.3) in the present report. The quantity $dr/d\theta$ is a parameter which allows for focusing [Fig. 8] or defocusing of horizontal ray paths caused by departures of the atmosphere from perfect stratification (i.e., horizontal variations) and formally is defined as the ray channel width per unit angle θ with which horizontal ray paths exit from the source location. For a perfectly stratified atmosphere but with the earth curvature correction (see Sec. 3.1.1 of the present report) included, it is given by

$$db/d\theta = r_e \sin(r/r_e) \tag{4.15}$$

The function $\psi(s,t,\theta)$ which appears in Eq. (4.11) is given by

$$\psi(s,t,\theta) = \frac{T_Y}{\pi\tau_D} \int_0^\infty \mathrm{Ai}\left[\frac{\tau_a - t}{\tau_D} + \mu\frac{T_Y}{\tau_D}\right] M(\mu)d\mu \tag{4.16}$$

where $\mathrm{Ai}(x)$ is the Airy function, defined by

$$\mathrm{Ai}(x) = \frac{1}{\pi}\int_0^\infty \cos(v^3/3 + xv)dv \tag{4.17}$$

and where

$$\begin{aligned} M(\mu) &= \int_0^\mu (1 - \xi)\exp(-\xi)[\mu - \xi]^{-1/2}\, d\xi\, U(\mu) \\ &= \left\{\sqrt{\mu} + (1 - 2\mu)\exp(-\mu)\int_0^{\sqrt{\mu}} \exp(y^2)dy\right\} U(\mu) \end{aligned} \tag{4.18}$$

gives the characteristic waveform time dependence for the Lamb edge mode in the intermediate field (before dispersion has had an appreciable accumulative effect). A plot of this function is given in Fig. 11 .

In Eq. (4.11), we have also made the abbreviations

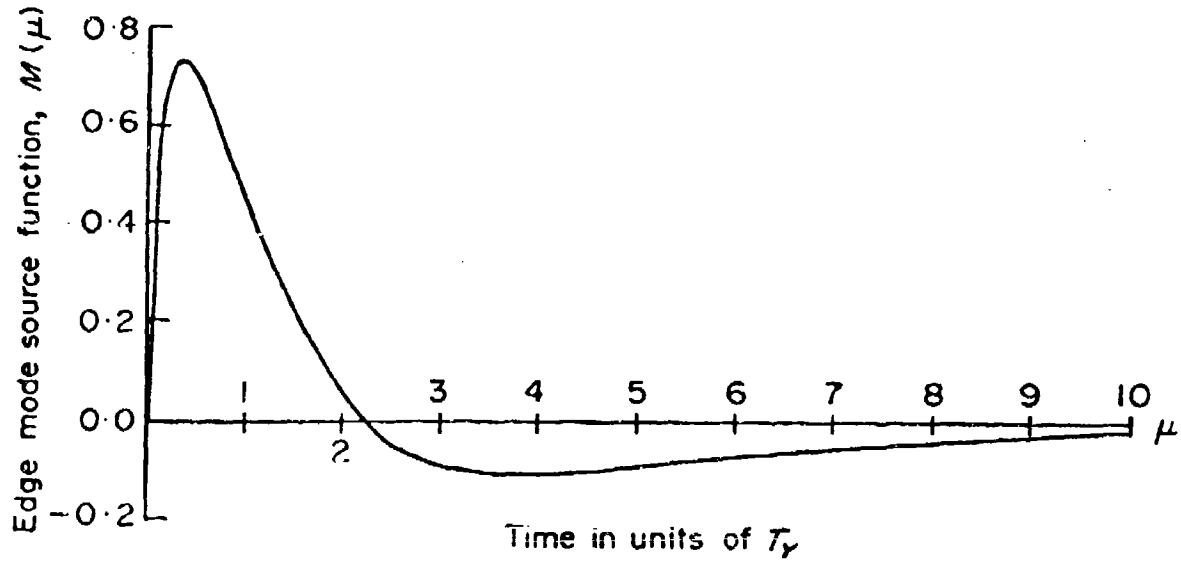

Figure 11. Source function, M(μ), describing the time variation of the effective source for Lamb mode excitation by nuclear explosions. Here $\mu = t/T_Y$, where T_Y is a characteristic time for the explosion.

$$\tau_a = \int_0^s (1/c_e)ds \tag{4.19a}$$

$$\tau_D = 3\left\{\int_0^s (h_{kk}/c_e^4)ds\right\}^{1/3} \tag{4.19b}$$

for the two characteristic functions s which appear in the integral. Both of these quantities have the uni of time and are here referred to as the waveform arrival time and the characteristic dispersion time, respectively. The parameter s is related to distance ℓ along a horizontal ray path (see Fig. 8) by the equation

$$\frac{ds}{d\ell} = \frac{c_L + v_{Lk}}{|c_L \vec{e}_k + \vec{v}_L|} = \frac{c_L + v_{Lk}}{[c_L^2 + 2c_L v_{Lk} + v_L^2]^{1/2}} \quad . \tag{4.20}$$

For typical winds in the atmosphere it would appear sufficient to take $s = \ell$.

In the often realized limit of propagation distances sufficiently large that $T_Y / \tau_D << 1$ and for arrivals sufficiently early that $t - \tau_a << \tau_D^2/T_Y$, Pierce and Posey [1971] argue that the function ψ may be suitably approximated by

$$\psi = (2/\sqrt{\pi})(T_Y/\tau_D)^{3/2} PP([t - \tau_a]/\tau_D) \tag{4.21}$$

where PP(x) is the function

$$PP(x) = \int_0^\infty Ai'(\alpha^2 - x)d\alpha \quad . \tag{4.22}$$

In the limit represented by Eq. (4.21), the acoustic overpressure p, as given by Eq. (4.11), is directly proportional to the energy release E . This is clear since the only other parameter in the formulation which varies with energy yield is T_Y and since the $T_Y^{3/2}$ factor in Eq. (4.21) cancels the corresponding factor in the denominator in Eq. (4.11). Note that this is in accord with the numerical study of Pierce, Posey, and Iliff [1971], the results of which are summarized in Sec. 3.3 of the present report. The result quoted there that, for smaller yields or lower heights

of burst, the amplitude of the first few peaks varies with source height z_0 as $[1/p_o(z_0)]^{(\gamma-1)/\gamma}$ is also indicated by Eq. (4.11).

The value 0.50 of the dimensionless constant K quoted in Eq. (4.12) turns out to be applicable to both above ground and near surface explosions since the alternative choices of Δp_{ref} and t_{ref} discussed in Secs. 3.2.1 and 3.2.2 are such that $\Delta p_{ref} t_{ref}^2$ is the same in both cases. [See Eq.(3.10).] However, in the computation of T_Y as given by Eq. (3.3), one should use $t_{ref} = 0.33$ sec and $t_{ref} = 0.416$ sec for above ground and near surface explosions, respectively.

The general shape of the Lamb mode waveform is fully described apart from a multiplicative time independent quantity by the function ψ. The numerical plots in Figs. 12 and 13 should give a general indication of the predictions of Eq. (4.16) for various T_Y/τ_D. The $T_Y/\tau_D = 0.1$ curve in Fig.12 is close to the limiting case represented by Eq.(4.21). It may be noted from Fig. 13 that the theory predicts the first peak to be smaller than the second as long as $T_Y/\tau_D < 0.34$. The ratios of the periods to τ_D in the first few cycles would appear from Fig. 12 to be relatively insensitive to the value of T_Y/τ_D. Thus the period, first peak to second peak, is about $4.0\tau_D$ while the period, second peak to third peak, is about $2.6\tau_D$.

4.4 COMPARISON WITH MULTIMODAL COMPUTATIONS

A computer program encompassing the edge mode theory was written during the reporting period by Posey [1971]. The program is, strictly speaking, in its present form only applicable to atmospheres without horizontal variations, although it allows the user the option of specifying three separate model atmospheres for the computation. One atmosphere, the "source atmosphere" could be utilized in computing all quantities (0 subscript) in the coefficient of ψ in Eq. (4.11) which correspond to the atmosphere near the source and in the computation of T_Y. Another atmosphere (the "propagation atmosphere") could be utilized in finding those quantities appropriate to the atmosphere near and above the observer location. Finally, a third atmosphere could be utilized in the computation of τ_D and τ_a and in the computation of $\psi(s,t,\theta)$. The quantity $db/d\theta$ would either have to be estimated independently or taken to be given by Eq. (4.15) or by r if $r \ll r_e$.

The computer program mentioned above enabled us to check, for the case of a stratified atmosphere, the extent of validity of the single mode hypothesis (where all modes other than the Lamb edge mode are neglected) by comparison of waveforms calculated according to the Lamb edge mode theory with those computed by the multimode theory as represented by the computer program

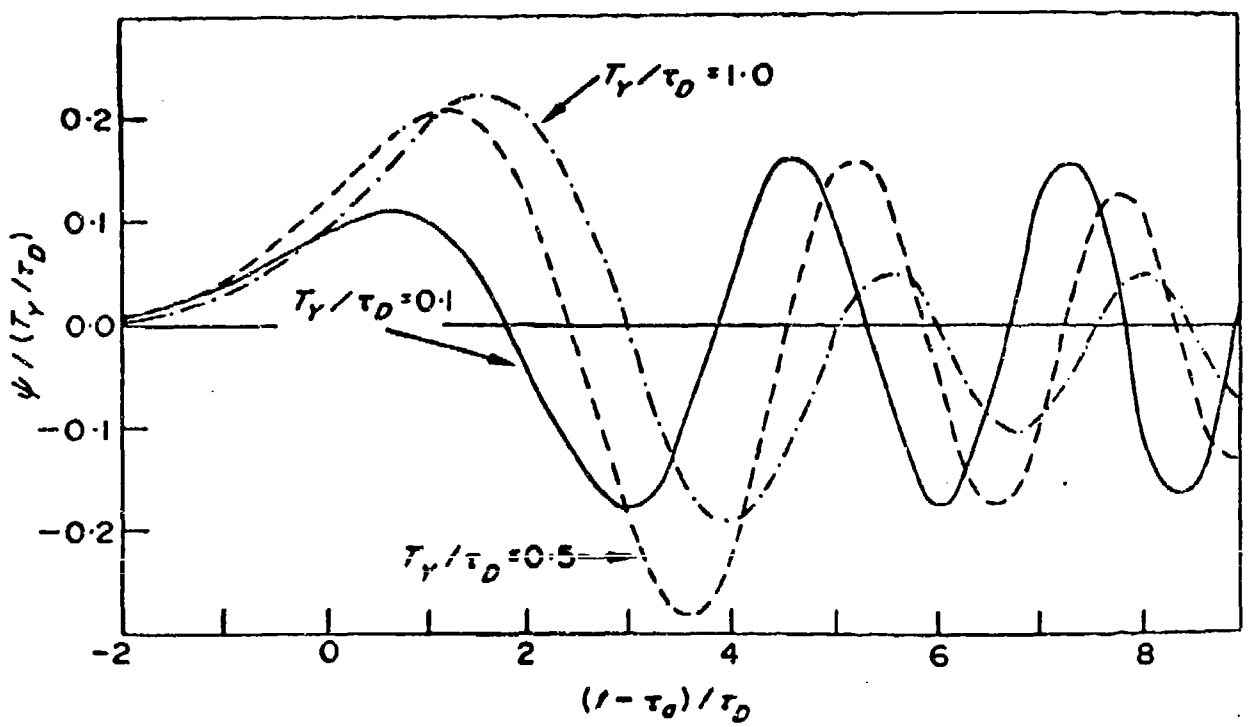

Figure 12. Variation of the waveform factor $\psi(t)$ with the parameter T_Y/τ_D. Here ψ is normalized with respect to T_Y/τ_D and the time is plotted relative to τ_a in units of τ_D.

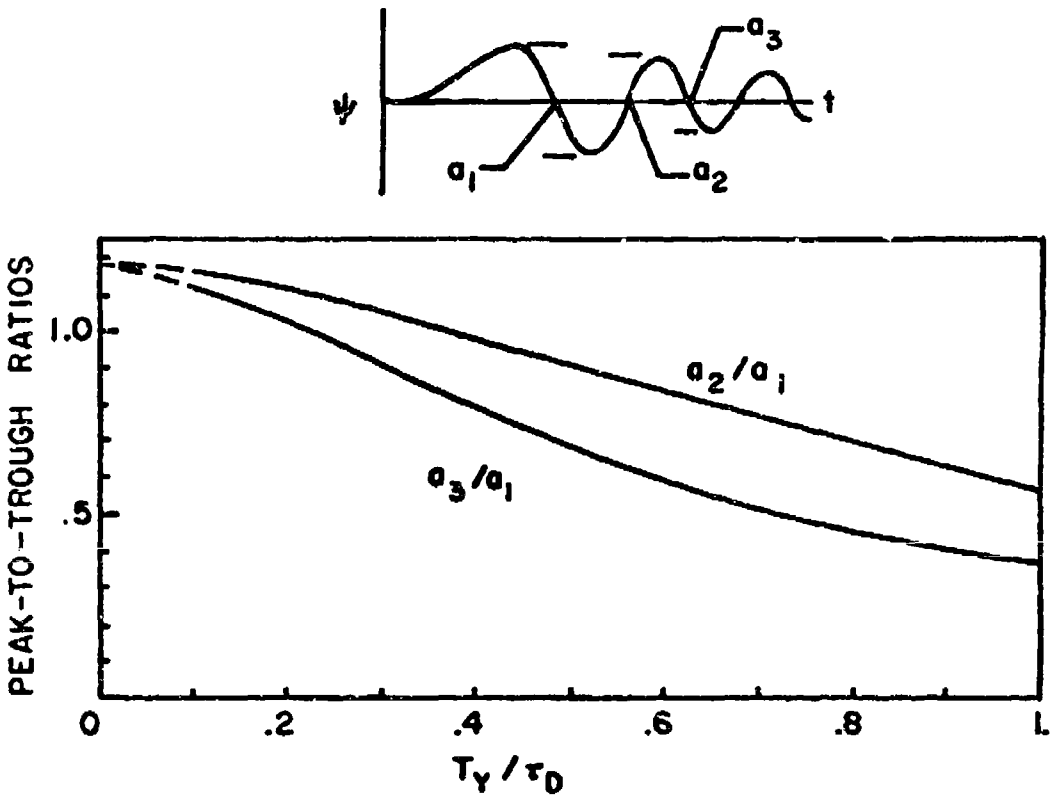

Figure 13. Predicted ratios a_3/a_1 and a_2/a_1 of successive peak to trough amplitudes a_1, a_2, and a_3 in far-field edge mode waveforms produced by nuclear explosions.

INFRASONIC WAVEFORMS. An example we chose for comparison is that where the source was a hypothetical 10MT burst at 3 km above Johnson Island and the observer was at ground level at r = 5600 km at Berkeley, California. The model atmosphere is as described previously, corresponding to the dispersion curves shown in Fig. 9. The numerical calculations give c_L = 0.312 km s^{-1}, v_{Lk} = 0.005 km s^{-1}, the source characteristic time T_Y as 12 s, the effective low-frequency sound speed c_e as 0.318 km s^{-1}, the dispersion constant h_{kk} as 0.13 $km^3 s^{-1}$, the arrival time τ_a as 17600 s (4.9 hr), while the characteristic dispersion time τ_D is 60 s. Thus T_Y/τ_D is 0·2.

In Fig. 14, the first 15 min of (1) an experimental waveform, (2) a waveform computed according to the multimode theory, and (3) a waveform computed according to the edge mode theory are simultaneously plotted. The experimental waveform is that recorded at Berkeley, California following the megaton class Housatonic shot of 1962 October 30 and which is given by Donn and Shaw [1967] in an inverted form (Professor Donn has informed us that the maximum peak-to-trough amplitude of this record is about 350 μbar). The second waveform, based on the multimode theory, has what we regard, albeit subjectively, as a relatively good agreement in waveform shape and period-time variation with the experimental record. The comparison of central concern here, however, is that between the second and third records. One should note that over the first three cycles the agreement is substantial. The zero crossings coincide almost exactly, while the heights of individual peaks or depths of individual troughs agree well except for a discrepancy of 30 per cent in the first peak and first trough. The greater disagreement at later times is to be expected, in view of the fact that the higher frequencies arriving at these times may be carried in other modes corresponding to natural channeling within an altitude region of lower effective sound speed.

As for those discrepancies which do exist at earlier times, particularly the 'precursor' dip in the multimode synthesis, it is difficult a priori to say which theory gives the more nearly correct prediction. The edge mode theory presented here is sufficiently simple that negligible numerical errors arise in the computation. On the other hand, the multimode synthesis is based on numerical computations of inverse Fourier transforms (the integration variable being frequency), where the limits of integration are truncated. The truncations having the most significant effect are those at the low frequency cut-offs shown in Fig. 9 which correspond to the transition from fully-ducted modes to leaky modes [Harkrider & Wells 1968]. The neglect of these leaky modes may place spurious precursors in the synthesized waveforms with periods of the order of the lower cutoff frequency, although hopefully this neglect will have negligible effect on the dominant portion of the waveform (the high-frequency part of the apparent precursor is due to the choice of upper integration limit). In contrast, within the context of the

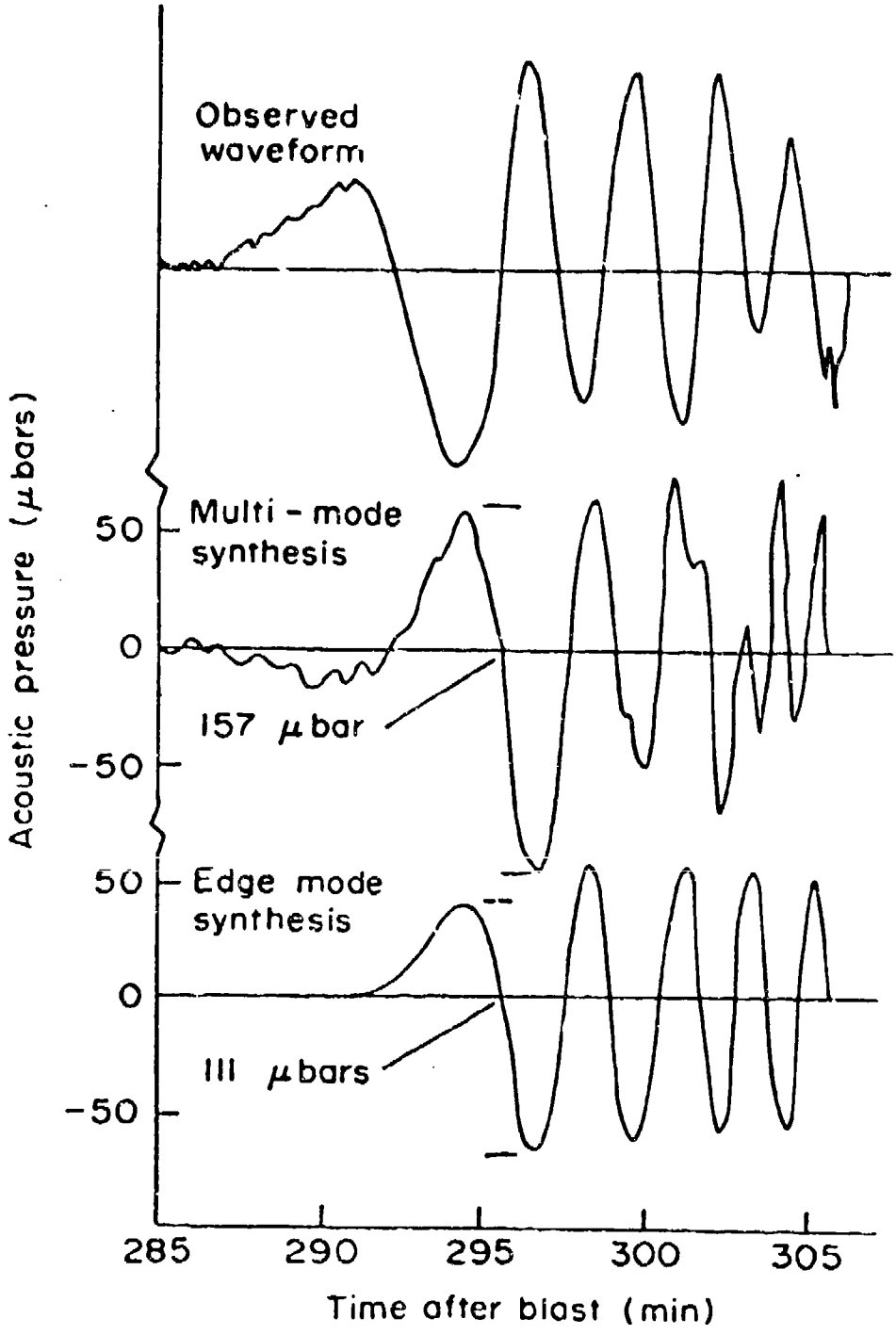

Figure 14. Observed and theoretical pressure waveforms at Berkeley, California, following the Housatonic detonation at Johnson Island on October 30, 1962. The observed waveform is taken from Donn and Shaw [1967]. The energy yield assumed in the theoretical computations was 10 MT. The maximum peak to trough amplitude of the experimental waveform is about 350 μbar.

edge mode theory presented here, the edge mode is formally fully ducting down to zero frequency, and there is no occasion to decide whether or not one should include leaky modes in his computation scheme.

4.5 IMPLICATIONS OF THE EDGE MODE THEORY

The edge mode model, being a simplified approximate model, certainly cannot give a detailed explanation of the existing data, and in many instances may lead to predictions which disagree significantly with the data. However, if one adopts the view that the edge mode model provides a framework for discussion of the data, then there is perhaps some merit in listing a number of the implications of the model, with various idealizations as to the atmospheric structure. If the predictions do not agree with the data in some respect, then we may seek to find what modifications or extensions are necessary to the theory, rather than to abandon the edge mode model completely.

4.5.1 Variation of waveform period with distance

The theory, in the normal limit when $T_Y/\tau_D<1$, predicts that the period, first peak to second peak, should increase with distance r from the source as $r^{1/3}$ for the stratified atmosphere model. This follows from Fig. 12 and Eq. (4.19b). The data does show some trend towards longer periods at greater distances, but the spatial variations with azimuthal angle are substantial. Since this is a relatively weak dependence on r, it is difficult to check quantitatively.

4.5.2 Ratios of successive periods

The waveform factors plotted in Fig. 12 suggest that the ratio of the first two periods (first peak to second peak, second peak to third peak) should be 4/2.6≈1.5. On the whole, the agreement with data of this prediction is fair. Periods tend to decrease with increasing time within a waveform, and in those instances where the peaks may be clearly identified, the ratio varies between 1.3 and 1.8. For example the New Orlea ,La., record of 1961 October 30, the ratio (depending on what one interprets as the first and third peaks) might be evaluated as 1.5.

4.5.3 Record begins with pressure rise

That the theory predicts this is clear from the curves in Fig. 12. This, while admittedly a qualitative rather than quantitative prediction, is reasonably well supported by the data. For example, in those records

given by Donn et al. [1963] where the positive pressure direction is indicated, and where one can distinguish the signal onset from the noise, the first positive pressure peak precedes the first trough.

4.5.4 Ratio of successive peaks

If T_Y/τ_D is small (which, as may be noted from the numerical example in the preceding section, is the normal case) then the first peak should be lower than the second peak and the ratio, first trough to second peak divided by first peak to first trough, should be about 1.2. The agreement of this prediction with the data is negligible. On many records the second peak is actually smaller, and the ratios of the two seem random. The disagreement may be due to a variety of causes: instrument response, interference from other modes, higher-order terms in the dispersion relation, interference from ambient noise, etc.

4.5.5 Variation of waveform amplitude with distance

In the case when there is negligible focusing of horizontal edge mode rays, the theory, Eqs. (4.11) and (4.15) , predicts that wave amplitude varies with great circle distance r as $[\sin(r/r_e)]^{1/2}\psi$, while individual peaks of the waveform factor ψ, for the stratified atmosphere mode, decrease with r in the limit of small T_Y/τ_D as $\tau_D^{-3/2}$ or as $r^{-1/2}$ from Eqs. (4.19) and (4.21). Thus amplitude varies in the idealized case as $r^{-1/2}[\sin(r/r_e)]^{-1/2}$. This variation, as previously discussed by Harkrider [1964], agrees relatively well with the data of Wexler and Hass [1962], although there are substantial variations of amplitude with azimuth angle. In Fig. 15, maximum amplitudes of synthesized Lamb mode waveforms [Posey, 1971] are compared with similar results presented by Harkrider [1964] for synthesized multi-mode waveforms [multiplied by $p_o(z_o)/p_o(z_g)$ as suggested by Pierce, 1965] and with the empirical data presented by Wexler and Hass. The atmospheric model and the source parameters used in the Lamb mode syntheses are the same as used by Harkrider; i.e., a 58 MT explosion at an altitude of 3.66 km in the ARDC standard atmosphere, as shown in Harkrider's Fig. 1, with no winds.

4.5.6 Determination of Explosion Energy from Pressure Waveforms

One of the more intriguing consequences of the Lamb edge mode theory is that it affords a simple method which is relatively insensitive to atmospheric structure for estimating an explosion's energy yield from experimental pressure records. As noted in Sec. 4.3, the shape of the waveform factor ψ is determined solely by the value of T_Y/τ_D .

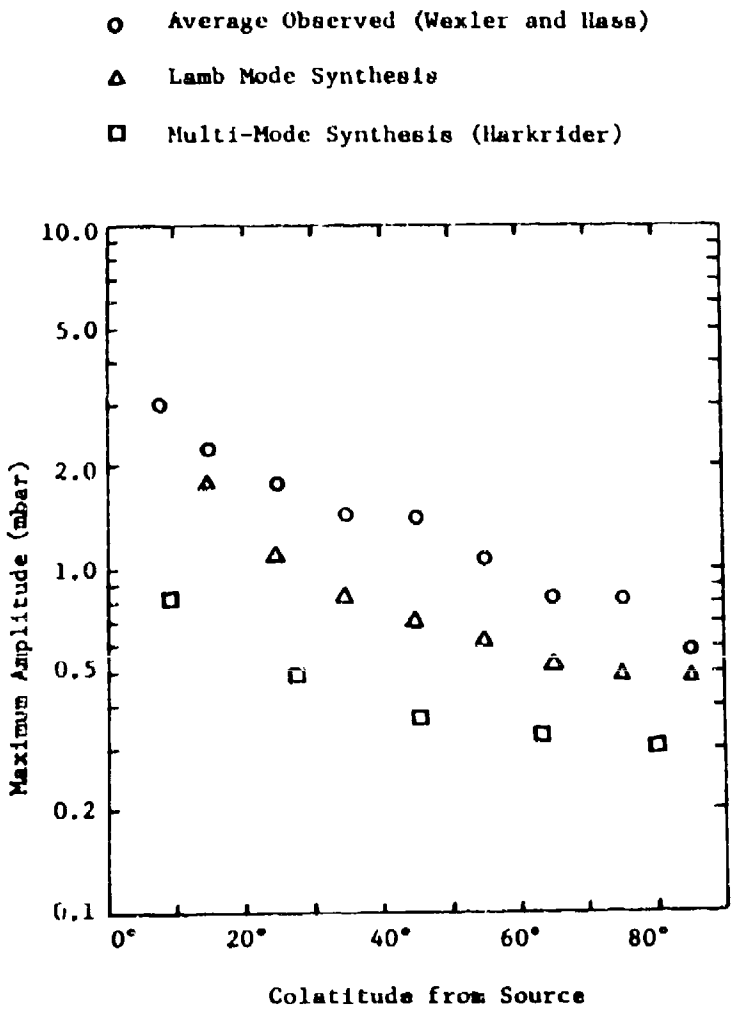

Figure 15. Comparison of observed and theoretical variation of maximum amplitude with distance from the source. The results of a series of Lamb mode syntheses are compared with observations reported by Wexler and Hass [1962] and with the results of waveform syntheses performed by Harkrider [1964] using a multi-mode formulation. (Harkrider's reported amplitudes are here corrected by the factor $p_o(z_o)/p_c(z_g)$ suggested by Pierce [1965], which in this case is about 0.76.)

Moreover, the ratios of the periods to τ_D in the first few cycles would appear from Fig. 12 to be relatively insensitive to this ratio. One finds, in particular, the period $T_{1,2}$ between first and second peaks is given by $4.0\ \tau_D$. Thus one can replace the largely a priori unknown quantity τ_D in the theoretical expressions by $T_{1,2}/4$. The plots in Fig. 12 also show that the quantity a_1, representing the first peak to first trough amplitude of ψ, is a slowly varying function of T_Y/τ_D. A relatively good approximation (within 10%) for most cases of interest is to set

$$a_1/(T_Y/\tau_D)^{3/2} \approx 0.9 \tag{4.23}$$

With the above approximations in mind, one may note that if Eq. (4.11) is written

$$p = G\psi \tag{4.24}$$

where G is an abbreviation for the quantity in braces in Eq. (4.11), then the absolute pressure variation p_{FPT} from the first peak to the first trough should be given by

$$p_{FPT} = G\, a_1 \tag{4.25}$$

or, from Eq. (4.23) and the approximation $\tau_D = T_{1,2}/4$, as

$$p_{FPT} = (G)(0.9)(4T_Y/T_{1,2})^{3/2} \tag{4.26}$$

When the expression for G is inserted and one solves for E, one finds

$$E = \left\{ \frac{c_{Lo}^{7/2}(db/d\theta)^{1/2}}{7.2\ D\ V\ g} \right\} p_{FPT}\ T_{1,2}^{3/2} \tag{4.27}$$

where the various quantities are as defined in Sec. 4.3.

This can be further simplified if a number of plausible assumptions are made: (1) the atmosphere is assumed to be horizontally stratified; (2) the ground level pressure at source and observer is taken to be one atmosphere; (3) the observer is considered to be on the ground; and (4) wind

velocities are considered small compared to the sound speed. In this event, one finds the energy yield to be given by (in equivalent kilotons of TNT)

$$Y = B \sin^{1/2}(r/r_e)[p_o(\vec{x}_o)]^{1-(1/\gamma)}[c(\vec{r}_o)\ T_{1,2}]^{3/2} p_{FPT} \qquad (4.28)$$

where $B = 0.199$ if p_o is measured in atmospheres, p_{FPT} is measured in μbar, c in km/sec, $T_{1,2}$ in seconds, and Y in KT.

Equation (4.28) would enable one to estimate the yield Y if the height of burst were known. Usually, this is not the case. However, the dependence on ambient pressure or burst height is relatively weak. The variation only amounts to 30% even for heights as great as 10 km. The speed of sound at the source can also vary, but generally stays within 15% of 310 m/sec for the first 60 km. Thus, it would appear expedient and not too gross an approximation to set $p_o(\vec{x}_o)$ equal to 1 atm and to set $c(\vec{x}_o)$ equal to 310 m/sec. When this is done one finds

$$Y = B' \sin^{1/2}(r/r_e)\ T_{1,2}^{3/2}\ p_{FPT} \qquad (4.29)$$

where B' has a value of

$$B' = 0.034\ \ \mu bar^{-1}\ sec^{-3/2}\ KT \qquad (4.30)$$

Because of the nature of the approximation outlined above, this prediction of energy yield may be too large for high altitude explosions or for records at long ranges from small yield explosions (i.e., $T_Y/\tau_D < 0.2$) and too small for records at short ranges from large yield sources (i.e., $T_Y/\tau_D > 0.2$).

The waveform parameters $T_{1,2}$ and p_{FPT} read from an observed microbarogram should properly be used in the above yield estimation formula only when the record prior to the second peak represents almost solely the Lamb mode pressure perturbation. In principle, this can only be the case when there is negligible background noise, when there is not yet appreciable contribution to the record from other modes, and when there is negligible phase shift due to instrument response.

In order to check the agreement between the approximate Lamb mode relation and the empirical waveforms, the quantities p_{FPT} and $T_{1,2}$ were measured on a number of records presented by Harkrider [1964] and by Donn and Shaw [1967]. The explosion sources for the records (generally recorded at more than one geographic location) are labeled a through n (see Table II).

event	date	Båth's Yield Estimate (MT)	R(km)	$T_{1,2}$(sec)	p_{FPT}(μbar)	Source of Microbarogram
a	9/10/61	10	3676	193	100	DS
			6644	280	70	DS
b	9/11/61	9	8000	229	125	H
c	9/14/61	7	6569	258	61	DS
d	10/4/61	8	8000	220	80	H
e	10/6/61	11	6674	300	59	DS
			8000	390	45	H
f	10/20/61	5	8000	310	21	H
g	10/23/61	25	6677	376	280	DS
h	10/30/61	58	6688	400	500	DS
			5631	540	133	DS
			8000	690	140	H
i	10/31/61	8	5717	386	25	DS
j	5/4/62	3	5375	200	36	DS
k	6/10/62	9	2177	187	125	DS
l	6/12/62	6	2172	200	55	DS
m	6/27/62	24	2192	187	264	DS
			5393	433	83	DS
			9307	500	90	DS
			9350	467	90	DS
n	7/11/62	12	2185	200	180	DS

Table II. Observed amplitudes and periods. This data corresponds to empirical microbarographs published by Donn and Shaw [1967] and by Harkrider [1964], refered to as DS and H, respectively. (a-i, U.S.S.R. explosions; j-n, U.S. explosions).

The records used include all of those in these two data collections for which Bath [1962] gives a source yield estimate, for which the pressure scale could be determined and for which the first cycle of the signal is recognizable above the background noise. Pressure amplitudes for Harkrider's records were computed using his microbarograph response data. Pressure amplitudes for the Donn and Shaw records were determined according to the premises (W. Donn, private communication) that (a) all records recorded by Lamont type A microbarographs are to the same scale and (b) the clip to clip amplitude of off scale oscillations was 350 μbars. The ordinate in Fig. 16 gives $p_{FPT}/[Y\sin^{-1/2}(r/r_e)]$ in μbar MT^{-1} where Y is the explosion yield in MT. The abscissa gives the period $T_{1,2}$ in s . Note that the plot is full logarithmic. The solid line represents the theoretical relation of Eqs. (4.29) and (4.30).

Although Posey and Pierce [1972] have demonstrated that the value of the constant B' in Eq. (4.29) is somewhat sensitive to the assumed form of the negative phase of the blast wave at close-in distances, it appears that the value actually derived gives the optimum fit to the data. The scatter about the theoretical curve could be due to various causes other than interference with the Lamb mode by other modes and by noise. One possibility which seems especially likely is the variation in amplitude due to the horizontal refraction and subsequent focusing and defocusing caused by departures of the atmosphere from perfect stratification.

One may properly argue that the plot in Fig. 16 at best only demonstrates that estimates of yield based on the theory outlined here are consistent with Bath's estimates. Thus it may be of some interest here to briefly review the basis for Bath's estimates.

According to Bath, the yields of the U.S.S.R. atmospheric tests of October 23 and October 30, 1961, were announced as 25 and 58 MT, respectively, and Bath says that American estimates set the height of burst for each at about 3600 meters. By ignoring height of burst effects and assuming a linear relation between yield and amplitude of the seismic surface wave as recorded at any given station in Sweden for all air blasts above the Novaya Zemlya test site, Bath estimates the yields of the remaining atmospheric explosions in the fall, 1961, Soviet test series. Each estimate is an average based on from 3 to 11 observations. Bath feels that these estimates (shown in his Table XII) are "fairly reliable". He also gives estimates for the yields of some of the atmospheric tests conducted by the U.S. near Christmas Island in 1962, apparently based on seismic energy estimates from seismic surface waves recorded at Uppsala, Sweden, and assuming a constant seismic coupling factor α [seismic energy/yield] of 2×10^{-5}. One might tend to believe that Bath's yield estimates for the Novaya Zemlya shots are probably more reliable than for the Pacific shots because results from several observations were averaged to get the former and because the latter were much further from Sweden. One may note also

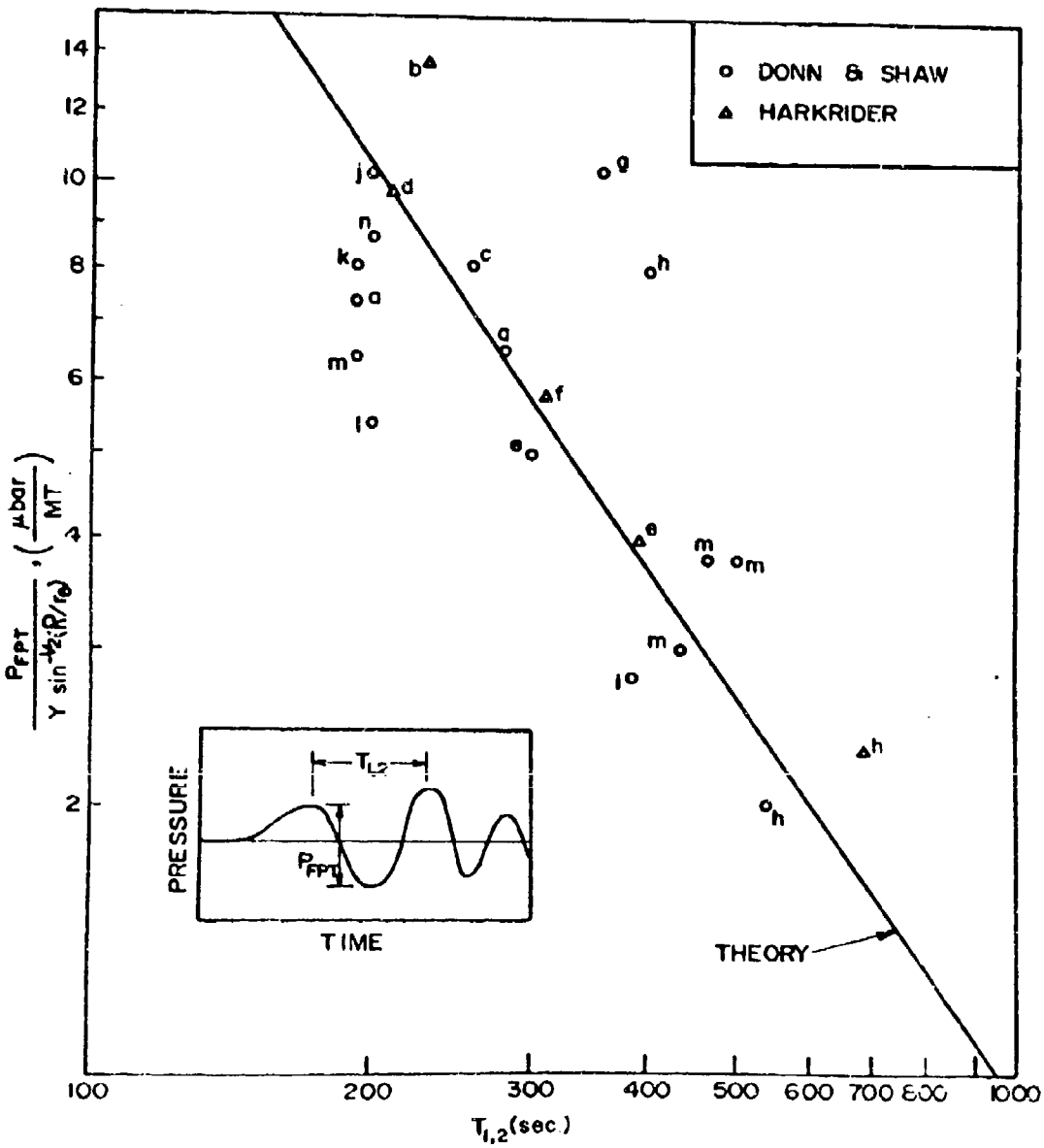

Figure 16. Comparison of data with the theoretical relation between amplitude and period of infrasonic waveforms generated by nuclear explosions. The data points are lettered a to n corresponding to particular events defined in the text.

that Bath's estimates are based on the following general relation between the yield and the Richter scale magnitude M:

$$M = 5.1 + 0.7 \log \alpha Y$$

where α is the seismic coupling factor.

4.5.7 The anomalous spatial variations in amplitude may be explained in terms of focusing or defocusing of horizontal ray paths

This prediction is based on the presence of the factor $(db/d\theta)^{-1/2}$ in the denominator of Eq. (4.11) where $(db/d\theta)d\theta$ is the ray channel width separating rays θ and $\theta + d\theta$. Such anomalous amplitude variations have been reported in some detail for pressure waves recorded following the Soviet explosion of 1961 October 30, by Wexler and Hass [1962]. For example, the amplitudes recorded in Illinois tended to be 2 to 4 times larger than those recorded in Nebraska or Kansas. The ray equations suggest that, if $|\vec{v}_L| << c_L$, the ray paths are nearly perpendicular to lines connecting stations which receive the pressure wave simultaneously. Thus the model would suggest that one might be able to predict regions where anomalously high or low amplitude waveforms are recorded from an examination of lines of constant arrival time. This is in fair accord with the data exhibited by Wexler & Hass.

Wexler and Hass [1962] give lines of constant arrival times over the entire globe and lines of constant amplitude over the northern hemisphere for the wave generated by the Soviet explosion of October 30, 1961, at Novaya Zemlya. Records from about 1000 barographs were used in determining these lines. They also show a plot of average amplitude vs. colatitude from the source. For the most part, these were meteorological barographs designed to record much slower pressure variations than the 1 to 10 minute periods characteristic of the strongest portion of the explosively generated acoustic-gravity waves. Wexler and Hass also state that most of the charts had a recording speed of only 9 hour/in. This suggests that they might be relatively insensitive to the details of oscillations with periods of 15 minutes or less such as are of interest here and that one could introduce significant time errors through inaccurate mounting of the paper (15 min is only 1/36 inch on the chart). While the above considerations suggest that one not place too great a reliance on the quantitative results presented, some valuable qualitative information on large scale anomalies in waveform arrival time and amplitude is certainly present. (One may note that the greatest rippling in the lines of constant arrival occur in the U.S. and Western Europe, where the density of reporting stations is large.)

For the reasons discussed above, we decided for the present that detailed or elaborate computations of Lamb mode propagation parameters from

existing atmospheric data were not warranted by the accuracy of Wexler and Hass' arrival time and amplitude data (a portion of which is reproduced in Figs. 17 and 18 here). Instead, it seemed appropriate to conduct a simple qualitative comparison between the Wexler and Hass data and the portions of the sea level and 500 mb (about 6 km) northern hemisphere weather maps for 1200 GMT, October 30, 1961, which are reproduced in Figs. 19 and 20, respectively. That is, by an examination of the weather maps, assuming that the average c_L is about the same for rays which are never separated by more than a few hundred kilometers, and taking winds to be geostrophic (parallel to the isobars, clockwise around a high pressure area and counterclockwise around a low in the northern hemisphere, and monotonically increasing in strength with the pressure gradient), one should be able to judge qualitatively how c_E, which is approximately $c_L + v_{Lk}$, varies and whether or not the undulations in the lines of constant arrival and/or the amplitude anomalies reported by Wexler and Hass are due to this variation. Of course, implicit in such a comparison is the assumption, which is not necessarily true, that both the earliest observation and the wave's largest amplitude are due to the Lamb edge mode. The former is more likely true than the second.

For the sake of simplicity, it is assumed that the general atmospheric circulation pattern, i.e., the variation of $\vec{v}_L$, is qualitatively represented by the winds at 500 mb. In Fig. 21, the major centers of low or high ambient pressure indicated in Fig. 20 are shown and numbered (L_1 through L_6 for the lows, and H_1, H_2 and H_3 for the highs). At each location the direction of the geostrophic wind is indicated by the arrows. The location of the 58 MT blast at Novaya Zemlya (73.82°N, 53.57°E according to Donn and Shaw [1962]) is shown by a star. As a ray propagates through the center of a low pressure system, the rays to its right should propagate more rapidly and those to its left more slowly because of the counterclockwise circulation. The opposite is true at the center of a high.

An unrefracted ray (great circle path from source) through low pressure center L_1 would pass through Alaska, so that the Lamb wave should be retarded in its arrival along the northern coast of Alaska and western Canada relative to its arrival just to the west. The presence of the high H_1 indicates a retarded c_E over the northern Canadian islands relative to the western coast of Greenland and an increased c_E down the eastern coast. All of these contentions are supported by the undulations of the 1200 GMT arrival line shown in Fig. 17.

The low pressure center L_4 is just about on the 1300 GMT line, so that its effect should be evident in the changes from 1200 to 1400 GMT, and, indeed, while the former is fairly straight north of L_4, the latter displays a wiggle consistent with increasing c_E from east to west just below L_4.

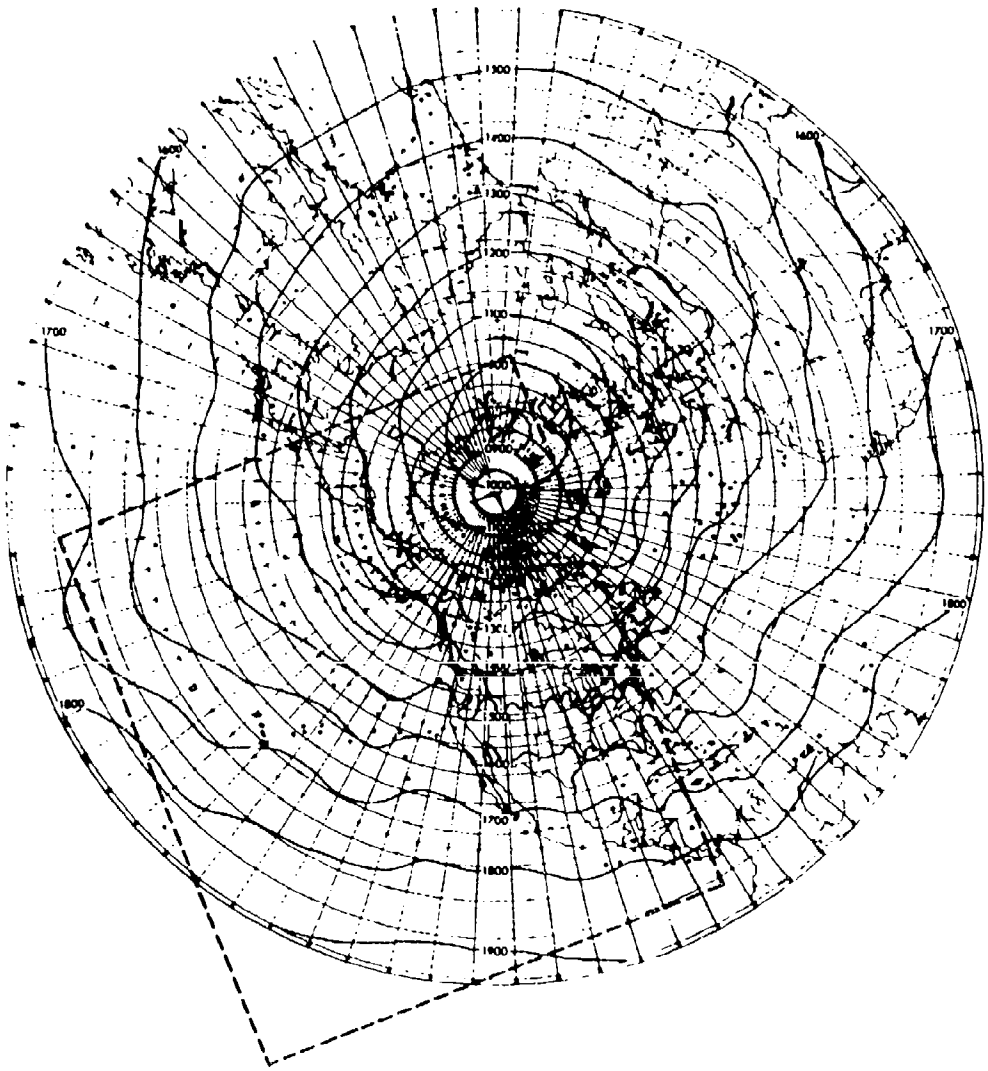

Fig. 17. Observed Arrival Time of an Infrasonic Wave. The source of the wave is the Soviet thermonuclear blast over Novaya Zemlya, October 30, 1961, at about 0830 GMT, and the recording instruments are barographs at weather stations or on ships. The dashed rectangle indicates the portion of the northern hemispheric map shown in Figs. 19-21 . **(Extracted from paper by Waxler and Hass** [1962].)

Fig. 18. Maximum Observed Amplitude of an Infrasonic Wave. This map is for the same disturbance as in Fig. 17, and is derived from the same records. The amplitude is given in mbars. (Extracted from paper by Wexler and Hass [1962].)

Similarly, the effect of L_2 is seen to be consistent with expectation from a comparison of the 1200 and 1400 GMT lines in its vicinity. The effect of L_3 can be seen by comparing the 1400 and 1600 GMT lines between about 150°E and 170°W. Changes in c_E due to winds about H_2, L_5, H_3 and L_6 are not as clear, but, as can be seen in Fig. 20, each of these except L_5 is a weak pressure center surrounded by relatively small pressure gradients and winds. In the portion of the northern hemisphere not shown in the 500 mbar map of Fig. 20, there were only three strong pressure systems, of which two, a low just east of Iceland and a high over the Caspian Sea, seem to produce undulations in the time lines consistent with the assumed variation of $\vec{v}_L$.

The above comparison shows that many of the irregularities of the order of 1000 km in the lines of constant arrival time can be qualitatively attributed to the variation of $\vec{v}_L$. Some other large scale irregularities cannot be explained by the assumed circulation pattern and are probably due to strong winds above the 500 mb level which do not conform to that pattern or to variations in c_L, which are ignored. A portion of the smaller scale irregularities could be due to instrumentation errors.

While the earliest portion of an explosively generated acoustic-gravity wavetrain is most likely due to the Lamb mode, the largest amplitude may or may not be due solely to the Lamb mode, depending primarily upon ducting conditions above the observer. Thus, it would not be suprising should the amplitude anomalies of Fig. 18 not be as easily explained by the Lamb mode theory as are the arrival time irregularities.

In order to determine whether the observed large scale variations in overpressure amplitude (of the order of 1000 km) are the result of horizontal refraction due to variations in c_E, the empirical lines of constant arrival are assumed to be lines of constant phase for the Lamb mode. That is, rays should be nearly perpendicular to these lines, so that a concave line would lead to focusing of the Lamb mode rays while a convex line would lead to defocusing. This effect is witnessed in some instances, such as in the Atlantic, where the convex lines of constant phase in the east are accompanied by small observed amplitudes and the concave lines in the middle Atlantic are accompanied by larger amplitudes. However, some of the pronounced amplitude variations, such as the increase over Indochina, cannot be explained by the assumed Lamb mode refraction pattern.

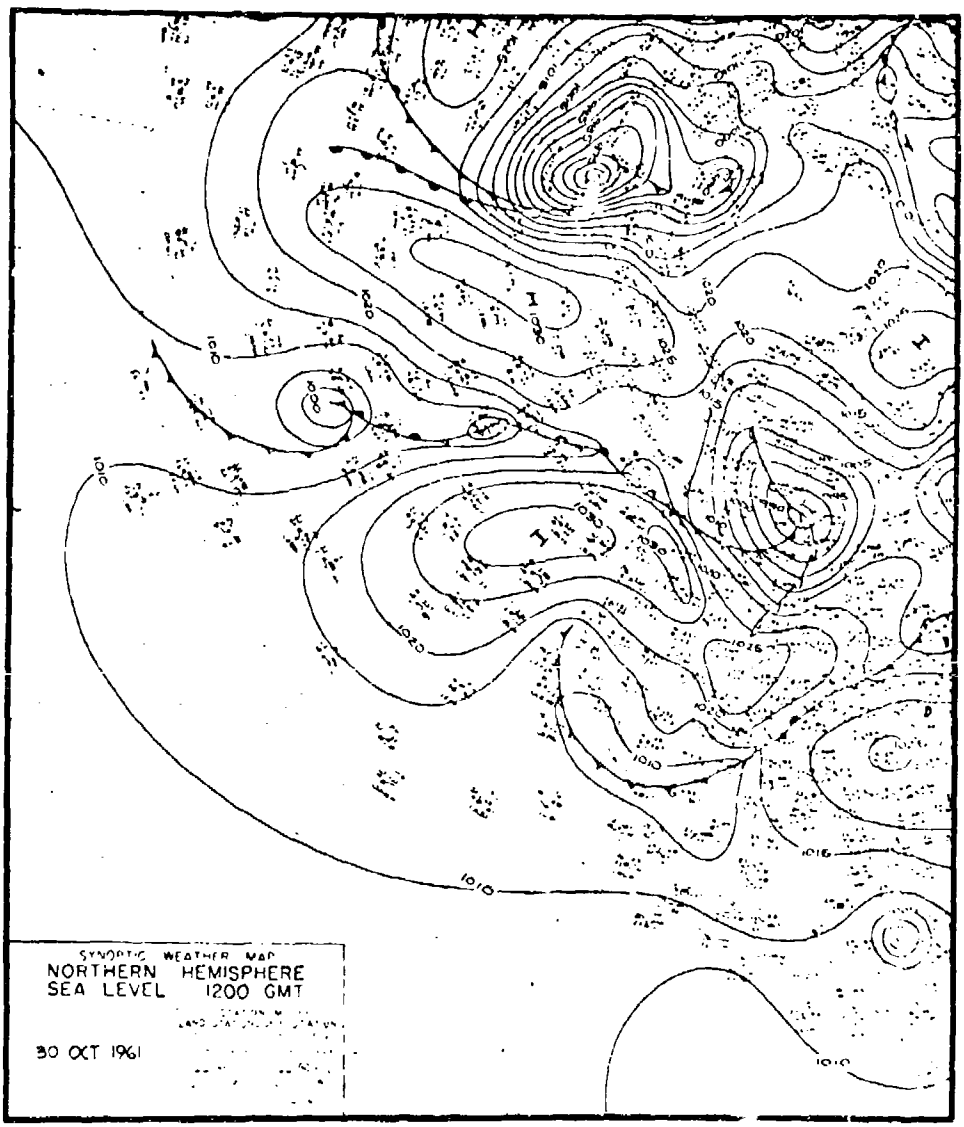

Fig. 19. Sea Level Synoptic Weather Map for the Northern Pacific Ocean and North America. The portion of the northern hemispheric map indicated by the dashed box in Fig. 17 is shown here.

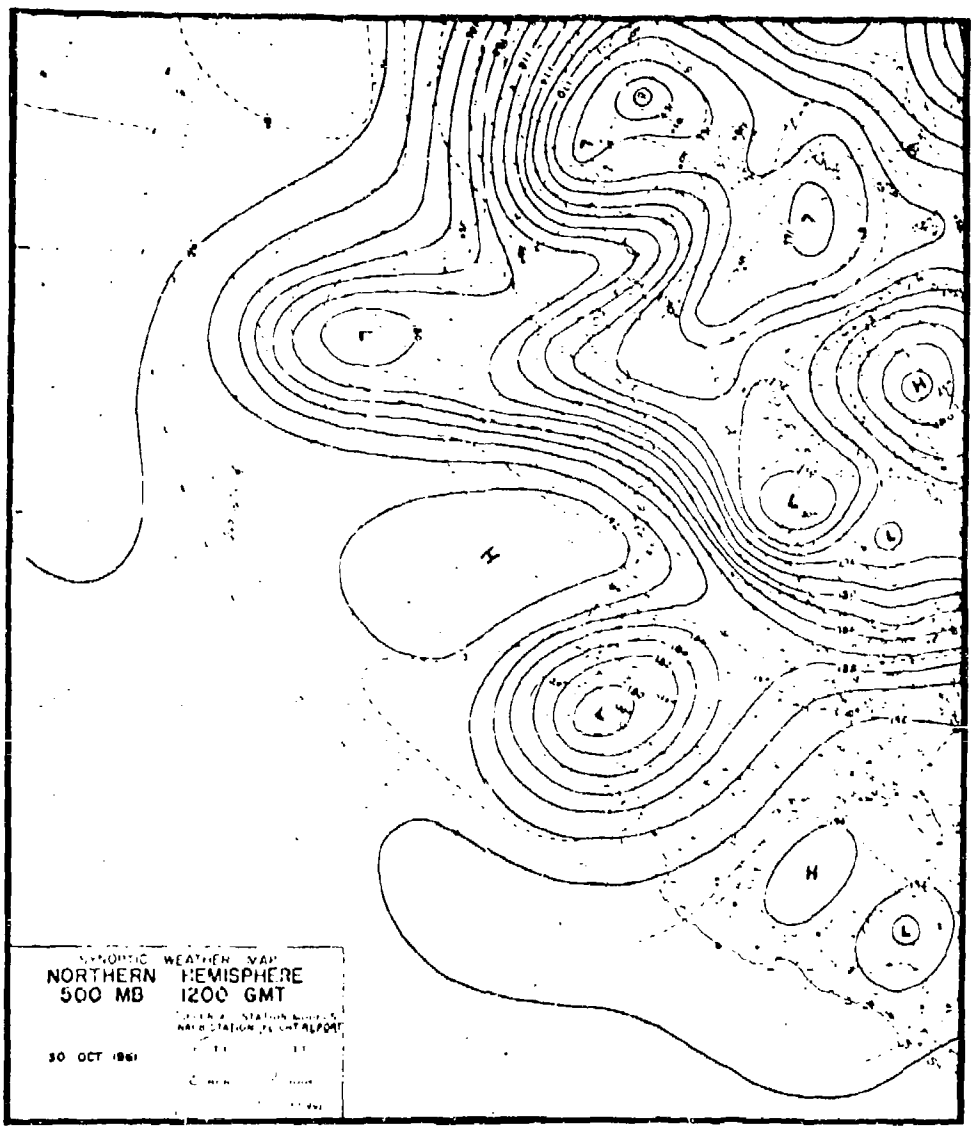

Fig. 20. 500 mbar Synoptic Weather Map for the Northern Pacific Ocean and North America. The portion of the northern hemispheric map indicated by the dashed box in Fig. 17 is shown here.

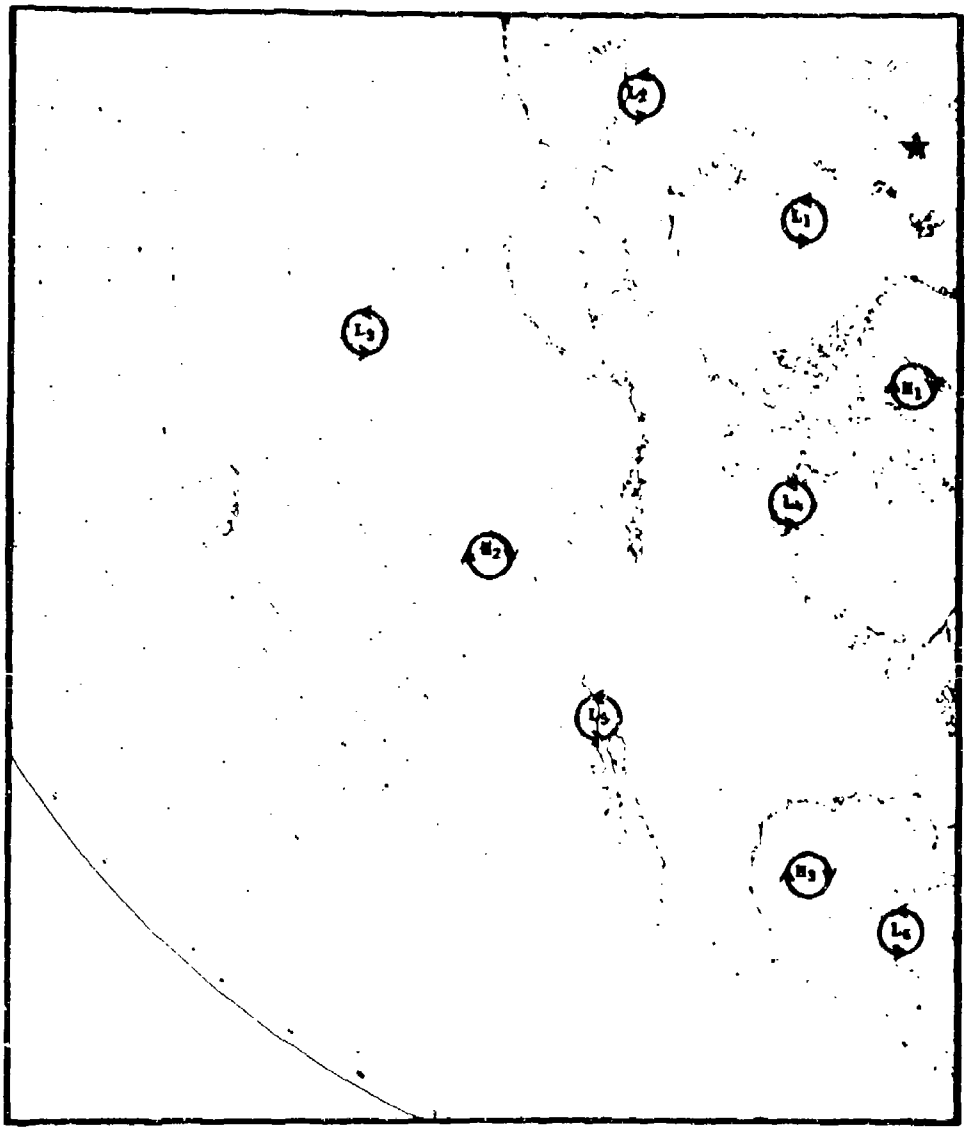

Fig. 21. High and Low Ambient Pressure Centers. The high and low pressure centers shown in Fig. 20 are labeled and the direction of circulation about each noted. The location of the Soviet explosion of October 30, 1961, is indicated by a star.

CHAPTER V

A SHORT PERIOD MODEL FOR WAVES GENERATED BY EXPLOSIONS

5.1 INTRODUCTION

The theories and computational techniques described in the previous two chapters apply best for interpretation of the lower frequency (2 to 15 minute periods) recorded at very large distance from megaton class nuclear explosions. We have recently started to develop an alternative theory applicable to shorter period signals generated by lower yield explosions or observed at closer-in distances. In the present chapter, the salient features of this theory are briefly reviewed.

5.2 RAY PATHS

The basic mathematical model presumes that the pressure wave disturbance at any given point somewhat removed from the immediate vicinity of the point of detonation can be expressed in the form

$$p(\vec{x},t) = \sum_{\text{rays}} p_{\text{ray}}(\vec{x},t) \qquad (5.1)$$

where the sum includes one term for each of the geometric acoustic ray paths which connect the point of detonation with the observer location, including those rays which may have been reflected one or more times at the ground. (In order to facilitate bookkeeping, it is assumed that the observation point is never identically on the ground, although it may be a very small distance above it.)

In the simpler version of the theory, presently under study, it is presumed that these ray paths may be taken to be those appropriate for higher frequency low amplitude disturbances. In the limit, the paths are independent of frequency and wave amplitude. This approximation does not necessarily imply a neglect of nonlinear effects or of frequency dispersion and has some precedence in the contemporary theories of sonic boom propagation [Whitham, 1956; Hayes, Haefeli, and Kulsrud 1969] where nonlinear affects are neglected in the determination of ray paths but included in the consideration of propagation along ray tubes.

The method of determination of such ray paths for a temperature and wind stratified atmosphere has previously been described by one of the authors in some detail [Pierce, 1966] and a computer program based on that method is presently in use by W. Donn and coworkers at Lamont-Doherty

Preceding page blank

Geological Observatory. (see, for example, Donn and Rind [1971]). A sample plot of such ray paths is shown in Fig. 22. The appropriate ray tracing equations on which such plots are based are

$$\frac{d\vec{x}}{d\tau} = c\,\vec{e}_\kappa + \vec{v} \qquad (5.2a)$$

$$\frac{d\vec{\kappa}}{d\tau} = -\kappa\nabla c - (\vec{\kappa}\cdot\nabla)\vec{v} - \vec{\kappa}\times(\nabla\times\vec{v}) \qquad (5.2b)$$

where, for variable τ, $\vec{x}(\tau)$ traces out the ray path. Here the ambient sound speed c and the wind velocity v are considered as functions of position x. The quantity κ is an auxiliary quantity termed the wave slowness vector (units of reciprocal velocity) which also is a function of the ray time parameter τ. At all points $\vec{\kappa}$ is related to $\vec{v}$ by the equation

$$(1 - \vec{\kappa}\cdot\vec{v})^2 = c^2\kappa^2 \qquad (5.3)$$

In Eq. (5.2a), $\vec{e}_\kappa$ is the unit vector in the direction of $\vec{\kappa}$. Note that in the absence of winds, $\kappa = 1/c$ and $\vec{e}_\kappa$ is the ray direction.

Initial conditions on the integration of Eq. (5.2) are that $\vec{x}$ at $\tau = 0$ represent the point of detonation and that the ray direction point in some given direction specified by parameters (θ_o,ϕ_o) which give the polar and azimuthal angles which $d\vec{x}/d\tau$ initially makes in a coordinate system with the z axis passing vertically through the point of detonation. Thus θ_o and ϕ_o form a means of labeling all rays which emanate from the source.

When a ray meets the ground it is assumed that it reflects specularly such that incident and reflected rays locally near the ground make the same angle with the ground. The horizontal components of $\vec{\kappa}$ do not change on reflection but the vertical component changes sign. It is of course assumed that there is no vertical component of wind velocity at the ground.

In the computation scheme we envision, one of the initial steps would be to find all initial ray parameter pairs (θ_o,ϕ_o) which correspond to rays which are governed by the equations described above and which connect the source and observer positions. Each such ray would then correspond to a term in Eq. (5.1).

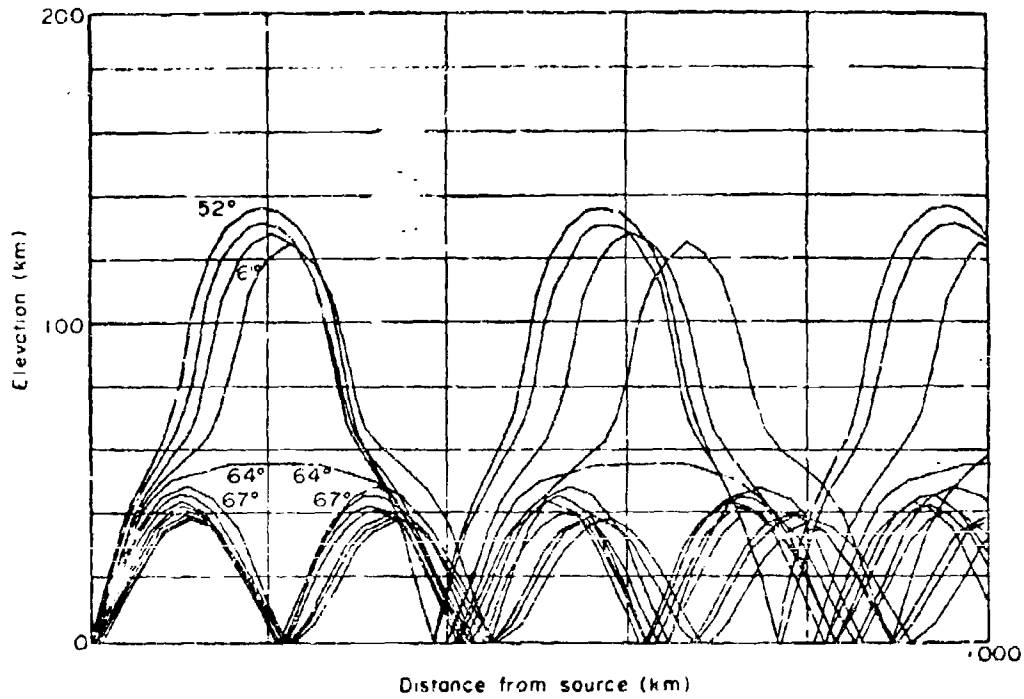

Figure 22. Computer generated plots of ray paths from a point source to the east in summer. (Extracted from paper by Donn and Rind [1971].)

5.3 PROPAGATION ALONG A RAY SEGMENT

For simplicity in the description of the overall computation scheme we speak of a ray segment as a portion of a ray path which contains no ground reflection and along which the ray does not intersect any of its neighboring rays (i.e., the ray does not touch a caustic or, equivalently, the ray tube area does not vanish). While the existence of caustics (i.e., the surfaces in space composed of points at which such intersections occur) must be taken into account in any theory seeking to describe waveforms at all but very close-in distances, the consideration of these is postponed until Sec. 5.5.

Along a given segment, the pressure contribution due to that ray is taken to be of the following form

$$p_{ray} = J(s)\psi(t,s) \tag{5.4}$$

where s is a parameter characterizing distance along a ray path, specifically related to distance ℓ along the path by a relation analogous to that of Eq. (4.20), i.e.

$$\frac{d\ell}{ds} = \frac{c + \vec{v}\cdot\vec{e}_\kappa}{\left|c\vec{e}_\kappa + \vec{v}\right|} \tag{5.5}$$

such that $s = \ell$ for a windless atmosphere. The parameter s is defined such that it is zero at the point of detonation. Thus any given ray segment will in general correspond to a finite range of s.

The parameter $J(s)$ in Eq. (5.4) is independent of time and defined to vary with s in such a manner that wave action [Bretherton and Garrett, 1968] or, equivalently, the Blokhintzev invariant [Blokhintzev, 1946] is conserved. Thus

$$\frac{d}{ds}\left\{\frac{J^2\left|d\vec{x}/d\tau\right|A}{\rho_o c^2(1 - \vec{\kappa}\cdot\vec{v})}\right\} = 0 \tag{5.6}$$

where ρ_o is ambient density, $\left|d\vec{x}/d\tau\right|$ is the ray speed of Eq. (5.2a) and A is ray tube area. Here A is defined as the (s variable) cross-sectional area of any given (small) fixed tube of rays which includes the ray in question. Note that the quantity in braces in Eq. (5.6) is

independent of s. Thus, if J is known at any given value of s, it can be found easily for any other value of s.

In the simplest limit of geometrical acoustics with nonlinear effects neglected, with the neglect of dissipation and with the neglect of any dispersion induced by the effects of gravity, the remaining factor ψ in Eq. (5.4) satisfies the one dimensional wave equation

$$\frac{\partial \psi}{\partial t} + (c + \vec{v}\cdot\vec{e}_s)\frac{\partial \psi}{\partial s} = 0 \tag{5.7}$$

which has the general solution

$$\psi = f(t - \int_0^s \frac{ds}{c_{eq}}) \tag{5.8}$$

where $f(t)$ is any arbitrary function and where we have abbreviated

$$c_{eq} = c + \vec{v}\cdot\vec{e}_s \tag{5.9}$$

as the effective wave speed. However, the approximation represented by the above equations may not be entirely sufficient, so we have sought a generalization of the Eq. (5.7) which incorporates other effects.

5.3.1 Dispersion Effects

To incorporate dispersion into Eq. (5.7) we recall that acoustic-gravity waves in an isothermal atmosphere with constant winds [Pierce, 1966] satisfy a dispersion relation of the general form

$$k_z^2 = (\Omega^2 - \omega_A^2)/c^2 - [(\Omega^2 - \omega_B^2)/\Omega^2](k_x^2 + k_y^2) \tag{5.10}$$

where $\Omega = \omega - \vec{k}.\vec{v}$ is the Doppler shifted angular frequency; k_x, k_y, k_z are the components of the wave propagation vector. Here ω_A and ω_B are the well known characteristic atmospheric frequencies given by

$$\omega_A = (\gamma/2)g/c \tag{5.11a}$$

$$\omega_B = (\gamma-1)^{1/2}g/c \tag{5.11b}$$

If this above dispersion relation is solved for ω, one finds to lowest order in $1/k$ that $\omega = c_{eq}k$, corresponding to nondispersive propagation. If the next nonzero term is included, one finds

$$\omega = c_{eq}k + \frac{1}{2}\,\omega_0^2/\omega \tag{5.12}$$

where

$$\omega_0^2 = \omega_A^2 - \{(k_x^2 + k_y^2)/(k_x^2 + k_y^2 + k_z^2)\}\,\omega_B^2 \tag{5.13}$$

is a positive quantity which depends on the direction of the wave propagation vector $\vec{k}$, but not on its magnitude.

Suppose now that $\psi(s,t)$ in Eq. (5.4) is specified as a function of t at some point s_o on a ray segment. Then if ψ propagates according to the dispersion relation (5.12), its time variation at any other point s on the same ray segment should be given by

$$\psi(t,s) = \mathrm{Re} \int_0^\infty \hat{\psi}(\omega) e^{-i[\omega T + \frac{1}{2}Q/\omega]}\,d\omega \tag{5.14}$$

where

$$T = t - \int_{s_o}^{s} \frac{ds}{c_{eq}} \tag{5.15}$$

$$Q = \int_{s_o}^{s} \frac{\omega_o^2 ds}{c_{eq}} \tag{5.16}$$

and where the Fourier transform $\hat{\psi}_o(\omega)$ is defined such that

$$\psi(t,s_o) = \mathrm{Re} \int_0^\infty \hat{\psi}_o(\omega) e^{-i\omega t}\,d\omega \tag{5.17}$$

Note that the resulting expression for $\psi(t,s)$ represented by Eq. (5.14) would reduce to Eq. (5.8) were it not for the factor $\exp[-i(1/2)Q/\omega]$ in the Fourier transform. It should be understood, of course, that $\hat{\psi}_o(\omega)$ is considered to be largest for higher frequencies than ω_o. Consistent with this, one may rewrite (5.14) in the form

$$\psi(t,s) = R_e \int_0^\infty \hat{\psi}_o(\omega) e^{-i\omega t} e^{i t_{prop} (\omega^2 - \omega_{eff}^2)^{1/2}} d\omega \quad (5.18)$$

where

$$t_{prop} = \int_{s_o}^{s} \frac{ds}{c_{eq}} \quad (5.19a)$$

$$\omega_{eff}^2 = Q/t_{prop} \quad (5.19b)$$

may be interpreted as the propagation time and an averaged value of ω_o^2 along the ray segment, respectively.

One may next reexpress Eq. (5.18) as a convolution integral in the form

$$\psi(t,s) = \int_{-\infty}^{t} G(t - t_o, s, s_o)\psi(t_o, s,)dt_o \quad (5.20)$$

where the Green's function is given by

$$G(t - t_o, s, s_o) = \frac{1}{2\pi} \int_{-\infty}^{\infty} e^{-i\omega(t-t_o)} e^{i t_{prop}(\omega^2 - \omega_{eff}^2)^{1/2}} d\omega \quad (5.21)$$

Here the integration contour extends slightly above the real axis and the branch cut extends from $-\omega_{eff}$ to $+\omega_{eff}$ along the real axis. The integral with some effort may be evaluated as

$$G = \delta(t-t_o-t_{prop}) - \omega_{eff}(\omega_{eff} t_{prop})\{J_1(D)/D\} \quad (5.22)$$

$$\times H(t-t_o-t_{prop})$$

where $J_1(D)$ is the Bessel function of first order and where we have abbreviated D as the positive square root of

$$D^2 = \omega_{eff}^2 \left[(t-t_o)^2 - t_{prop}^2\right] \tag{5.23}$$

The symbols δ and H in the above formulas represent the familiar Dirac delta function and Heaviside step function, respectively.

With the substitution of Eq. (5.22) into Eq. (5.20) one finds that the dispersed waveform is given by

$$\psi(t,s) = \psi\,(t-t_{prop},s_o) - \omega_{eff}^2 t_{prop} \int_{-\infty}^{t-t_{prop}} \{J_1(D)/D\}\psi(t_o,s_o)dt_o \tag{5.24}$$

One may also show that the quantity D may be further approximated as

$$D = \omega_{eff}(2\ t_{prop})^{1/2}(t-t_{prop}-t_o)^{1/2} \tag{5.25}$$

for all practical purposes if ψ is composed primarily of higher frequencies than ω_{eff}.

Although we have at present no computations of Eq. (5.24) to exhibit, it would appear (see Fig. 23) that what is being described by the mathematics in the case of, say, a N shaped wave is the development of an oscillatory tail whose amplitude and length increase with propagation distance and whose period at any given point tends to increase with time at any given point. The latter follows since the zeros of $J_1(D)$ occur at successively larger intervals of t for fixed t_{prop} and t_o. Also, it follows from the fact that the group velocity according to the dispersion relation of Eq. (5.12) tends to decrease with increasing period (decreasing ω).

5.3.2 Nonlinear Effects

If Eq. (5.7) were to be modified to incorporate nonlinear effects, a simple approach (which we in essence adopt here) would be for one to utilize Whitham's rule [Whitham, 1952, 1956] and to replace the travel speed $c + \vec{v}.\vec{e}_\kappa$ by that characteristic of the perturbed rather than the ambient medium, such that Eq. (5.7) becomes

$$\left(\frac{\partial\psi}{\partial t}\right) + c_{NL}\left(\frac{\partial\psi}{\partial s}\right) = 0 \tag{5.26}$$

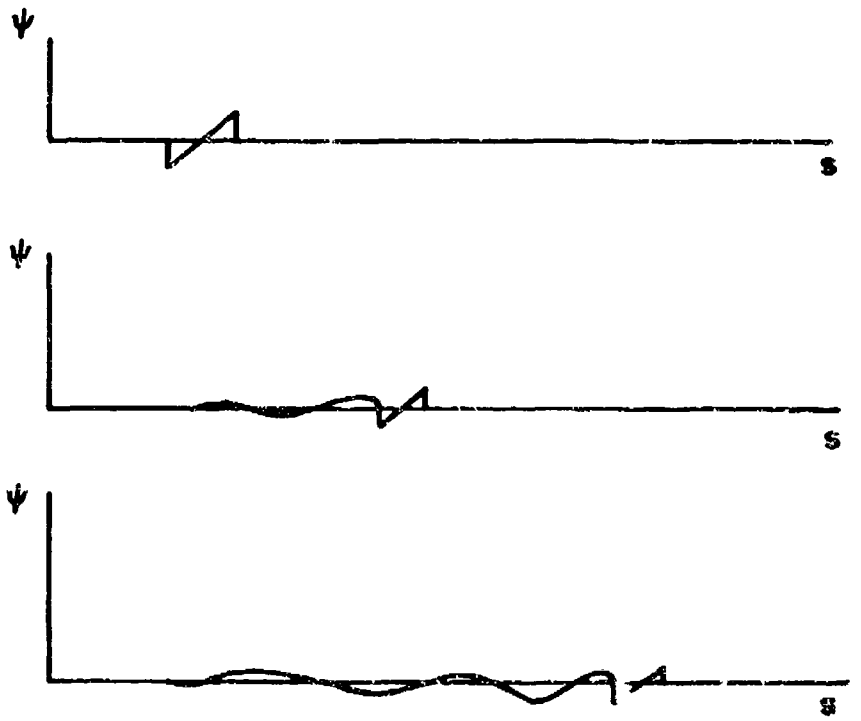

Fig. 23. Sketch of the effects of gravitationally induced dispersion on an originally N-shaped waveform. Successive plots correspond to later values of time. The parameter s is equivalent to distance along a ray path.

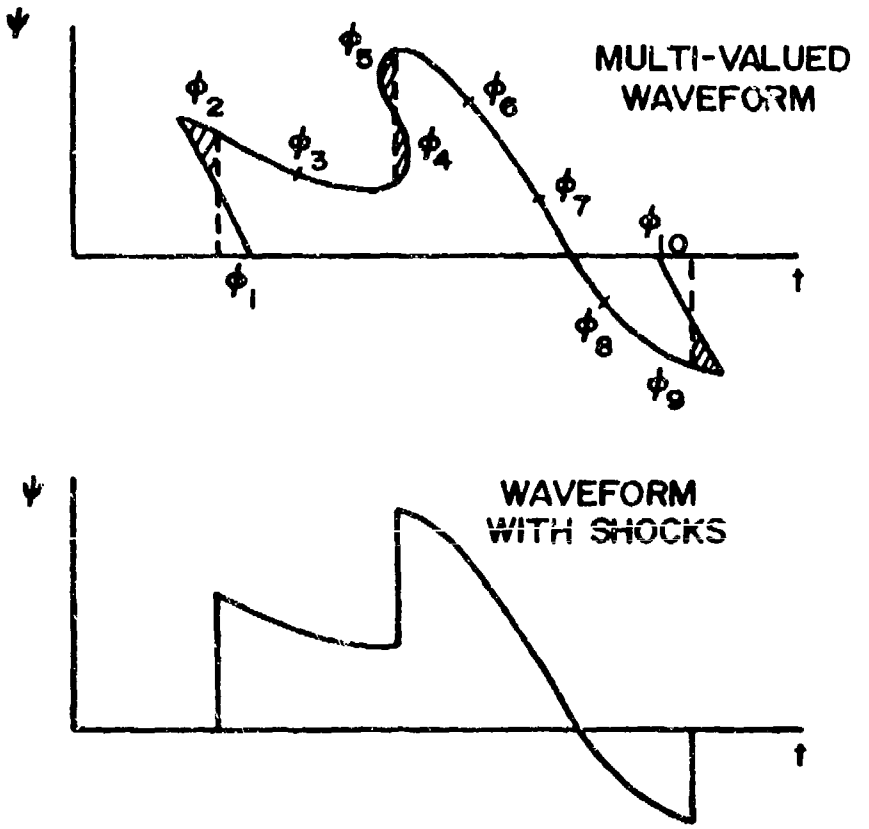

Fig. 24. Sketch of the application of the equal area rule to construct shock locations from a multi-valued waveform.

with the corrected wave speed

$$c_{NL} = c + \vec{v}\cdot\vec{c}_K + c[(\gamma+1)/(2\gamma)]p/p_o \tag{5.27}$$

The third term represents the first order correction to the sum of the sound speed and the fluid velocity for the case of a plane wave propagating in a homogeneous ideal gas. Here p is the acoustic pressure, p_{ray} in Eq. (5.4) , and p_o is the ambient pressure. Equation (5.26) is sometimes referred to as the inviscid Burger's equation.

The above derived nonlinear equation for ψ has the approximate solution which can be given in a parametric form as

$$\psi(s,t) = \psi_o(\phi) \tag{5.28}$$

$$t = \phi + t_{prop} - \mu(s,s_o)\psi_o(\phi) \tag{5.29}$$

where

$$\mu = [(\gamma+1)/(2\gamma)] \int_{s_o}^{s} (J/p_o)(1/c_{eq})ds \tag{5.30}$$

Here ϕ is an auxiliary parameter defined such that it equals time t when $s = s_o$. The function $\psi_o(t)$ gives $\psi(s,t)$ when $s = s_o$. Thus, were s specified, one could let ϕ run through a sequence of values and list corresponding values of ψ and t computed from the Eqs. (5.28) and (5.29). If these values were plotted to give ψ versus t, one would have a plot of $\psi(s,t)$ for fixed s and variable t . [The complication of shocks is considered below.]

In the event that the quantity ψ constructed for given s becomes multiple valued, it is postulated that discontinuities in the actual waveform (i.e., shocks) form. In the time interval between shocks, ψ versus t is still described parametrically by the above equations, only with a restricted range of ϕ. The approximate waveform which incorporates weak shocks may be found graphically by first plotting the multivalued function described parametrically by $[\psi_o(\phi), t(\phi)]$ for variable ϕ and then placing shocks (vertical lines on a ψ versus t graph) in such a way that the equal area rule is satisfied. Each such shock hits the graph at three points and delimits an upper loop on its left and a lower loop on its right (we

assume time runs to the right). The location of the shock is such that the area of the upper loop just equals that of the lower loop (see Fig. 24) and the shock replaces the two loops in the approximate waveform.

One may show, albeit with some effort, that the scheme described above is consistent with the Rankine-Hugoniot relations [see, for example, Landau and Lifshitz, 1959] in the limit of sufficiently weak shocks. Also, if the above method is used twice in succession; waveform at s_2 determined from waveform at s_1 which was previously found from waveform at s_o; then one can show that the resulting waveform is just the same as that which would be found if the waveform at s_2 were determined directly from that at s_o.

5.3.3 Composite Numerical Method

In order to take nonlinear effects and dispersion effects into account simultaneously, one may adopt the following method. Let a given ray segment be divided into a small number of segments, the length of which may be of the order of 100 km or less. The optimal length remains a topic for analytical investigation, although we doubt that one need take it less than 25 km. Let the distance parameter at the near end of one of these segments be s_o, that at the further end be s_1. Given $\psi(t,s_o)$ as a function of time, one seeks to determine $\psi(t,s_1)$ as a function of time.

The first step is to determine a function $\bar{\psi}(t,s_1)$ with the neglect of nonlinear effects, but with the consideration of dispersion. This intermediate waveform is found from Eqs. (5.24) and (5.25), as is discussed in Sec. 5.3.1. Next one defines

$$\bar{\psi}(t,s_o) = \bar{\psi}\ (t + t_{prop},s_1) \tag{5.31}$$

as that waveform which would have resulted in $\bar{\psi}(t,s_1)$ were the propagation from s_o to s_1 to take place without dispersion. This dispersed but time shifted waveform is then used to define $\psi_o(\phi)$ in Eq. (5.28). The nonlinear propagation equations (5.28) and (5.29), along with the method for constructing shocks described in Sec. 5.3.2, are then used to find the function $\psi(t,s)$.

Alternately, one could consider nonlinear effects first, then time shift back, and construct the dispersed waveform from the nonlinearly distorted waveform. Both methods should give virtually the same result if the distance from s_o to s_1 is sufficiently short. What is assumed is that over short distances the two forms of distortion, nonlinear and dispersive, are additive. Over large distances the distortion due to either may be large, but the distortion is an accumulative effect which is small over short distances.

The above scheme can be used repeatedly over a sequence of subsegments such that one can in principle with, hopefully, only a modest amount of computing find the waveform at the further end of a chain of subsegments from a knowledge of the waveform at the nearer end.

Similar considerations may be employed to incorporate viscous and thermal dissipation into the calculation, although we have not yet derived the appropriate waveform distortion equations.

5.4 INITIAL CONDITIONS

We here consider that ray segment of a given ray which begins at the point of detonation. It should be clear from the general formulation given in the preceding sections that one needs to know the waveform factor $\psi(t,s)$ at some relatively close-in value of s in order to find the waveform at all larger values of s. This should in principle be accomplished by matching Eq. (5.4) to the blast wave at some relatively close-in distance yet sufficiently far out that the weak shock theory should be applicable. Since this leaves considerable lattitude in the starting value s_{start} of s, the initial conditions are not completely clear. The situation is further complicated by the fact that, if the explosion is moderately strong or if it takes place at higher altitudes, then one may expect the effects of the atmosphere's density stratification to be appreciable before the shock has become a weak shock (say, less than 10% ambient pressure). This would imply that one might not be able to use calculations or data which pertain or conform to the idealized case of a blast wave propagating with spherical symmetry in a homogeneous atmosphere.

In order to circumvent such difficulties, we sought to find just what properties of the blast wave were at least asymptotically independent of distance s along a ray path. In this regard, one may note that, among other quantities, the blast wave passing a given point may be characterized by an overpressure P_s and a positive phase derivation T_s. Both P_s and T_s vary with s, P_s decreasing and T_s increasing with distance from the explosion, but two aggregate quantities, even with nonlinear effects taken into account, tend to remain invariant. These are

$$I_1 = P_s T_s / J \tag{5.32a}$$

$$I_2 = T_s J / P_s - [(\gamma+1)/(2\gamma)] \int_a^s [J/(c_{eq} p_o)] ds \tag{5.32b}$$

where J is the quantity satisfying Eq. (5.6) and where a is any convenient nonzero constant. Although J is arbitrary to the extent of a constant

multiplicative factor, the choice of that factor will not affect the invariance of I_1 and I_2 with s. (The proof of the invariance of the two quantities I_1 and I_2 is based on the idealization that, in the positive phase of the blast wave, the plot of pressure versus time at a fixed point is a straight line which goes from P_s to 0 in a time interval T_s. For brevity, the proof is omitted here.)

It is possible to choose a such that I_2 is identically zero. If this is done for some value of s, then I_2 will be zero for all s for the same choice of a. Let us denote this choice of a by a^*. Then a^* may also be regarded as an invariant.

Once a^* and I_1 are known, then the positive phase durvation T_s and the shock overpressure P_s at any value of s (assumed sufficiently large that the weak shock theory is applicable) may be found from the relations

$$T_s = \{[(\gamma+1)/(2\gamma)]I_1 \int_{a^*}^{s} [J/(c_{eq}p_o)]ds\}^{1/2} \qquad (5.33a)$$

$$\frac{P_s}{J} = \frac{I_1^{1/2}}{\{\frac{\gamma+1}{2\gamma} \int_{a^*}^{s} [J/(p_o(c_{eq})]ds\}^{1/2}} \qquad (5.33b)$$

Thus a^* may be considered as that point on the ray where the weak shock theory formally predicts T_s to be zero and P_s to be infinite. Even though the weak shock theory is clearly not applicable for s near a^*, we may still regard a^* as a convenient parameter characterizing the explosion.

The values of a^* and I_1 for a given nuclear explosion may be estimated from Brode's [1954] computations of the blast wave generated by a point energy source in a homogeneous atmosphere. From examination of his figures which show the blast wave at larger distances from the source we estimate (taking $\gamma = 1.4$ and requiring that $J = 1/s$ at sufficiently small values of s)

$$a^* = 0.7\ (E_H/p_o)^{1/3} \qquad (5.34a)$$

$$I_1 = 1.0\ (E_H/p_o)^{2/3}\ p_o/c \qquad (5.34b)$$

Here E_H is the total hydrodynamic energy (taken to be half the total energy E released) and p_o and c are the ambient pressure and sound speed at the source.

The above assumes the explosion to be some distance above the ground. For an explosion very close to the ground, it would appear to be more accurate to replace E_H by $2E_H$ in the above and to only consider rays which propagate initially horizontally or obliquely upwards.

In so far as the source model is concerned, our choice for the present is that: (1) J as a function of s be computed from Eq. (5.6) subject to the requirement that J reduce to $1/s$ in the limit of small s, an initial ψ at $s=s_{start} = 5a^*$ be taken of the general form of a "Glasstone pulse"

$$\psi(t,s_{start}) = [1/J(s_{start})]P_s(1-\Delta t/T_s)e^{-\Delta t/T_s}H(\Delta t) \qquad (5.35)$$

where P_s and T_s are found from Eqs. (5.33) and where Δt is $t-t_{start}$. Here t_{start} is the time that the blast wave first arrives at the point s_{start} on the ray in question. A suitable approximate expression for this quantity would appear to be

$$t_{start} = \int_{2a^*}^{s_{start}} \frac{ds}{c_{eq}} - \int_{2a^*}^{s_{start}} \frac{(\gamma+1)}{(2\gamma)} \frac{1}{c_{eq}} \frac{P_s}{p_o} ds \qquad (5.36)$$

where P_s is given as a function of s by Eq. (5.33b). Note that the time origin ($t = 0$) corresponds to the time the blast first reaches the point $2a^*$. It is tacitly assumed that departures of the blast from spherical symmetry are negligible before that time.

5.5 PROPAGATION PAST CAUSTICS AND GROUND REFLECTION

Let us suppose that a given ray under consideration touches a caustic (see Fig. 25) at a point where $s=s_c$. The computational procedure described in the previous sections is assumed to have been carried to the point where at some value of s slightly less that s_c, say $s_c-\varepsilon$, one knows that the two factors $J(s_c-\varepsilon)$ and $\psi(t,s_c-\varepsilon)$ which, according to Eq. (5.4), describe the waveform shortly before it reaches the caustic. The task which now

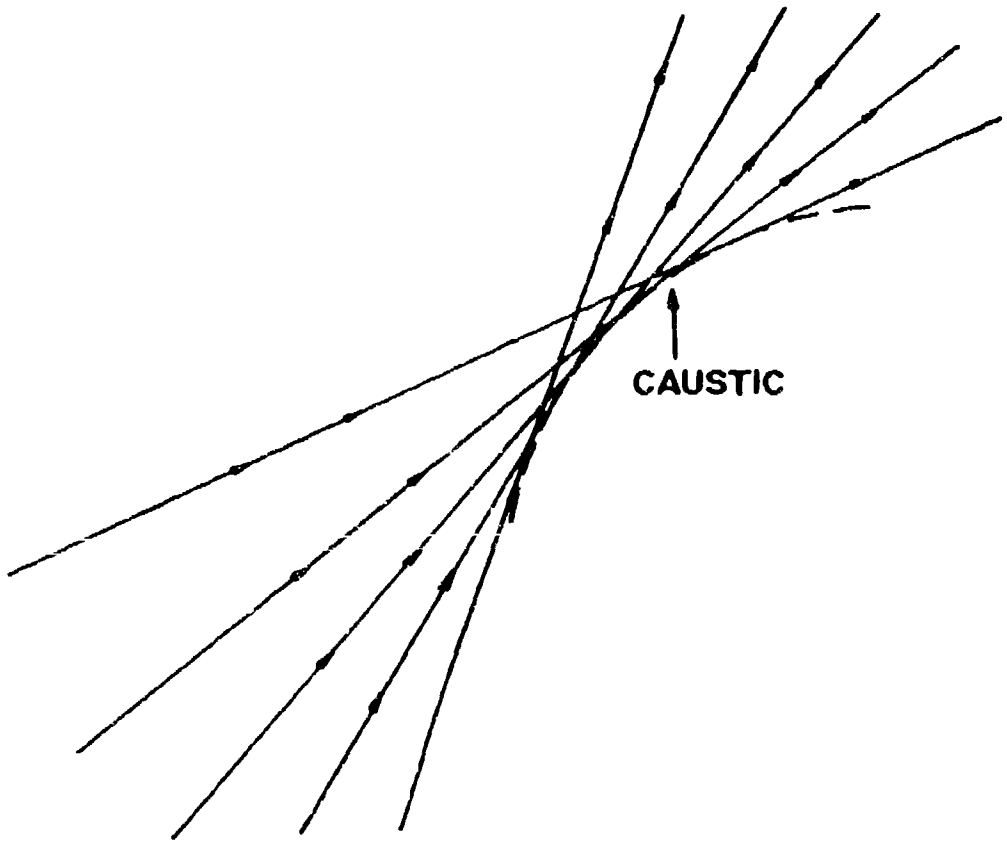

Fig. 25. Sketch of rays in the vicinity of a caustic (which forms the locus of points of intersection of adjacent rays). Here, for simplicity, the radius of curvature of the caustic is considered to be substantially less than that of the rays, although this is not always the case.

presents itself is the determination of J and ψ at some point, say $s_c+\epsilon$, on the ray past the caustic.

As is well known [see, for example, Maglieri, Hilton, Huckel, Henderson, and McLeod, 1970], waveforms on passing caustics undergo a considerable alteration in shape. This alteration takes place within a relatively short distance of several wavelengths; and subsequently the waveform propagates along the ray with relatively little additional distortion. Thus we can adopt the idealization that the alteration is abrupt and the choice of ϵ becomes largely immaterial.

For simplicity, we ignore nonlinear effects in the vicinity of the caustic and take the alteration of waveform to be as predicted by linear acoustics. The linear acoustic theory which includes diffraction effects of waveform alteration at a caustic is now relatively well known and has been discussed in the literature by, among others, Friedlander [1958], Tolstoy [1965, 1968], Ludwig [1966] and by Sachs and Silbiger [1971]. The general prediction of the linear theory as applied to the problem at hand is that J at $s_c+\epsilon$ may be found by requiring that the quantity in braces in Eq. (5.6) is the same at $s_c+\epsilon$ and $s_c-\epsilon$. The choice of J is understood to be a positive quantity. Then the function $\psi(t, s_c+\epsilon)$ is predicted to be the Hilbert transform of $\psi(t-t_{prop}, s_c-\epsilon)$ such that

$$\psi(t, s_c+\epsilon) = \frac{1}{\pi} P\int_{-\infty}^{\infty} \frac{\psi(t_o-t_{prop}, s_c-\epsilon)}{t_o - t}\, dt_o \tag{5.37}$$

where

$$t_{prop} = \int_{s_c-\epsilon}^{s_c+\epsilon} \frac{ds}{c_{eq}} \tag{5.38}$$

is the small increment of time required for a wave to propagate from $s_c-\epsilon$ to $s_c+\epsilon$. In Eq. (5.37), the capital P implies that the principal value should be taken, i.e., for any function $f(t)$

$$\frac{1}{\pi} P\int_{-\infty}^{\infty} \frac{f(t_o)}{t_o-t}\, dt_o = \frac{1}{\pi} \int_0^{\infty} \left\{ \frac{f(t+\xi) - f(t-\xi)}{\xi} \right\} d\xi \tag{5.39}$$

Note that, as long as $f(t)$ is continuous, the integrand on the right hand side remains bounded, even in the limit of small ξ.

In order to give the reader some additional insight into the waveform alteration represented by a Hilbert transform, we show in Fig. 26 some plots of functions and their transforms which were extracted from the paper by Sachs and Silbiger [1971].

One of the complications which must be considered in reference to the above described theory is that, if the incident waveform has any discontinuities (corresponding to weak shocks), then its Hilbert transform will have a logarithmic singularity. The existence of such singularities should be evident in the plots in Fig. 26. In particular, if the function $f(t)$ in Eq. (5.39) has a positive jump upwards of Δ at a value t_j of t, then the Hilbert transform (i.e., the integral) will be dominated at times near t_j by a term of the form

$$\text{log sing.} \approx \frac{\Delta}{\pi} \ln \{1/|t-t_j|\} \tag{5.40}$$

While the presence of such singularities would add a certain unrealism to the theory, a formal application of the nonlinear propagation theory described in Sec. (5.32) using the equal area rule to locate and define shocks would indicate that each such singularity is immediately transformed into a finite strength shock as it propagates past the caustic.

A given logarithmic singularity described by, say, Eq. (5.40) after propagating some distance according to Eqs. (5.28) and (5.29) will be described locally by the two lines

$$t - t_j - t_{prop} = \pm e^{-\pi\psi/\Delta} - \mu\psi \tag{5.41}$$

obtained by eliminating ϕ from Eqs. (5.28) and (5.29). These two lines describe a drooped singularity such as sketched in Fig. 27a. The multivalued configuration is reduced to a finite amplitude single valued waveform by placing a shock at t_s which intersects the unmodified waveform in Fig. 27a at ψ_a, ψ_b, and ψ_c, such as is sketched. The equal area rule requires areas A_1 and A_2 sketched in the figure to equal area A_3. One may easily check that, even though the unmodified waveform is singular, the area A_1 is finite and, moreover, given by

$$A_1 = \frac{2\Delta}{\pi} e^{-\pi\psi_a/\Delta} \tag{5.42}$$

Once one works out expressions for the other areas, he finds the equal area rule implies that

$$\psi_a - \psi_c = (1.20)(2\Delta/\pi) \tag{5.43}$$

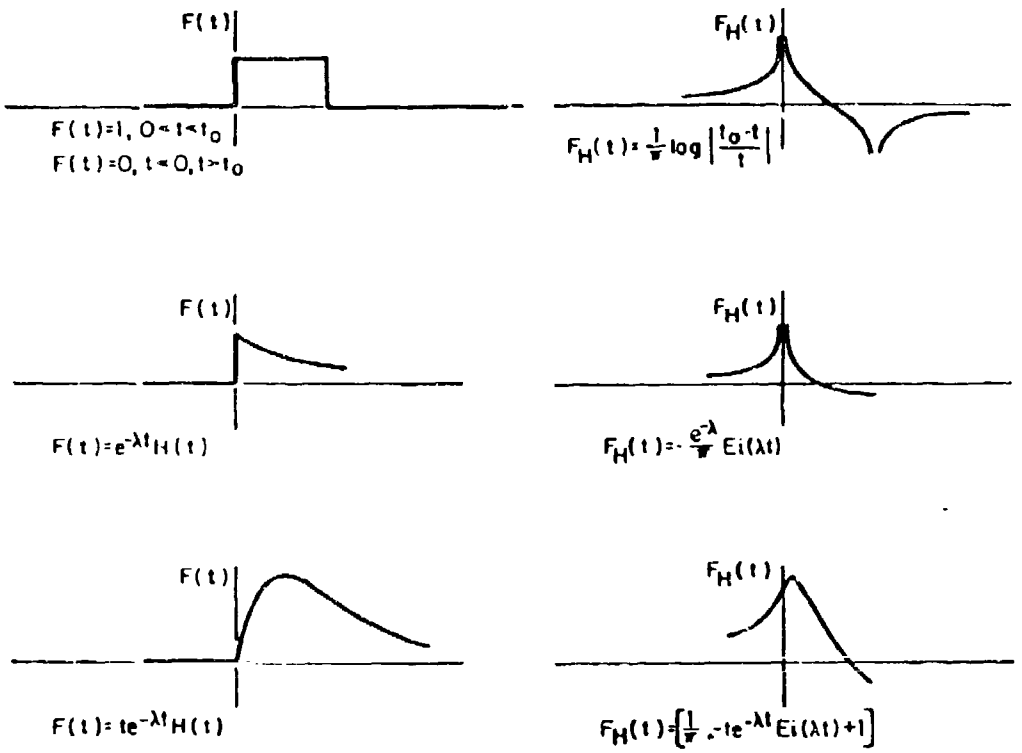

Figure 26. Three simple pulse shapes and their Hilbert transforms. (Extracted from paper by Sachs and Silbiger [1971].)

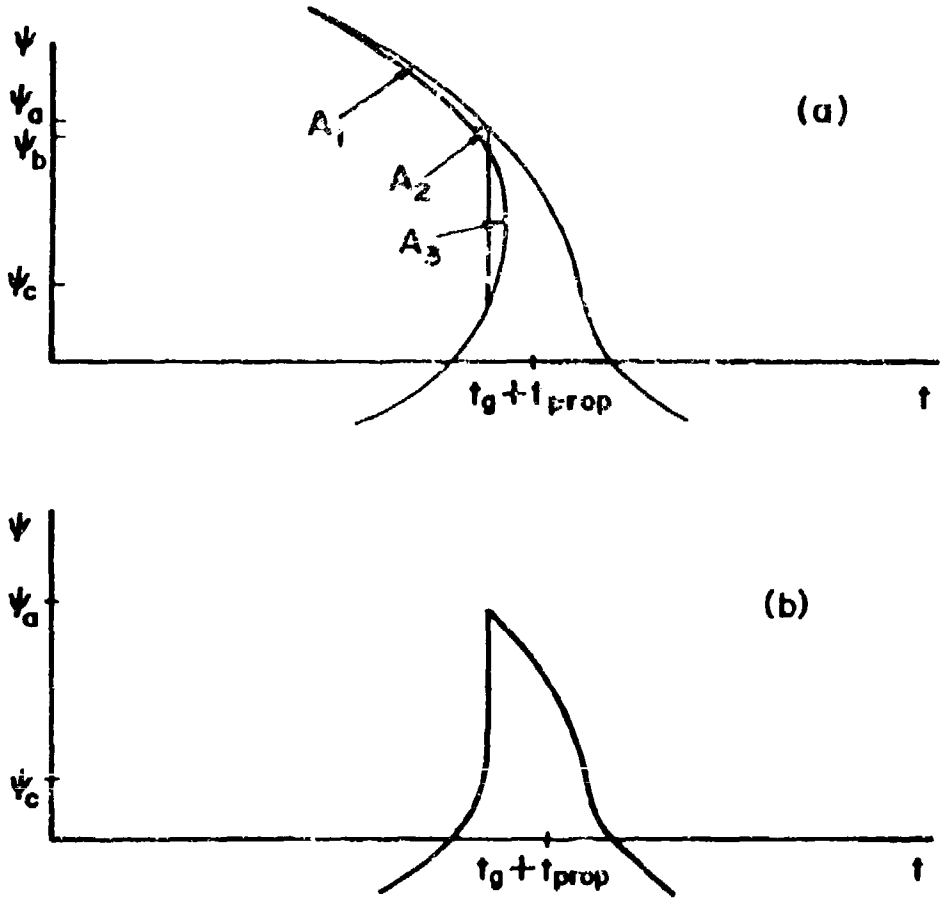

Fig. 27. Sketch of how nonlinear effects reduce a logarithmic singularity to a shock of finite amplitude. (a) Unmodified multivalued waveform, illustrating application of equal area rule. (b) Modified waveform with constructed shock.

where the factor 1.20 represents the root of the trancendental equation

$$x = \coth x \tag{5.44}$$

Thus, in so far as the singularity dominates the Hilbert transformed waveform, the net discontinuity is independent of μ and hence of propagation distance. The peak value ψ_a of ψ depends, however, on μ, being given by

$$\psi_a \simeq \frac{\Delta}{\pi} \ln\left(\frac{20\pi}{\mu\Lambda}\right) \tag{5.45}$$

which reduces rapidly as μ increases.

If we use the prescription outlined above, we may take the waveform which is received just past the caustic to be finite and we may therefore analyze its subsequent propagation on the ray segment beyond the caustic according to the method outlined in Sec. 5.3.

The only other case which requires special consideration is reflection of a wave at the ground. Consistent with the other approximations we have made it would appear that we should take J and $\psi(s,t)$ to be the same for both incident and reflected rays on the ground.

5.6 REMARKS

The general method for finding a given ray's contribution to the overall pressure waveform is to take p_{ray} in the form $J\psi$ as in Eq. (5.4) where the values of $J(s)$ and $\psi(t,s)$ at a relatively close-in value of s are found according to the procedure outlined in Sec. 5.4. The distortion of the waveform propagating along the ray is then computed, ray segment by ray segment, with suitable alterations at caustics and upon ground reflection, according to the method outlined in Secs. 5.3 and 5.5 . The total waveform is then found by a summation of all such ray waveforms which correspond to ray paths which connect the point of detonation with the observation point.

The method has a number of limitations which should be pointed out. First we are tacitly ignoring all nonlinear interactions between rays which pass through the same point. In particular, nonlinear interaction between incident and ground reflected waves is ignored. Also, we have not taken into account any nonlinear contributions to ray refraction since ray paths are taken from linear acoustics. Diffraction, which, among other things, is largely responsible for the excitation of the Lamb edge mode discussed in Chapter 4, is handled only in a gross way with its effects considered

only when we take into account the distortion at a caustic. The general method breaks down when the observation point is very near a caustic since the nonlinear effects at a caustic have been neglected. Also, the method of incorporating frequency dispersion into the theory is such that one cannot have any confidence in the lower frequency contribution to the overall waveform, especially for frequencies much less than a representative lower atmosphere ω_A (corresponding to a period of the order of 4 minutes).

Nevertheless, if one specifically wishes to consider the higher frequency portion of the waveform corresponding to periods less than, say, two minutes, the method outlined above could very possibly give theoretical waveforms which have more than token resemblance to actual waveforms recorded in the field. The overall method would appear to be somewhat more sophisticated than any existing computational scheme based primarily on geometrical acoustic concepts in that it considers frequency dispersion and distortion at caustics in addition to nonlinear effects. It does seem feasible, however, to develop a general computer program encompassing the method which could complement the program INFRASONIC WAVEFORMS described in Chapter 3 in regards to the domain of application.

Chapter VI

A MODEL FOR ACOUSTIC-GRAVITY EXCITATION BY FIREBALL RISE

6.1 INTRODUCTION

The models of acoustic-gravity wave excitation by nuclear explosions discussed in the preceding chapters of this report are based on the general tenet that the near field blast wave is the source of acoustic gravity waves observed at large distances. The authors believe, however, that the processes associated with the rise of the fireball subsequent to the generation of the blast wave may be an important source of waves in some instances. These instances include the later arriving lower frequency waves which might be observed directly below the source or at high altitudes. Fireball rise is probably not a significant source of the earlier arriving waves observed at ground level at large horizontal distances, however.

We may note that fireball rise was previously considered and subsequently dismissed as a significant source of far field radiation by Hunt, Palmer, and Penney [1960]. We believe, however, that these authors' arguments in support of this tenet are fallacious since they are based on the assumption that the wave amplitudes generated by fireball rise should fall off with increasing distance faster than those generated by the blast wave and since there is no apriori reason to believe the fireball rise generated waves to be less susceptible to channeling or guiding by the inhomogeneous atmosphere than those arising from the blast wave. They would, however, arrive later.

More recently, the question of fireball rise as a possible source mechanism was reopened by Tolstoy and Lau [1971]. These authors argued that the rise mechanism may well be the dominant source of wave generation, especially at larger periods, if the fireball is of substantially large radius. The present authors found Tolstoy and Lau's excellent discussion of this topic to be most intriguing and consequently sought to refine the Tolstoy-Lau model to include a more realistic and less phenomenological source mechanism. The source model used by Tolstoy and Lau consisted, among other features, of a point vertical force term on the right hand side of the Euler's equation (i.e., Newton's second law for a fluid) in its linearized form. The point of application of the force was presumed to be rising at constant speed through the atmosphere. The magnitude of the force was inferred from Warren's [1960] calculations of the wave drag on a rigid sphere rising at constant speed in a density stratified medium. Thus the force depended, among other quantities, on the radius of the sphere, the density of the fluid, and the velocity. The radius of the sphere and its velocity were estimated independently from other known features of a nuclear explosion.

In the present chapter, we propose a somewhat different model which takes into account the entrainment of air by the rising fireball and which incorporates a dynamical model of fireball rise into the formulation. We do not explicitly use Warren's [1960] wave drag expression as it is difficult to ascertain the extent to which a rising turbulent fireball may be simulated by a rigid sphere. An earlier version of the theory given here is reported in t' · paper by Pierce [1972].

It should be noted that a somewhat similar model of wave generation by fireball rise is presented in the recent paper by Murphy and Kahalas [1972]. [Unfortunately, at the time of this writing we hav not yet had sufficient time to make a detailed comparison of the two models.]

6.2 DYNAMICAL MODEL OF FIREBALL RISE

According to the computations of Brode [1955], the blast wave propagating out from the point of detonation carries away a finite amount of mass, such that, in the absence of gravitational effects, there remains a spherically shaped region of negligible density. The radius of this region appears [Pierce, 1968] to be of the general order of magnitude of

$$R_o = 0.4(E_H/p_o)^{1/3} \tag{6.1}$$

where E_H is the hydrodynamic energy release (taken as one half of the total energy released) and p_o is the ambient pressure at the source location.

We may expect that such a bubble will rise under the influence of gravity in such a manner that it retains its identity, if not its spherical shape. Taylor [1950] argues on the basis of potential flow in the air directly above the bubble and assuming constant pressure within the bubble that the initial rate of rise should be

$$v_{init} = (2/3)\ (g\ R_o)^{1/2} \tag{6.2}$$

Scorer [1957], on the basis of similitude considerations and from experimental data on the motion of globular masses of different density under the influence of buoyancy in a incompressible fluid, finds that the velocity of "bubble" rise may be represented by the semi-empirical equation

$$v = 1.2(g[(\rho_o - \rho_1)/\rho_c]R)^{1/2} \tag{6.3}$$

where R is a length analogous to radius which may be interpreted as the radius of a sphere of the same volume and where ρ_i is the density of the substance inside the "bubble". This agrees with Taylor's formula except for the magnitude of the coefficient. Since some definite choice should be made at this point, we choose to use Eq. (6.3) in the discussion that follows.

One may note that Eq. (6.3) may be interpreted as the velocity of a bubble rising with negligible acceleration such that the net buoyancy force exerted on it is counterbalanced by a drag force, i.e.

$$F_D = g(\rho_o - \rho_i)\left(\frac{4}{3}\pi R^3\right) \tag{6.4}$$

The relation of this drag force to the velocity may be inferred from an elimination of ρ_i from Eqs. (6.3) and (6.4) with the net result that

$$F_D = \frac{(4/3)\pi}{(1.2)^2} R^2 \rho_o v^2 \tag{6.5}$$

One may note that this drag force is proportional to the square of the velocity, to the apparent surface area of the bubble, and to the density of the surrounding medium. Apart from the numerical coefficient, this formula might also be inferred from similitude considerations.

Given an expression for the drag force, one may conjecture that a suitable form of Newton's second law for the motion of the fireball might be

$$\frac{d}{dt}\left\{(M + K M_{disp})\frac{dz}{dt}\right\} = (M_{disp} - M)g \mp F_D \tag{6.6}$$

where the sign of F_D is opposite to that of the velocity and where M is the mass of gas within the fireball, M_{disp} is the mass displaced,

$$M_{disp} = (4/3)\pi R^3 \rho_o \tag{6.7}$$

and K has a magnitude such that $K M_{disp}$ represents the effective inertia of the surrounding air. Alternately, one may interpret K to be of the magnitude such that

$$\frac{1}{2} K M_{disp} (dz/dt)^2 = (KE)_{outside} \qquad (6.8)$$

equals the kinetic energy of the air exterior to the fireball. One possible choice for K is the value of 1/2 which would be applicable to the case where the fireball is a rigid sphere and the surrounding medium is incompressible and homogeneous. (See, for example, Lamb [1879, 1945], p. 124). Our present opinion is that, for the actual inhomogeneous and compressible atmosphere, K may vary from 0 to 1/2. Its value during the early stages of fireball rise and growth would probably be more nearly 1/2, while that at the later stages is conjectured to be closer to zero. (These remarks are, however, largely unsubstantiated at present.) In order to have a definitive model, we take $K = 1/2$ in what follows.

The entrainment of mass by the rising fireball may be formally taken into account by considering M as well at z to be a dependent variable in Eq. (6.6). An additional equation describing the entrainment of mass may be taken as

$$\frac{dM}{dt} = \alpha(4\pi R^2)\rho_o \left|\frac{dz}{dt}\right| \qquad (6.9)$$

where the entrainment constant α is inferred from Scorer's [1957] experiments to have a value of 1/4. Note that the above assumes the entrainment rate to be proportional to the area, the velocity, and the density of the outside medium.

To complete the dynamical model, a third equation is needed, since R and ρ_i cannot be apriori specified as functions of time. For this purpose, a suitable approximate equation may be derived by considering the net change in density ρ_i in some time interval Δt as formally equivalent to a two step process. First R expands by $(\Delta R)_a$ with no net change in density distribution such that a net mass increment

$$\Delta M = (4\pi R^2)\rho_o \Delta R_a \qquad (6.10)$$

is added. This mass then mixes irreversibly with the mass inside to give a new averaged density

$$\rho_i + \Delta\rho_i = \rho_i + \frac{3(\Delta R)_a}{R}(\rho_o - \rho_i) \qquad (6.11)$$

Thus the contribution of the entrainment process to the net rate of change of density is

$$\left(\frac{\partial \rho_i}{\partial t}\right)_{\text{entrainment}} = (\rho_o - \rho_i)\ \frac{1}{V}\ \frac{dV}{dt} \tag{6.12}$$

where V is the volume enclosed. Throughout the process just described it is presumed that the pressure inside the bubble remains always equal to that of the surrounding medium. When the bubble rises to a layer of different ambient pressure, the density is assumed to readjust itself adiabatically, such that the contribution of the external pressure variation to the net rate of change of internal density is

$$\left(\frac{\partial \rho_i}{\partial t}\right)_{\text{pressure}} = \frac{\rho_i}{\gamma p_o}\ \frac{dp_o}{dt} \tag{6.13}$$

Thus, after adding Eqs. (6.12) and (6.13), we find

$$\frac{d\rho_i}{dt} = \frac{\rho_i}{\gamma p_o}\ \frac{dp_o}{dt} + (\rho_o - \rho_i)\ \frac{1}{V}\ \frac{dV}{dt} \tag{6.14}$$

or, with the use of $\rho_i V = M$ and $\rho_o V = M_{disp}$ and, after some algebra, we find

$$\frac{d}{dt}\left\{\ell n(\rho_o V^\gamma)\right\} = \frac{\gamma}{\rho_o V}\ \frac{dM}{dt} \tag{6.15}$$

Let us next note that Eqs. (6.6), (6.9), and (6.15) may be considered as three simultaneous ordinary differential equations for z, M, and V (or R) as functions of time. Suitable initial conditions would appear to be that, at $t = 0$: (1) R equal the R_o given by Eq. (6.1); (2) z equal the height of detonation z_o; (3) dz/dt be given by $1.2(g\ R_o)^{1/2}$ and (4) the initial mass M be zero. Once the ambient pressure and density are specified as functions of z, it would appear to be a straightforward matter to numerically integrate these equations on a computer and thus fully describe M, V, R, or z as a function of time t.

6.3 APPROXIMATE SOLUTION OF FIREBALL RISE EQUATIONS

Some remarks may be in order at this point concerning the nature of the solution of the equations presented in the previous section. Up to a time somewhat before the velocity first becomes zero, it would appear that a reasonable approximation might be to neglect the inertial term in Eq. (6.6). In this event, it is convenient to consider z rather than t as the independent variable, such that Eq. (6.6) becomes

$$\frac{dt}{dz} = \frac{1}{(1.2\, g\, R)^{1/2}} \left[1 - \frac{M}{\rho_o V} \right]^{-1/2} \tag{6.16}$$

where

$$V = (4/3)\pi R^3 \tag{6.17}$$

Equation (6.9) may also be rewritten as

$$\frac{dM}{dz} = \alpha (4\pi R^2) \rho_o \tag{6.18}$$

while Eq. (6.15) becomes

$$\frac{d}{dz} \ell n (p_o V^\gamma) = \frac{\gamma}{\rho_o V} \frac{dM}{dz} \tag{6.19}$$

If one eliminates dM/dz from the latter two of the above equations, he finds after some algebra that

$$\frac{d}{dz} \left[R\, p_o^{1/(3\gamma)} \right] = \alpha\, p_o^{1/(3\gamma)} \tag{6.20}$$

which integrates to

$$R = R_o + \alpha\, p_o^{-1/(3\gamma)} \int_{z_o}^{z} p_o^{1/(3\gamma)}\, dz \tag{6.21}$$

This may in turn be inserted into Eq. (6.18), yielding M as the integral over z from z_o to z of the right hand side. Then Eq. 6.16 may be integrated directly. Although the integrations are cumbersome, they are straightforward.

In the case of an isothermal atmosphere, Eq. (6.21) integrates to

$$R = R_o + \gamma 3\gamma H[e^{\zeta/(3\gamma H)} - 1] \tag{6.22}$$

where

$$H = c^2/(\gamma g) \tag{6.23}$$

is the scale height and we have abbreviated ζ for $z - z_o$. Thus, R tends to first increase linearly with z but, once ζ becomes comparable to several scale heights (if the sphere actually rises that far), the growth is exponential.

An estimate of the peak height of rise may be taken as that value of z for which dt/dz in Eq. (6.16) becomes singular, i.e. where $M = \rho_o V$, or equivalently; where

$$3\alpha \int_{z_o}^{z} \rho_o R^2 \, dz = \rho_o R^3 \tag{6.24}$$

In the case of an isothermal atmosphere, this requires that R_o and z jointly satisfy the transcendental equation

$$\gamma[(B + N - 1)^3 - (N - 1)^3] - B(2 - \gamma)(N^{3\gamma} - 1)$$

$$- \frac{6\gamma B}{3\gamma - 1}(N^{3\gamma} - N) - \frac{3\gamma}{3\gamma - 2}(N^{3\gamma} - N^2) = 0 \tag{6.25}$$

where we have abbreviated

$$B = (R_o/H)/(3\gamma\alpha) \tag{6.26a}$$

$$N = e^{(z - z_o)/(3\gamma H)} \tag{6.26b}$$

In the nominal limit (which is not necessarily of greatest interest) of very small explosions at lower altitudes, where $R_o \ll H$, the solution of Eq. (6.25) is found to be

$$z - z_o = \gamma H B^3 \tag{6.27}$$

Since R_o is proportional to the cube root of yield, this would suggest that the net rise is proportional to the yield for smaller yield bursts. We at present have no information as to whether this is consistent with what has been observed.

The presence of the inertia term in Eq. (6.6) implies that the fireball does not simply rise to the equilibrium altitude, but, instead, overshoots and then oscillates, such as is sketched in Fig. 28, with a period of roughly the Brunt-Väisälä period at the stabilization altitude. The oscillatory phase of the motion may be described approximately if one formally considers $z - z_M = \Delta z$ to be small, where z_M is the stabilization altitude or, equivalently, that where M first equals $\rho_o V$. Thus, we set $M = M_M + \Delta M$ and $V = V_M + \Delta V$, where M_M and V_M are the corresponding values of mass and volume when this altitude is reached. The "linearized" versions of Eqs. (6.9) and (6.15) then require

$$\frac{d}{dt}(\Delta M) = [4\pi R^2 \rho_o \alpha]_M \left|\frac{d}{dt}(\Delta z)\right| \tag{6.28}$$

$$\rho_o \frac{d}{dt}(\Delta V) = \frac{d}{dt}(\Delta M) + \frac{M_o g}{c^2} \frac{d}{dt}(\Delta z) \tag{6.29}$$

Note that the assumed nature of the entrainment process is such that the mass continues to grow. However $\rho_o \Delta V - \Delta M$ is independent of entrainment.

In Eq. (6.6), if we discard terms of higher than first order (with the exception of the drag force, which we retain), we find that

$$\frac{d}{dt}\{(1 + K)M_o \frac{d}{dt}(\Delta z)\} + M_o \omega_B^2 \Delta z = \mp F_D \tag{6.30}$$

where

$$\omega_B^2 = -\frac{1}{\rho_o}\frac{d\rho_o}{dz} - \frac{g}{c^2} \tag{6.31}$$

should be positive and is recognized as the square of the Brunt-Väisälä

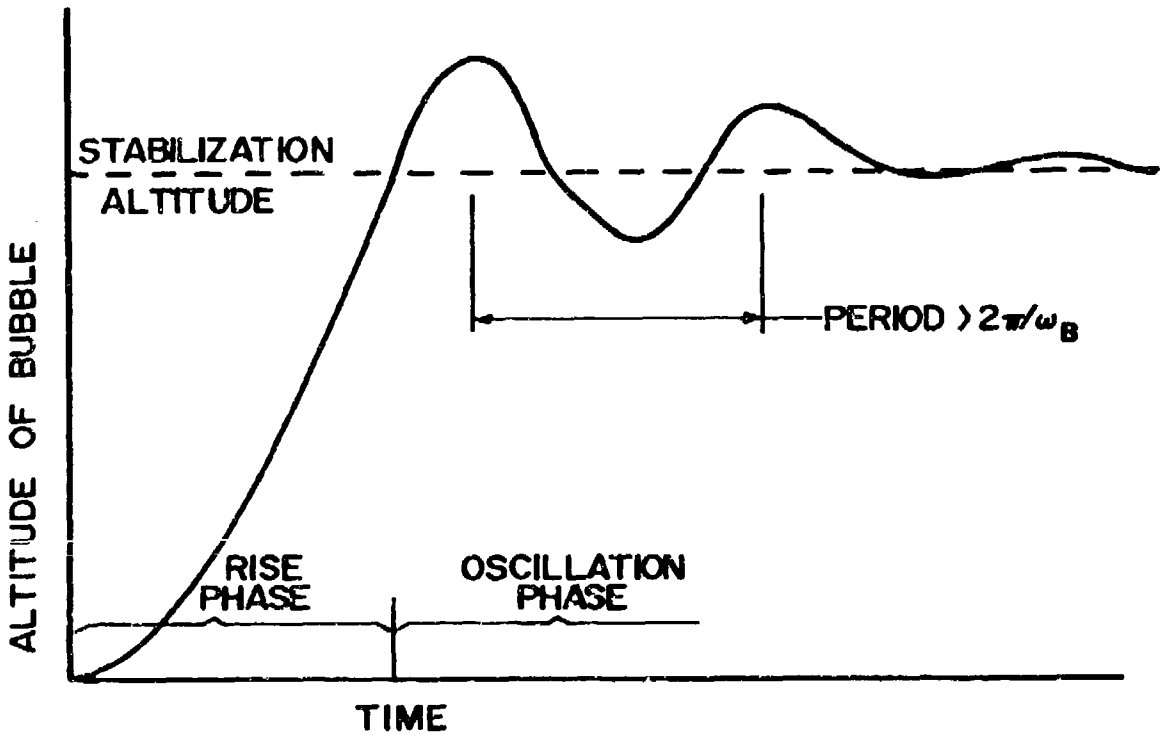

Fig. 28. Sketch of the prediction of the theory outlined in the text in regards to the height of a rising fireball (or hot gaseous bubble) as a function of time.

frequency at the stabilization altitude. It is interesting that Eq. (6.30) is independent of the entrainment coefficient.

Preparatory to solving Eq. (6.30), it is convenient to rewrite it in the form

$$(1 + K)M_o \frac{d^2}{dt^2}(\Delta z) + M_o \omega_B^2 \Delta z = \mp M_o (R_D)^{-1} [d(\Delta z)/dt]^2 \qquad (6.32)$$

where from the expression, Eq. (6.5), for F_D, we identify the constant R_D as

$$R_D = (1.2)^2 R_M \qquad (6.33)$$

Next, one may note that Eq. (6.32) has the energy integral

$$\{(1 + K)v^2 - \frac{1}{4} R_D^2 \omega_B^2 [1 \mp 2(\Delta z)/R_D]\} e^{\mp 2(\Delta z)/R_D} \qquad (6.34)$$

where the upper or lower signs are to be used depending on whether the "bubble" is rising or descending. This quantity should remain constant for any phase of the motion during which the sign of v remains unchanged. During the initial rise phase, it is clear that the constant must be identically zero since, otherwise, the solution would not match on to that represented by Eq. (6.16). Thus, up until v first becomes zero, we have

$$v = \left[\frac{1}{4(1 + K)}\right]^{1/2} \frac{\omega_B R_D}{\sqrt{R_D}} [R_D - 2(\Delta z)]^{1/2} \qquad (6.35)$$

For Δz negative and $|\Delta z| >> R_D$ this should reduce to Eq. (6.16). Note that the net amount of overshoot is $R_D/2$.

After v first reverses sign, one finds in a similar fashion that

$$v = -\left[\frac{1}{4(1 + K)}\right]^{1/2} \frac{\omega_B R_D}{\sqrt{R_D}} [2\Delta z + R_D - 2R_D \phi]^{1/2} \qquad (6.36)$$

where we have abbreviated

$$\phi = \exp [-1 + 2\Delta z/R_D] \qquad (6.37)$$

The above expression for v indicates a second turning point (such that rise recommences) when

$$\Delta z = -.39 R_D \qquad (6.38)$$

Expressions describing subsequent oscillations of the fireball can be worked out in analogous fashion. The above would indicate that the amplitude of the oscillation is initially of the same order of magnitude as the fireball radius. The period would appear also (taking K to be between 0 and 1/2) to be of the order, but slightly in excess of, the Brunt-Väisälä period.

6.4 DERIVATION OF SOURCE TERMS

The presence of the rising and subsequently oscillating fireball in the atmosphere can be formally taken into account in so far as wave generation is concerned by adding source terms to the right hand sides of the linearized equations of atmospheric fluid dynamics. For simplicity, in the present discussion we neglect winds, such that these equations become

$$\frac{\partial \rho_1}{\partial t} + \nabla \cdot (\rho_o \vec{u}_1) = S_M \tag{6.39a}$$

$$\rho_o \, \partial \vec{u}_1 / \partial t + \nabla p_1 + g \rho_1 \vec{e}_z = \vec{S}_\pi \tag{6.39b}$$

$$\partial p_1 / \partial t + \gamma \nabla \cdot (p_o \vec{u}_1) + (\gamma - 1) \rho_o g u_{1z} = (\gamma - 1) S_E \tag{6.39c}$$

where the zeroth order equations require

$$dp_o/dz = -g\rho_o \, . \tag{6.40}$$

Here ρ_1, $\vec{u}_1$, and p_1 are the acoustic perturbations (first order quantities) to density, fluid velocity, and pressure. The quantities S_M, $\vec{S}_\pi$ and S_E are source terms, whose detailed forms are discussed below.

In the paper by Pierce [1972], a general derivation is given for these source terms which may be applied here. Let $\vec{r}_c(t)$ be the position of the center of the rising fireball which is specified as a function of time, such as would be obtained from a solution of the equations presented in the previous

sections. Then one may formally consider each source term to be formally expandable as a sum of monopoles, dipoles, quadrupoles, etc., where each is centered at $\vec{x} = \vec{r}_c$. Thus, for example,

$$S_M = S_{Mo}\,\delta(\vec{x} - \vec{r}_c) + S_{M1}\,\frac{\partial}{\partial z}\,\delta(\vec{x} - \vec{r}_c) + \ldots \qquad (6.41)$$

where the first term is identified as the mass monopole source and the second term as the mass dipole source. (Note that we have here defined our symbols somewhat differently from that of the paper by Pierce [1972].) The reason that the mass dipole source term involves only a z derivative is because of the assumed axial symmetry of the fireball.

6.4.1 Monopole Source Terms

As long as we restrict ourselves to the consideration of acoustic-gravity radiation with wavelengths somewhat larger than the diameter of the rising fireball, the importance of the source terms should diminish rapidly with increasing order. Thus, a first approximation would be to take just the monopole terms (i.e., those containing a delta function rather than a derivative of a delta function) as sources. The corresponding coefficients for these monopole sources turn out to be

$$S_{Mo} = -\frac{d}{dt}\,(M - M_{disp}) \qquad (6.42a)$$

$$\vec{S}_{\pi o} = -(d/dt)(\vec{\pi} - \vec{\pi}_{disp}) - (M - M_{disp})g\,\vec{e}_x \qquad (6.42b)$$

$$S_{Eo} = -(d/dt)(\mathcal{E} - \mathcal{E}_{disp}) - g(\vec{\pi} - \vec{\pi}_{disp}) \cdot \vec{e}_z \qquad (6.42c)$$

where M, $\vec{\pi}$, and $\mathcal{E}$ are the mass, momentum, and energy of the fireball, while M_{disp}, $\vec{\pi}_{disp}$, and $\mathcal{E}_{disp}$ are the corresponding quantities which would hold for a volume of the same size of the ambient atmosphere which would occupy the same region of space if the fireball were not present. Since the ambient atmosphere is quiescent, $\vec{\pi}_{disp}$ is zero, although M_{disp} is not. The quantity $\mathcal{E}_{disp}$ may be considered as just the thermal energy of the ambient air. However, since the fireball is assumed to have the same pressure as the ambient air, the thermal energy of the fireball per unit volume (not per unit mass) will be the same as that of the air. Thus the difference $\mathcal{E} - \mathcal{E}_{disp}$ should be the kinetic energy of the gas inside the fireball. [Note

that in the aforementioned paper by Pierce [1972], there are some obvious misprints and that the correction of the source terms to account for the presence of the ambient atmosphere was erroneously omitted in Eqs. (18) of that paper.]

Since the fireball is rising vertically, the only nonzero component of $\vec{S}_{\pi o}$ is the vertical component, which, with reference to Eq. (6.6), is just

$$S_{\pi oz} = \pm F_D - \frac{d}{dt}\left(KM_{disp}\frac{dz_c}{dt}\right) \tag{6.43}$$

Also, Eq. (6.9) allows us to write the mass source coefficient in the form

$$S_{Mo} = 4\pi R^2 \rho_o \left\{\frac{dR}{dt} - \alpha\left|\frac{dz_c}{dt}\right|\right\} + V\frac{d\rho_o}{dz}\frac{dz_c}{dt} \tag{6.44}$$

The remaining source term coefficient S_{Eo} may be estimated by taking the kinetic energy of the gas inside the fireball to be the same as that for a Hill spherical vertex [Lamb, 1879, 1945], which turns out to be just twice that for a rigid sphere of the same mass rising at speed dz_c/dt. Thus

$$\mathcal{E} - \mathcal{E}_{disp} = M_{disp}(dz_c/dt)^2 \tag{6.45}$$

and one accordingly obtains

$$S_{Eo} = -\frac{d}{dt}\left\{M(dz_c/dt)^2\right\} - g\,M\,dz_c/dt \tag{6.46}$$

In order to find these three coefficients S_{Mo}, $S_{\pi oz}$, S_{Eo} explicitly as functions of time, one must in principle first find M, z_c, R, and V from the solution of the fireball rise equations, then insert these into the equations derived above.

It may be of some interest at this point to compare our expression, Eq. 6.43, for $S_{\pi oz}$ with that used in the aforementioned paper by Tolstoy and Lau [1971]. These authors in effect take

$$S_{\pi oz} = + F_2 \tag{6.47}$$

for a rising fireball where F_2 is approximated by

$$F_2 = \frac{\gamma^2 g^4 \quad R^6 \rho_o}{\pi^2 c^4 \quad (dz_c/dt)^2} \qquad (6.48)$$

Here we have made appropriate insertions into Tolstoy and Lau's Eqs. (38) and (71) to put it into the notation of the present report. The above expression should be contrasted with the Eq. (6.5) given previously which was extracted from Scorer's experiments. The discrepancy appears to be considerable when one considers the disparate velocity dependences of the drag forces in the two expressions. There seems at present to be no clear cut means of deciding which of the two is more nearly correct, although a force which increases with increasing velocity would seem to be more physically plausible.

6.4.2 Mass Dipole Source

Although we do expect the influence of higher order multipole source terms to diminish rapidly as the multipole order increases, the possibility may be considered that the mass dipole term may lead to significant wave generation. Here we estimate the magnitude of the mass dipole source term following the general formulation of Pierce [1972].

The coefficient S_{M1} which appears in Eq. (6.41) for the mass dipole coefficient is given by an integral of the form

$$S_{M1} = - \int (\psi_M') \ (z - z_c) \ d A \qquad (6.49)$$

where the integration is over an area A enclosing the fireball and where ψ_M', given by,

$$\psi_M = \rho_o \vec{u}_1 \cdot \vec{n} \qquad (6.50)$$

represents the mass flowing out through the bounding surface per unit time per unit area to first order. As a rough approximation to this, we let

$$\vec{u}_1 \cdot \vec{n} = \overset{o}{z}_c \vec{e}_z \cdot \vec{n} \qquad (6.51)$$

and disregard the z dependence of ρ_o. Doing this gives

$$S_{M1} \approx - \rho_o \overset{o}{z}_c \int R \cos^2 \theta \ d A$$

$$\approx - \overset{o}{z}_c M_{disp} \qquad (6.52)$$

where M_{disp} is the mass idsplaced by the rising fireball.

6.5 REMARKS

The solution of Eqs. (6.39) for the special case of an isothermal atmosphere is easily derived [Liu and Yeh, 1972; Pierce, 1972] and may be used to gain insight into the generation of waves in more realistic atmospheres. For brevity, this solution is not reproduced here although some of its features should be evident without reference to the detailed derivation.

One may note that, during the rise phase of the fireball motion, the time dependence of the various source terms is not oscillatory. The dominant property of the source terms (other than magnitude) is that their point of application is rising. Thus one would expect a wave wake trailing the fireball which is composed primarily of waves whose phase velocity is less than the vertical source velocity. Since lower frequency waves (depending on their frequency) may have phase velocities considerably less than the sound speed, it is not necessary that the source rise at supersonic speeds in order to have appreciable wave generation. However, a subsonic source will predominantly excite waves of frequency less than the Brunt-Vaisala frequency.

A second feature of interest is the fact that, after the rise phase, the analysis indicates that the fireball, and hence the source term point of application, should oscillate with a frequency somewhat less than ω_B. To first order in z_c, the mass dipole source term would appear to be equivalent to a stationary source whose strength is oscillating in the same manner as the velocity. Since the governing equations are linear one would expect a radiated wave which oscillates with the same period as the fireball itself. Source terms which are of second order in z_c may be expected to generate waves of twice the frequency or half the period. Since waves with periods near the Brunt period travel extremely slowly (the group velocity is nearly zero) one might expect that at larger distances and earlier times the dominant frequency of the wave generated by the fireball oscillation is more nearly twice the Brunt-Vaisala frequency.

At larger distances, it may be more nearly appropriate to solve Eqs. (6.39) by the guided mode method. In this event, it would appear to be a straightforward task to extend the existing program INFRASONIC WAVEFORMS discussed in Chapter 3 of the present report to include rising and oscillating sources, and to include the source model introduced here in particular. Additional comments concerning the implementation of the theory may be found in Sec. 7.4.

Chapter VII

CONCLUSIONS AND RECOMMENDATIONS

7.1 MULTIMODE SYNTHESIS

The computer program INFRASONIC WAVEFORMS appears to be a relatively useful tool for the analysis and interpretation of infrasonic pressure signatures detected at large distances from nuclear explosions. The program is now in use in a number of laboratories and has already given us some interesting insights into the dependence of waveforms on atmospheric temperature and wind profiles, and on energy yield and height of burst.

The limitations of the present program are, nevertheless, somewhat stringent and it is to be hoped that future work may be devoted to removing these limitations. It would appear entirely feasible, for example, to modify the program such as to include leaking modes in the synthesis. Also, the method of integration over frequency might be improved such that analytic asymptotic expressions for the Fourier transforms are utilized to extend the range of integration over a wider range of frequencies, especially higher frequencies and very low frequencies.

One also should be able to extend the model such that it would be applicable to atmospheres where the temperature and wind-velocity profiles vary with horizontal coordinates.

The present source model might also be improved. In the present version, a distinction must be made between near surface bursts and air bursts. It would seem feasible to have a somewhat generalized model which takes the nonlinear reflection of shocks at the ground into account and which gives a source model whose parameters depend continuously on the height of burst.

The development of a source model which adequately describes higher altitude bursts appears to be a relatively difficult problem, and it is clear that additional efforts are required to devise such a model. Perhaps the departures from spherical symmetry of shocks generated by high altitude bursts may be taken into account with the incorporation of dipole and higher order multipole terms in the source term expressions which we add to the linearized equations of atmospheric fluid dynamics.

Finally, we may note that the wide latitude in choice of input parameters (number of modes, range of frequencies and phase velocities, etc.) in the present version of the program may lead to some ambiguities in its numerical predictions of waveforms. It would appear feasible to modify the program such that the user not be forced to make too many seemingly arbitrary

Preceding page blank

decisions regarding input parameters. Thus, for example, the computer may decide internally, subject to requirements of numerical accuracy, just how many and which modes are required for an adequate synthesis and over just which ranges of frequencies the integration should extend. In this manner, the output of the program will become more standardized.

7.2 LAMB EDGE MODE SYNTHESIS

The hypothesis that the dominant portion of the early arriving lower frequency parts of the waveforms observed at large distances is carried by the real atmosphere's counterpart of Lamb's edge mode for the isothermal atmosphere seems to be amply substantiated by the numerical studies carried out during the contract. The hypothesis leads to a number of interesting implications which are mentioned in Sec. 4.5 of the present report. One of the most intriguing of these is that an estimate of energy yield which is relatively insensitve to details of atmospheric structure may be obtained from the period and amplitude of the earlier portion of the waveform. Our analysis indicates that such yield estimates agree fairly well with Bath's estimates based on seismic records.

The principal advantage of the edge mode theory is its simplicity. Numerical synthesis based on this theory requires only a small fraction of the computer time required by the multimode synthesis program INFRASONIC WAVEFORMS. Also, this simplicity makes the theory much more readily amenable to the consideration of horizontal variations in atmospheric structure.

The present edge mode synthesis program, written by Posey [1971], as mentioned in Chapter 4, strictly holds only for perfectly stratified atmospheres. However, the incorporation of horizontal variations into the program seems to be a task of considerably smaller magnitude than that required for the present multimode synthesis program. Thus, one would recommend that a suitable modification to the Lamb edge mode program be made within the near future.

A possible improvement to the edge mode model might be the inclusion of the next higher order term in the dispersion relation. Also, the question of the truncation of integration over height discussed in Sec. 4.2 might be examined in some more depth.

Undoubtedly, any theory based on the propagation of just one mode, even though it may be a composite mode, is going to have considerable limitations. Thus it would appear to be of interest to investigate ways in which the model might be augmented to include waves other than the edge mode. There are two ways in which this might be done. One is simply to identify one or more other guided modes which may contribute to the waveform and to develop a theory of comparable simplicity for their excitation and propagation. The other way

would be to add on a higher frequency wave which propagates out from the burst according to a geometrical acoustics' theory. Thus one might, for example, simply add the wave given by the edge mode theory to that which would be found by the method outlined in Chapter V.

7.3 HIGHER FREQUENCY MODEL

The theoretical model discussed in Chapter V of the present report appears to have some promise for the interpretation of portions of wave trains which have periods somewhat less than 2 minutes. The question of the range of frequencies whose propagation is adequately described by this model remains somewhat open, but it would appear that the range should extend up to periods as long as 30 sec. and perhaps as long as 2 minutes. Numerical experimentation would undoubtedly help in resolving this question.

The model contains three principal innovations which should help to offset the limitations which one normally associates with a ray theory computation. One of these is the incorporation of nonlinear effects in the propagation along ray paths, similar to what is currently done in sonic boom propagation computations. Another is the incorporation of gravitationally induced dispersion into the propagation. The third innovation is the use of the Hilbert transform to describe the alteration in shape of the waveform when it passes a caustic. [Although the use of such a technique appears to be relatively well known to workers in underwater acoustics, it has evidently not yet been incorporated in a general purpose computer program for arbitrarily stratified oceans.]

The method we suggest for incorporation of the source into the higher frequency propagation model appears to be somewhat more satisfactory than those presently used for the multimode and edge mode syntheses in that it takes into account the interaction of near field nonlinear effects with the variation of atmospheric density. Thus the model may be applicable for a somewhat higher range of burst altitudes.

While there are a number of limitations to the model, towards the removal of which future theoretical efforts might be directed, our present view is that the model is sufficiently promising in its present form to warrant its implementation in the form of a digital computer program. Once such a program is written, it would appear to be of considerable interest to compare its predictions with data. In this respect, one might note that the data for such a comparison need not be restricted to just nuclear explosions, but could include high energy (HE) explosion data or data taken following accidental natural gas explosions.

7.4 WAVES EXCITED BY FIREBALL RISE

The model described in Chapter VI for the generation of acoustic-gravity

waves by rising and subsequently oscillating fireballs has two principal features. First, one has a model for the dynamics of the fireball motion which tacitly ignores wave generation. Next, one has a scheme [Pierce, 1972] for deriving effective source terms for the linearized equations of atmospheric fluid mechanics from the previously derived properties of the fireball. The actual solution of the resulting linearized equations can, at least for larger horizontal distances, be found by using a multimode synthesis program only slightly different from the present INFRASONIC WAVEFORMS.

The model suggested for the fireball dynamics is probably still too simplistic for actual events, although there appears to be very little information in this regard pertaining directly to nuclear explosions in the open literature. The model suggested here has the one principal advantage that it relies on a minimum of empirical parameters. Given the yield and height of burst, the model will give a relatively complete (albeit, perhaps not entirely correct) description of the fireball motion.

It is important that one realize that the technique for extracting source terms from properties of fireball dynamics as described here and in the paper by Pierce [1972] is not necessarily restricted to the particular model of fireball dynamics described in Secs. 6.2 and 6.3 of the present report. Thus, should one devise a more accurate or detailed model of fireball rise, he still should be able to use the same technique.

As yet, we have not carried the fireball rise wave generation model to the point of making detailed numerical predictions. While this would appear to be a relatively uncomplicated task, it might be appropriate to first review all other sources of information pertinent to the phenomenology of fireball rise. In the absence of one's finding any more realistic model in the near future which is not so complicated as to be excessively difficult to use in the source term formulation, the implications of the present model should be explored, if only to give some clearer indication of the magnitude and general qualitative nature of the contribution of fireball rise to the far field waveforms. In particular, one might examine some of the assertions made in the article by Tolstoy and Lau [1972].

7.5 OTHER TOPICS

The work done under the contract on the generation of infrasound by natural sources (such as turbulence and severe weather) is only briefly described in the present report. The paper by Moo and Pierce [1972], the abstract of which is included in Chapter II of the present report, gives the status of this research as of April 1972. Further work has since been done towards the prediction of the frequency spectra of infrasonic waves propagated at large distances from localized tropospheric disturbances with given statistical properties. Since this work is still in progress and will shortly be described in some depth in a doctoral thesis by C. A. Moo, it was decided that a detailed description of the work accomplished to date in the

present report would be unwarranted. Some further indication of the work done in this respect may be found in the following abstract of a paper currently in preparation for presentation at the April 1973 meeting of the Acoustical Society of America.

Nonlinear Theory of Infrasonic Fluctuation Spectra. C. A. Moo and A. D. Pierce, Massachusetts Institute of Technology, Cambridge, Mass. 02139. In a previous paper [AGARD Conference Proceedings No. 115 (1972)] the authors have suggested that the 2-5 minute period oscillations observed in the ionosphere during periods of thunderstorm activity in the troposphere may be explained in terms of the interaction of the velocity fluctuation fields in thunderstorm regions. This analysis is here extended to the investigation of the nonlinear interactions of a system of propagating and evanescent internal acoustic-gravity waves. The development rests on Hamilton's principle for nonlinear acoustic-gravity waves with the Lagrangian approximated to third order. The coherent nonlinear interaction problem is discussed with the artifice of two primary waves which interact in a restricted region of space. Although two interacting gravity waves cannot produce a third propagating gravity wave of second order they may produce an acoustic wave in the atmosphere. The general problem of interacting random wave fields is formulated and the evolution of an initially monotonic gravity wave spectrum due to nonlinear interactions is discussed. In addition to affording a possible explanation of the anomalous ionospheric oscillations, the nonlinear interaction theory may explain the well known spectral gap which is found in the kinetic energy spectrum of atmospheric turbulence during periods of convective activity.

7.6 CONCLUDING REMARKS

The subject matter of the present report has primarily been concerned with the prediction of acoustic-gravity waveforms at large distances following a nuclear explosion in the atmosphere. The emphasis of this research has essentially been on the development of one or more theoretical models which give a sufficiently detailed numerical prediction to enable either a qualitative or quantative comparison with data. Our development of such models has been guided largely by what has been done by other workers in the past, by a consideration of those physical phenomena which appear most important, and by a desire that the model be the simplest possible (at least in conceptual terms) to explain or interpret those features of the data which appear pertinent.

Since the atmosphere is always changing, it is always imperfectly known at any given instant. Since the waveform one receives at a given point is a functional of this atmosphere, it appears that detailed agreement of theory with experiment will never be possible. However, what does appear to be the case is that certain features of the waveform may be less sensitive to small details of atmospheric structure than others. This became vividly apparent

to the authors when they found that the Lamb edge mode model predicted the product of period to the three-halves power and amplitude to correlate better with energy yield than either period or amplitude, separately, for the case of the early arriving low frequency signal. This type of result exemplifies what we hope should emerge from further studies of this type. Computer programs such as INFRASONIC WAVEFORMS may be useful in this respect primarily because they allow one to carry out numerical experimentation, from which simple trends (such as yield-amplitude proportionality) might be discovered. Once such trends are discovered, they may guide one in the development of simpler models which emphasize the essential physics of the phenomena without unnecessary complications.

REFERENCES

Baker, D. M., Acoustic Waves in the Ionosphere following Nuclear Explosions, in Acoustic-Gravity Waves in the Atmosphere (U. S. Government Printing Office, 1968) pp. 79-86.

Baker, D. M., and K. Davies, Waves in the Ionosphere produced by Nuclear Explosions, J. Geophys. Res. 73, 448-451 (1968).

Baker, D. M., and K. Davies, F2-Region Acoustic Waves from Severe Weather, J. Atmos. Terrest. Phys. 31, 1345-1352 (1969).

Balachandran, N. K., Acoustic-Gravity Wave Propagation in a Temperature- and Wind-Stratified Atmosphere, J. Atmos. Sci. 25, 818-826 (1968).

Balachandran, N. K., Acoustic-Gravity Waves in the Neutral Atmosphere and the Ionosphere, in Effects of Atmospheric Acoustic Gravity Waves on Electromagnetic Wave Propagation, AGARD Conference Proceedings No. 115 (Harford House, London, 1972) pp. 9-1 to 9-9.

Balachandran, N. K., and W. L. Donn, Dispersion of Acoustic-Gravity Waves in the Atmosphere, in Acoustic-Gravity Waves in the Atmosphere (U. S. Government Printing Office, 1968) pp. 179-193.

Barry, G., Ray Tracings of Acoustic Waves in the Upper Atmosphere, J. Atmos. Terrest. Phys. 25, 621-629 (1963).

Bath, M., Seismic Records of Explosions - Especially Nuclear Explosions, Pt. III, Rept. A 4270-4271, Seismological Inst., Univ. Uppsala, Sweden (1962).

Berthet, C., M. Bertin and D. Massignon, Experimental Confirmation of the Nonlinear Acoustic Propagation Theory in the Atmosphere, C. r. Acad. Sci. Paris 268, 650-652 (1969).

Berthet, C., and R. Rocard Theory of Atmospheric Acoustic Propagation, in Effects of Atmospheric Acoustic Gravity Waves on Electromagnetic Wave Propagation, AGARD Conference Proceedings No. 115 (Harford House, London, 1972) pp. 11-1 to 11-16.

Bethe, H. A., and K. Fuchs, Asymptotic Theory for Small Blast Pressure, in Blast Wave, Los Alamos Sci. Lab. Report LA-2000, August 1947, pp. 135-176.

Blokhintzev, D. I., The Propagation of Sound in an Inhomogeneous and Moving Medium I, J. Acoust. Soc. Amer. 18, 322-328 (1946).

Bretherton, F. P., Lamb Waves in a Nearly Isothermal Atmosphere, Q. J. Roy. Met. Soc. 95, 754-757 (1969).

Bretherton, F. P., and C. J. R. Garrett, Wavetrains in Inhomogeneous Moving Media, Proc. Roy. Soc. London A302, 529-576 (1968).

Brode, H. L., Numerical Solutions of Spherical Blast Waves, J. Appl. Phys. 26, 766-775 (1955).

Brode, H. L., Review of Nuclear Effects, in Annual Review of Nuclear Science, edited by E. Segre (Annual Reviews, Inc., Palo Alto, 1968) pp. 153-202.

Brune, J. N., J. E. Nafe, and L. E. Alsop, The Polar Phase Shift of Surface Waves on a Sphere, Bull. Seism. Soc. Amer. 51, 247-257 (1961).

Brunt, D., The Period of Simple Vertical Oscillations in the Atmosphere, Q. J. Roy. Met. Soc. 53, 30-31 (1927).

Clarke, R., The Effect of Wind on the Propagation Rate of Acoustic-Gravity Waves, Tellus 15, 287-296 (1963).

Cook, R. K., Atmospheric Sound Propagation, in Proc., Scientific Meetings of the Panel on Remote Atmospheric Probing, Vol. 2 (Natl. Acad. Sci. U. S., Wash., D. C., 1969) pp. 633-667.

COSPAR International Reference Atmosphere (North Holland, Amsterdam, 1965).

Daniels, G. M., Acoustic-Gravity Waves in Model Thermospheres, J. Geophys. Res. 72, 2419-2427 (1967).

Daniels, G. M., Ducted Acoustic-Gravity Waves in a Nearly Isothermal Atmosphere, J. Acoust. Soc. Amer. 42, 384-387 (1967).

Davies, K., and J. E. Jones, Ionospheric Disturbance in the F2-Region originating in Severe Thunderstorms, J. Atmos. Sci. 28, 254-262 (1971).

Dikii, L. A., Green's Function for Weak Disturbances in a Baroclinic Isothermally Stratified Atmosphere, Doklady Acad. Sci. USSR 143, 97-100 (1962).

Donn, W. L., and M. Ewing. Atmospheric Waves from Nuclear Explosions - Part II: The Soviet Test of October 30, 1961, J. Atmos. Sci. 19, 264-273 (1962).

Donn, W. L., R. L. Pfeffer and W. Ewing, Propagation of Air Waves from Nuclear Explosions, Science 139, 307-317 (1963).

Donn, W. L., and D. Rind, The Natural Infrasound as an Atmospheric Probe, Geophys. J. Roy. Astron. Soc. 26, 111-133 (1971).

Donn, W. L., and D. M. Shaw, Exploring the Atmosphere with Nuclear Explosions, Rev. Geophys. 5, 53-82 (1967)

Donn, W. L., D. M. Shaw, and A. C. Hubbard, The Microbarographic Detection of Nuclear Explosions, IEEE Trans. Nuclear Sci. NS-10, 285-296 (1963).

Friedlander, F. G., Sound Pulses (Cambridge Univ. Press, 1958).

Garrett, C. J. R., The Fundamental Mode of Acoustic-Gravity Wave Propagation in the Atmosphere, Fluid Mech. Trans. Warsaw 4, 707-719 (1969a)

Garrett, C. J. R., Atmospheric Edge Waves, Q. J. Roy. Met. Soc. 95, 731-753 (1969b).

Gazaryan, Yl L., Infrasonic Normal Modes in the Atmosphere, Soviet Phys., Acoust. 7, 17-22 (1961).

Georges, T. M., A Program for Calculating Three-Dimensional Acoustic-Gravity Ray Paths in the Atmosphere, NOAA Technical Report ERL 212-WPL 16, Boulder, Colorado, August 1971.

Glasstone, S., The Effects of Nuclear Weapons (U. S. Government Printing Office, 1957, revised edition, 1962).

Greene, J. S., Jr., and W. A. Whitaker, Theoretical Calculations of Travelling Ionospheric Disturbances Generated by Low Altitude Nuclear Explosions, in Acoustic-Gravity Waves in the Atmosphere (U. S. Government Printing Office, 1968) pp. 54-64.

Groves, G., Acoustic Pulse Characteristics from Explosive Releases in the Upper Atmosphere, in AFCRL-64-364, Project Firefly, N. Rosenberg, Ed. (Air Force Cambridge Research Laboratories, Bedford, Mass., 1964).

Harkrider, D. G., Theoretical and Observed Acoustic-Gravity Waves from Explosive Sources in the Atmosphere, J. Geophys. Res. 69, 5295-5321 (1964).

Harkrider, D. G., and F. Wells, Excitation and Dispersion of the Atmospheric Surface Wave, in Acoustic-Gravity Waves in the Atmosphere (U. S. Government Printing Office, 1968) pp. 299-313.
Hayes, W. D., Self-Similar Strong Shocks in an Exponential Medium, J. Fluid Mech. 32, 305-315 (1968).
Hayes, W. D., The Propagation Upward of the Shock Wave from a Strong Explosion in the Atmosphere, J. Fluid Mech. 32, 317-331 (1968).
Hayes, W. D., Conservation of Action and Modal Wave Action, Proc. Roy. Soc. London A320, 187-208 (1970).
Hayes, W. D., R. C. Haefeli and H. E. Kulsrud, Sonic Boom Propagation in a Stratified Atmosphere, with Computer Program, National Aeronautics and Space Administration Report, NASA CR-1299 (1969).
Herron, T. J., Group Velocities of Atmospheric Gravity Waves, J. Atmos. Sci. 28, 598 (1971).
Herron, T. J., I. Tolstoy and D. Kraft, Atmospheric Pressure Background Fluctuations in the Mesoscale Range, J. Geophys. Res. 74, 1321-1329 (1969).
Hines, C. O., Internal Atmospheric Gravity Waves at Ionospheric Heights, Can. J. Phys. 38, 1441-1481 (1960).
Hines, C. O., Atmospheric Gravity Waves, a New Toy for the Wave Theorist, Radio Sci. 69D, 375-380 (1965).
Hines, C. O., On the Nature of Travelling Ionospheric Disturbances Launched by Nuclear Explosions, J. Geophys. Res. 72, 1877-1882 (1967).
Hunt, J. N., R. Palmer and W. Penney, Atmospheric Waves caused by Large Explosions, Phil. Trans. Roy. Soc. London A252, 275-315 (1960).
Hurley, D. G., The Emission of Internal Waves by Vibrating Cylinders, J. Fluid Mech. 36, 657-672 (1969).
Jones, W. L., Ray Tracing for Internal Gravity Waves, J. Geophys. Res. 74, 2028-2033 (1969).
Jones, W. L., A Theory for Quasi-Periodic Oscillations Observed in the Ionosphere, J. Atmos. Terrest. Phys. 32, 1555-1566 (1970).
Kahalas, S. L., T. L. McLaren, and B. L. Murphy, Study of Acoustic-Gravity Wave Generation by Nuclear Detonations, Final Report, ARPA Order No. 1502, Contract F44620-71-C-0086, Mt. Auburn Research Assoc., Newton Upper Falls, Mass., April 1972.
Korteweg, D. J., and G. de Vries, On the Change of Form of Long Waves Advancing in a Rectangular Channel and on a New Type of Long Stationary Wave, Phil. Mag. 39, 422-443 (1895).
Lamb, H., Hydrodynamics (Dover Publications, New York, 1945, first edition published in 1879).
Lamb, H., On the Theory of Waves Propagated Vertically in the Atmosphere, Proc. London Math. Soc. 7, 122-141 (1908).
Lamb, H., On Atmospheric Oscillations, Proc. Roy. Soc. London A84, 551-572 (1910).
Landau, L. D., On Shock Waves at Large Distances from the Place of their Origin, J. Phys. USSR 9, 496-500 (1945).
Landau, L. D., and E. M. Lifshitz, Fluid Mechanics (Addison-Wesley, Reading, Mass., 1959).
Laumbach, D. D., and R. F. Probstein, A Point Explosion in a Cold Exponential Atmosphere, J. Fluid Mech. 35, 53-75 (1968).
Lehto, D. L., and R. A. Larson, Long Range Propagation of Spherical Shockwaves from Explosions in Air, Naval Ordnance Report NOLTR 69-88,

White Oak, Maryland (1969).
Levine, J., Spherical Vortex Theory of Bubble-Like Motion in Cumulus Clouds, J. Meteor. 16, 653-662 (1959).
Lighthill, M. J., On Sound Generated Aerodynamically. I. General Theory, Proc. Roy. Soc. A211, 564-587 (1952).
Lighthill, M. J., Group Velocity, J. Inst. Math. Applics. 1, 1-28 (1965).
Lilly, D. K., On the Numerical Simulation of Buoyant Convection, Tellus 14, 148-172 (1962).
Liu, C. H. and K. C. Yeh, Excitation of Acoustic-Gravity Waves in an Isothermal Atmosphere, Tellus 23, 150-163 (1971).
Liu, C. H., and K. C. Yeh, On Waves Generated by Stationary and Travelling Sources in an Isothermal Atmosphere Under Gravity, in Effects of Atmospheric Acoustic Gravity Waves on Electromagnetic Wave Propagation, AGARD Conference Proceedings No. 115 (Harford House, London, 1972) pp. 8-1 to 8-10.
Ludwig, D., Uniform Asymptotic Expansions at a Caustic, Commun. Pure and Appl. Math. 19, 215-250 (1966).
Lutzky, M., and D. L. Lehto, Shock Propagation in Spherically Symmetric Exponential Atmospheres, Phys. of Fluids 11, 1466 (1968).
MacKinnon, R. F., The Effects of Winds on Acoustic-Gravity Waves from Explosions in the Atmosphere, Quart. J. Roy. Meteor. Soc. 93, 436-454 (1967).
MacKinnon, R. F., Microbarographic Oscillations Produced by Nuclear Explosions as Recorded in Great Britain and Eire, Quart. J. Roy. Meteor. Soc. 94, 156-166 (1968).
Maglieri, D. J., D. A. Hilton, V. Huckel, H. R. Henderson, and N. J. McLeod, Measurements of Sonic Boom Signatures from Flights at Cutoff Mach Numbers, in (I. R. Schwartz, Ed.) Third Conference on Sonic Boom Research, NASA SP-255, pp. 243-254 (October, 1970).
Meecham, W. C., Simplified Normal Mode Treatment of Long Period Acoustic-Gravity Waves in the Atmosphere, Proc. IEEE 53, 2079-2087 (1965).
Meecham, W. C., Effect of Atmospheric Wind Sturcture on Shorter Period, Nuclear Generated Infrasound, J. Geophys. Res. 73, 377 (1968).
Moo, C. A., and A. D. Pierce, Generation of Anomalous Ionospheric Oscillation by Thunderstorms, in Effects of Atmospheric Acoustic Gravity Waves on Electromagnetic Wave Propagation, AGARD Conference Proceedings No. 115 (Harford House, London, 1972) pp. 17-1 to 17-6.
Morton, B. R., G. I. Taylor, and J. S. Turner, Turbulent Gravitational Convection from Maintained and Instantaneous Sources, Proc. Roy. Soc. London A234, 1-23 (1956)
Mowbray, D. E., and B. S. H. Rarity, A Theoretical and Experimental Investigation of Internal Waves of Small Amplitude in a Density Stratified Liquid, J. Fluid Mech. 28, 1-16 (1967).
Mowbray, D. E., and B. S. H. Rarity, The Internal Wave Pattern Produced by a Sphere Moving Vertically in a Density Stratified Liquid, J. Fluid Mech. 30, 489-495 (1967).
Murphy, B. L., and S. L. Kahalas, Modeling of Nuclear Sources of Acoustic-Gravity Waves, in Effects of Atmospheric Acoustic Gravity Waves on Electromagnetic Wave Propagation, AGARD Conference Proceedings No. 115 (Harford House, London, 1972) pp. 10-1 to 10-15.
Murphy, B. L., and A. D. Zalay, Study of Acoustic-Gravity Wave Generation

by Nuclear Detonations, Report for ARPA Order No. 1502, Contract No. F44620-71-C-0086, Mt. Auburn Research Assoc., Newton Upper Falls, Mass., Sept. 1971.

Nelson, R. A., H. E. Singhaus, and E. C. McNiel, Theory and Computation of the Generation of Acoustic-Gravity Waves from Explosive Sources, Stanford Research Institute, Report DASA 2120 (July, 1968).

Otterman, J., Finite-Amplitude Propagation Effect on Shock Wave Travel Times from Nuclear Explosions, J. Acoust. Soc. Amer. 31, 470-474 (1959).

Pekeris, C. L., Atmospheric Oscillations, Proc. Roy. Soc. 158, 650-671 (1937).

Pekeris, C. L., The Propagation of a Pulse in the Atmosphere, Proc. Roy. Soc. A171, 434-449 (1939).

Pekeris, C. L., The Propagation of a Pulse in the Atmosphere, Part II, Phys. Rev. 73, 145-154 (1948).

Pfeffer, R. L., A Multi-Layer Model for the Study of Acoustic-Gravity Wave Propagation in the Earth's Atmosphere, J. Atmos. Sci. 19, 251-255 (1962).

Pfeffer, R. L., and J. Zarichny, Acoustic-Gravity Wave Propagation from Nuclear Explosions in the Earth's Atmosphere, J. Atmos. Sci. 19, 256-263 (1962).

Pfeffer, R. L., and J. Zarichny, Acoustic-Gravity Wave Propagation in an Atmosphere with Two Sound Channels, Geofis. Pura et Appl. 55, 175-199 (1963).

Pierce, A. D., Propagation of Acoustic-Gravity Waves from a Small Source above the Ground in an Isothermal Atmosphere, J. Acoust. Soc. Amer. 35, 1798-1807 (1963).

Pierce, A. D., Propagation of Acoustic-Gravity Waves in a Temperature-and Wind-Stratified Atmosphere, J. Acoust. Soc. Amer. 37, 218-227 (1965).

Pierce, A. D., Comments on Paper by David G. Harkrider, 'Theoretical and Observed Acoustic-Gravity Waves from Explosive Sources in the Atmosphere,' J. Geophys. Res. 70, 2463-2464 (1965).

Pierce, A. D. Justification of the Use of Multiple Isothermal Layers as an Approximation to the Real Atmosphere for Acoustic-Gravity Wave Propagation, Radio Science 1, 265-267 (1966).

Pierce, A. D., Geometrical Acoustics Theory of Waves from a Point Source in a Temperature-and Wind-Stratified Atmosphere, Report AFCRL-66-454, Air Force Cambridge Research Laboratories, Beford, Mass. AD-636-159 (August, 1966).

Pierce, A. D., Propagation Modes of Infrasonic Waves in an Isothermal Atmosphere with Constant Winds, J. Acoust. Soc. Amer. 39, 832-840 (1966).

Pierce, A. D., The Multi-Layer Approximation for Infrasonic Wave Propagation in a Temperature - and Wind-Stratified Atmosphere, J. Comp. Phys. 1, 343-366 (1967).

Pierce, A. D., Theoretical Source Models for the Generation of Acoustic-Gravity Waves by Nuclear Explosions, in Acoustic-Gravity Waves in the Atmosphere (U. S. Government Printing Office, 1968) pp. 9-24.

Pierce, A. D., A Model for Acoustic-Gravity Wave Excitation by Buoyantly Rising and Oscillating Air Masses, in Effects of Atmospheric Acoustic

Gravity Waves on Electromagnetic Wave Propagation, AGARD Conference Proceedings No. 115 (Harford House, London, 1972) pp. 4-1 to 4-10.

Pierce, A. D., and S. C. Coroniti, A Mechanism for the Generation of Acoustic-Gravity Waves during Thunderstorm Formation, Nature 210, 1209-1210 (1966).

Pierce, A. D., and C. A. Moo, Theoretical Study of the Propagation of Infrasonic Waves in the Atmosphere, Report AFCRL-67-0172, Air Force Cambridge Research Laboratories, Bedford, Mass. (1967).

Pierce, A. D., and J. W. Posey, Theoretical Prediction of Acoustic-Gravity Pressure Waveforms Generated by Large Explosions in the Atmosphere, Report AFCRL-70-0134, Air Force Cambridge Research Laboratories, Bedford, Mass. (April, 1970).

Pierce, A. D., and J. W. Posey, Theory of the Excitation and Propagation of Lamb's Atmospheric Edge Mode from Nuclear Explosions, Geophys. J. Roy. Astron. Soc. 26, 341-368 (1971).

Pierce, A. D., J. W. Posey, and E. F. Iliff, Variation of Nuclear Explosion generated Acoustic-Gravity Waveforms with Burst Height and with Energy Yield, J. Geophys. Res. 76, 5025-5042 (1971).

Posey, J. W., Application of Lamb Edge Mode Theory in the Analysis of Explosively Generated Infrasound, Ph.D. Thesis, Dept. of Mech. Engrg., Mass. Inst. of Tech. (August, 1971).

Posey, J. W., and A. D. Pierce, Estimation of Nuclear Explosion Energies from Micobarograph Records, Nature 232, 253 (July 23, 1971).

Posey, J. W., and A. D. Pierce, Explosive Excitation of Lamb's Atmospheric Edge Mode, in Effects of Atmospheric Acoustic Gravity Waves on Electromagnetic Wave Propagation, AGARD Conference Proceedings No. 115 (Harford House, London, 1972) pp. 12-1 to 12-8.

Press, F., and D. G. Harkrider, Propagation of Acoustic-Gravity Waves in the Atmosphere, J. Geophys. Res. 67, 3889-3908 (1962).

Rayleigh, J. W. S., On the Vibrations of an Atmosphere, Phil. Mag. 29, 173-180 (1890)

Reed, S. G., Jr., Note on Finite Amplitude Propagation Effects on Shock Wave Travel Times from Explosions at High Altitudes, J. Acoust. Soc. Amer. 31, 1265 (1959).

Reed, S. G., Jr., N Wave Propagating into a Stratified Atmosphere, Phys. Fluids 3, 134 (1960).

Rohringer, G., Entrainment and Expansion Controlled Fireball Rise, GE TEMPO Report RM 63TMP-25, DASA Report 1409 (July 1963).

Rohringer, G., Properties of Ballistic Fireball Rise, GE TEMPO Report RM 63TMP-26, DASA Report 1410.

Row, R. V., Acoustic-Gravity Waves in the Upper Atmosphere due to a Nuclear Detonation and an Earthquake, J. Geophys. Res. 72, 1599-1610 (1967).

Sachs, D. A., and A. Silbiger, The Focusing and Refraction of Harmonic Sound and Transient Pulses in Stratified Media, J. Acoust. Soc. Amer. 49, 824-840 (1971).

Scorer, R. S., The Dispersion of a Pressure Pulse in the Atmosphere, Proc. Roy. Soc. London A201, 137-157 (1950).

Scorer, R. S., Experiments on Convection of Isolated Masses of Buoyant Fluid, J. Fluid Mech. 2, 583-594 (1957).

Scorer, R. S., and F. H. Ludlam, Bubble Theory of Penetrative Convection, Quart. J. Roy. Meteor. Soc. 79, 94-103 (1953).

Seliger, R. L., and G. B. Whitham, Variational Principles in Continuum Mechanics, Proc. Roy. Soc. A305, 1-25 (1968).
Simmons, W. F., A Variational Method for Weak Resonant Wave Interactions, Proc. Roy. Soc. London, A309, 551-575 (1969).
Solberg, H., Vibrations and Wave Motions in an Atmosphere whose Temperature Decreases with Height, Astrophys. Norweg. 2, 123-173 (1936).
Sutton, O. G., The Atom Bomb Trial as an Experiment in Convection, Weather 2, 105-110 (1947).
Symond, G. J., The Eruption of Krakatoa and Subsequent Phenomena (Trubner and Co., London, 1888).
Tang, L., Propagation of Guided Acoustic Gravity Waves in a Turbulent Atmosphere, M. S. Thesis, Department of Mechanical Engineering, Massachusetts Institute of Technology (May, 1971).
Taylor, G. I., Waves and Tides in the Atmosphere, Proc. Roy. Soc. London A126, 169-183 (1929).
Taylor, G. I., The Oscillations of the Atmosphere, Proc. Roy. Soc. London A156, 318-326 (1936).
Th as, J. E., and L. B. Craine, Acoustic-Gravity Wave Propagation in a Realistic Atmosphere, College of Engineering Research Report, University of Idaho, Moscow (1970).
Thomas, J. E., A. D. Pierce, E. A. Flinn, and L. B. Craine, Bibliography on Infrasonic Waves, Geophys. J. Roy. Astron. Soc. 26, 399-426 (1971).
Tolstoy, I., The Theory of Waves in Stratified Fluids including the Effect of Gravity and Rotation, Revs. Mod. Phys. 35, 207-230 (1963).
Tolstoy, I., Total Internal Reflection of Pulses in Stratified Media, J. Acoust. Sci. Amer. 37, 1153-1154 (1965).
Tolstoy, I., Long Period Gravity Waves in the Atmosphere, J. Geophys. Res. 72, 5-4622 (1967).
Tols I., Phase Changes and Pulse Deformation in Acoustics, J. Acoust. S Amer. 44, 679-683 (1968).
Tolstc ., and T. Herron, Atmospheric Gravity Waves from Nuclear Explosions, J. Atmos. Sci. 27, 55-61 (1960).
Tolstoy, I., and J. Lau, Generation of Long Internal Gravity Waves in Waveg des by Rising Buoyant Air Masses and other Sources, Geophys. J. Roy. Meteor. Soc. 26, 295-310 (1971).
Troutman W. W., and C. W. Davis, Jr., The Two-Dimensional Behavior of Shoc in the Atmosphere, Air Force Weapons Laboratory, Albuquerque, AFWL-TR-65-151 (September 1965).
Turner, J. S., The 'Starting Plume' in Neutral Surroundings, J. Fluid Mech. 13, 356-368 (1962).
Turner J. S., The Motion of Buoyant Elements in Turbulent Surroundings, J. Fluid Mech. 16, 1-16 (1963).
Turner, J. S., Model Experiments Relating to Thermals with Increasing Buoyancy, Quart. J. Roy. Meteor. Soc. 89, 62-74 (1963).
Turner, J. S. The Flow into an Expanding Spherical Vortex, J. Fluid Mech. 18, 195-208 (1964).
Turner J. S., The Dynamics of Spheroidal Masses of Buoyant Fluid, J. Fluid Mech. 19, 481-490 (1964).
Turner, J. S., The Constraints Imposed on Tornado-Like Vortices by the Top and Bottom Boundary Conditions, J. Fluid Mech. 25, 377-400 (1966).

Unno, W., and S. Kato, On the Generation of Acoustic Noise from the Turbulent Atmosphere, Pt. 1, Publ. Astron. Soc. Japan 14, 417-430 (1960).
Vaisala, V., On the Effect of Wind Oscillations on the Pilot Observations, Soc. Scientific Fennica, Commun. Phys. -Math. II 19, 1 (1925).
Valley, S. L., Handbook of Geophysics and Space Environments, Air Force Cambridge Research Laboratories, Bedford, Mass. (1965).
Van Hulsteyn, D. G., The Atmospheric Pressure Wave Generated by a Nuclear Explosion, J. Geophys. Res. 70, 257-278 (1965).
Warren, F. W. G., Wave Resistance to Vertical Motion in a Stratified Fluid, J. Fluid Mech. 7, 209-229 (1960).
Warren, F. W. G, and M. K. Arora, A Problem of Vertical Distribution of Mechanical Wave Energy in the Atmosphere, Quart. J. Mech. Appl. Maths. 20, 316-332 (1967).
Weston, D. E., Guided Propagation in a Slowly Varying Medium, Proc. Phys. Soc. 73, 365-384 (1959).
Weston, D. E., Horizontal Refraction in a Three-Dimensional Medium of Variable Stratification, Proc. Phys. Soc. 78, 48-52 (1961).
Weston, V. H., The Pressure Pulse Produced by a Large Explosion in the Atmosphere, Can. J. Phys. 39, 993-1009 (1961); Part II, Can. J. Phys. 40, 431-445 (1962).
Weston, V. H., and D. B. Van Hulsteyn, The Effects of Winds on the Gravity Wave, Can. J. Phys. 40, 797-804 (1962).
Wexler, H., and W. A. Hass, Global Atmospheric Pressure Effects of the October 30, 1961 Explosion, J. Geophys. Res. 67, 3875 (1962).
Whipple, F. J. W., The Great Siberian Meteor and the Waves, Seismic and Aerial, Which It Produced, Quart. J. Roy. Meteor. Soc. 56, 287-304 (1930).
Whipple, F. J. W., On Phenomena Related to the Great Siberian Meteor, Quart. J. Roy. Meteor. Soc. 60, 505-513 (1934).

Whitham, G. B., The Flow Pattern of a Supersonic Projectile, Commun. Pure Appl. Math. 5, 301-348 (1952).
Whitham, G. B., On the Propagation of Weak Shock Waves, J. Fluid Mech. 1, 290-318 (1956).
Whitham, G. B., On the Propagation of Shock Waves through Regions of Non-uniform Area or Flow, J. Fluid Mech. 4, 337-360 (1958).
Wu, J., Mixed Region Collapse with Internal Wave Generation in a Density Stratified Medium, J. Fluid Mech. 35, 531 (1969).
Yamamoto, R., A Dynamical Theory of the Microbarographic Oscillations Produced by the Explosions of Hydrogen Bombs, J. Meteor. Soc. Japan 35, 32-40 (1957).